Table 4. Correlation between NS5A and core protein polymorphisms and on-treatment virological responses of patients treated with PEG-IFN/RBV

Protein	Factor	Total[a]	RVR[b]	Non-RVR	EVR	Non-EVR	ETR	Non-ETR	p value		
									RVR vs. non-RVR	EVR vs. non-EVR	ETR vs. non-ETR
NS5A	IRRDR≥6	24	5 (21)[c]	19 (79)	17 (71)	7 (29)	21 (87)	3 (13)	0.12	0.04	0.026
	IRRDR≤5	44	3 (7)	41 (93)	19 (43)	25 (57)	26 (59)	18 (41)			
	Ala^{2360}	18	4 (22)	14 (78)	13 (72)	5 (28)	16 (89)	2 (11)	0.19	0.1	0.04
	Non-Ala^{2360}	50	4 (8)	46 (92)	23 (46)	27 (54)	31 (62)	19 (38)			
	ISDR≥2	18	6 (33)	12 (67)	9 (50)	9 (50)	11 (61)	7 (39)	0.003	0.79	0.39
	ISDR≤1	50	2 (4)	48 (96)	27 (54)	23 (46)	36 (72)	14 (28)			
Core	Wild-core (Arg^{70}/Leu^{91})	33	5 (15)	28 (85)	23 (70)	10 (30)	28 (85)	5 (15)	0.47	0.009	0.009
	Non-wild-core	35	3 (9)	32 (91)	13 (37)	22 (63)	19 (54)	16 (46)			
	Gln^{70}	21	2 (10)	19 (90)	6 (29)	15 (71)	10 (48)	11 (52)	1.0	0.009	0.02
	Non-Gln^{70}	47	6 (13)	41 (87)	30 (64)	17 (36)	37 (79)	10 (21)			
	Met^{91}	19	2 (11)	17 (89)	8 (42)	11 (58)	11 (58)	8 (42)	1.0	0.29	0.25
	Non-Met^{91}	49	6 (12)	43 (88)	28 (57)	21 (43)	36 (73)	13 (27)			

RVR = Rapid virological response; EVR = early virological response; ETR = end-of-treatment response; IRRDR = interferon/ribavirin resistance-determining region; Ala^{2360} = alanine at position 2360; ISDR = interferon sensitivity-determining region; Arg^{70} = arginine at position 70; Leu^{91} = leucine at position 91; Gln^{70} = glutamine at position 70; Met^{91} = methionine at position 91.

[a] Total number of isolates with a given factor. [b] Number of RVR, non-RVR, EVR, non-EVR, ETR or non-ETR cases with a given factor. [c] Values in parentheses are percentages.

Table 5. Correlation between NS5A and core protein polymorphisms

Factor	% (number of subjects/number of subtotal)[a]		p value
	IRRDR≥6	IRRDR≤5	
Ala^{2360}	50 (12/24)	14 (6/44)	0.003
Non-Ala^{2360}	50 (12/24)	86 (38/44)	
ISDR≥2	42 (10/24)	18 (8/44)	0.047
ISDR≤1	58 (14/24)	82 (36/44)	
Wild-core (Arg^{70}/Leu^{91})	67 (16/24)	39 (17/44)	0.04
Non-wild-core	33 (8/24)	61 (27/44)	
Gln^{70}	21 (5/24)	36 (16/44)	0.27
Non-Gln^{70}	79 (19/24)	64 (28/44)	

IRRDR = Interferon/ribavirin resistance-determining region; Ala^{2360} = alanine at position 2360; ISDR = interferon sensitivity-determining region; Arg^{70} = arginine at position 70; Leu^{91} = leucine at position 91; Gln^{70} = glutamine at position 70.

[a] Number of isolates with a certain factor/total number of HCV isolates with IRRDR≥6 or IRRDR≤5.

Correlation between NS5A and Core Polymorphisms

We then examined the possible correlation among the polymorphic factors in NS5A and core proteins. A significant correlation was observed between IRRDR≤5 and non-Ala^{2360} as the majority (86%) of HCV isolates with IRRDR≤5 had non-Ala^{2360} (p = 0.003) (table 5). Also, a significant correlation was obtained between IRRDR≤5 and ISDR≤1 since 82% of IRRDR≤5 were ISDR≤1 (p = 0.047). When IRRDR and core polymorphisms were compared, IRRDR≥6 was significantly correlated with wild-core (Arg^{70}/Leu^{91}) (p = 0.04). On the other hand, there was no significant correlation between IRRDR≥6 and non-Gln^{70}, or IRRDR≤5 and Gln^{70}, although the majority (79%) of IRRDR≥6 were non-Gln^{70}.

Influence of NS5A and Core Polymorphisms on HCV Clearance Kinetics during PEG-IFN/RBV Combination Therapy

To investigate the influence of NS5A and core polymorphisms on HCV-RNA kinetics during the entire course of PEG-IFN/RBV combination therapy, Kaplan-Meier HCV survival curve analysis was carried out based on HCV-RNA positivity according to NS5A and core polymorphisms. The result showed that HCV isolates of IRRDR≥6 were cleared from patients' sera more rapidly than those with IRRDR≤5 (fig. 2a). On the other hand, HCV-RNA clearance kinetics did not differ significantly between HCV isolates of ISDR≥2 and those of ISDR≤1 (fig. 2b). As for the core polymorphism, HCV isolates of non-wild-core or Gln^{70} persisted in patients' sera for longer periods of time than those of wild-core (Arg^{70}/Leu^{91}) or non-Gln^{70} (fig. 2c, d).

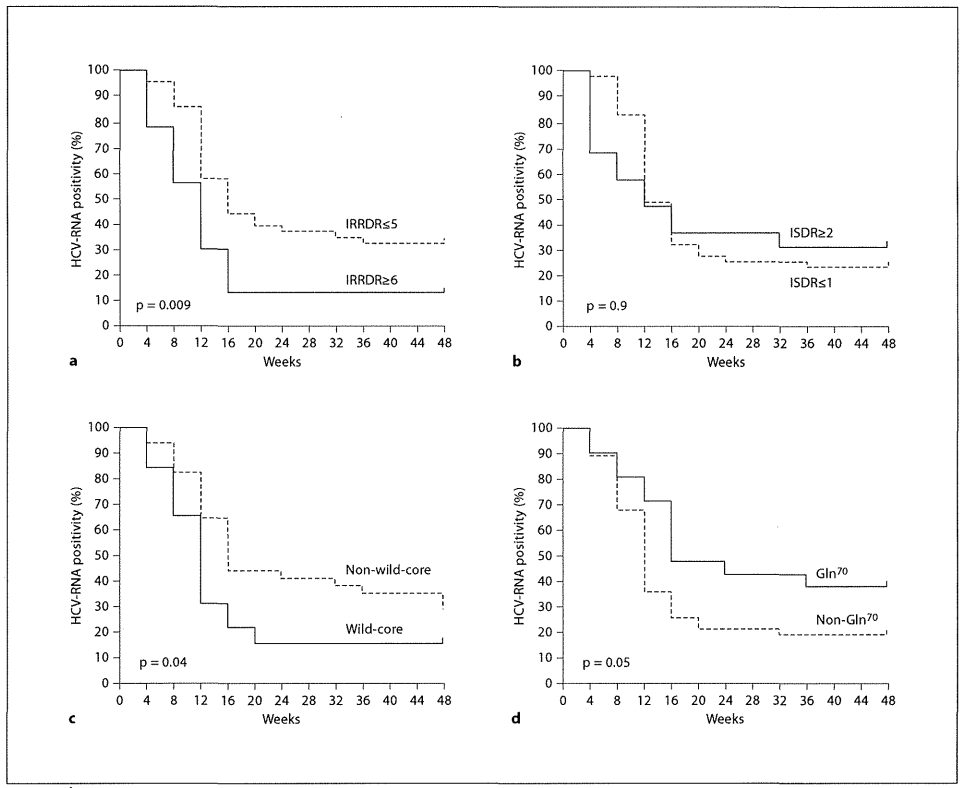

Fig. 2. Kaplan-Meier HCV survival curve analysis based on HCV-RNA positivity during the whole treatment course according to NS5A (**a**, **b**) and the core protein (**c**, **d**) polymorphisms. The difference between the analyzed groups was measured by the log-rank test.

Next, HCV clearance kinetics during the very early stages of the treatment course, e.g., 24 h, 1, 2 and 4 weeks after initiation of PEG-IFN/RBV therapy was examined. For this purpose, a possible correlation between the degree of IRRDR, ISDR and core polymorphisms and the proportion of patients who achieved significant reduction (1 log after 24 h, 1 log after 1 week, 1.5 log after 2 weeks, and 2 log after 4 weeks) of core antigen titers was analyzed. Interestingly, IRRDR≥6 was significantly associated with reduction and/or disappearance of serum HCV core antigen titers at 24 h, 1, 2 and 4 weeks after initiation of the treatment (table 6). Again, there was no significant correlation between ISDR sequence variation

Table 6. Correlation between the proportions of patients with rapid reduction of HCV core antigen titers and degree of NS5A and core protein polymorphisms

Protein	Criteria	Number of patients with significant reduction of HCV core antigen titers/number of total							
		24 h[a] (≥1 log)[b]	p value	1 week (≥1 log)	p value	2 weeks (≥1.5 log)	p value	4 weeks (≥2 log)	p value
NS5A	IRRDR≥6	20/23	0.0006	18/23	0.004	17/23	0.018	19/23	0.008
	IRRDR≤5	17/40		16/40		16/40		19/40	
	ISDR≥2	10/19	1.0	11/19	0.59	10/19	1.0	11/19	1.0
	ISDR≤1	24/44		21/44		22/44		27/44	
Core	Wild core (Arg^{70}/Leu^{91})	23/31	0.01	22/31	0.02	20/31	0.13	24/31	0.005
	Non-wild-core	13/32		13/32		14/32		13/32	
	Gln^{70}	6/19	0.03	5/19	0.01	6/19	0.06	6/19	0.004
	Non-Gln^{70}	28/44		27/44		26/44		32/44	

Note: Patients Nos. 108, 111, 129, 135 and 152 were excluded from this analysis because their core antigen titers at certain time points were missing.

IRRDR = Interferon/ribavirin resistance-determining region; ISDR = interferon sensitivity-determining region; Arg^{70} = arginine at position 70; Leu^{91} = leucine at position 91; Gln^{70} = glutamine at position 70.

[a] Period after initiation of IFN/RBV therapy.

[b] Criteria of significant reduction of HCV core antigen titers.

Table 7. Uni- and multivariate logistic regression analyses to identify independent predictive factors for success of PEG-IFN/RBV combination therapy

Univariate		Multivariate	
variable	p value	odds ratio (95% CI)	p value
IRRDR mutations (IRRDR≥6 vs. IRRDR≤5)	<0.0001	14.33 (2.24–91.65)	0.005
Ala^{2360}	0.01	1.75 (0.19–15.36)	0.62
Core polymorphism (wild-core vs. non-wild-core)	0.06	0.41 (0.05–3.28)	0.34
Gln^{70}	0.04		
RVR	<0.0001		
EVR	<0.0001	41.83 (6.12–285.68)	0.0001
ETR	<0.0001		
HCV core antigen, fmol/l	0.05		
Age	0.01	0.91 (0.84–0.99)	0.02
Platelets, $\times 10^4/mm^3$	0.07		
Hemoglobin, g/dl	0.006		

IRRDR = Interferon/ribavirin resistance-determining region; Ala^{2360} = alanine at position 2360; Gln^{70} = glutamine at position 70; RVR = rapid virological response; EVR = early virological response; ETR = end-of-treatment response.

(ISDR≥2 and ISDR≤1) and reduction of HCV core antigen titers during the very early stages of PEG-IFN/RBV therapy. On the other hand, non-wild-core or Gln^{70} were significantly associated with slow reduction and/or persistence of HCV core antigen in the patients' sera (table 6).

Identification of Independent Predictive Factors for SVR by Uni- and Multivariate Logistic Regression Analyses

Finally, in order to identify significant independent predictive factors of PEG-IFN/RBV treatment outcome, first, all available data of baseline patients' parameters, on-treatment responses and NS5A and core polymorphisms were entered in a univariate logistic analysis. This analysis yielded 11 factors that were correlated or nearly correlated with the treatment outcome; IRRDR mutations categorized as IRRDR≥6 and IRRDR≤5, Ala^{2360} and non-Ala^{2360}, core protein polymorphism categorized as wild-core (Arg^{70}/Leu^{91}) and non-wild-core, Gln^{70} and non-Gln^{70}, RVR and non-RVR, EVR and non-EVR, ETR and non-ETR, HCV core antigen titers, age, platelets count and hemoglobin levels (table 7). Subsequently, these 11 factors were entered in multivariate logistic regression analysis. This analysis yielded IRRDR mutations ($p = 0.005$), EVR ($p = 0.0001$) and age ($p = 0.02$) as independent predictive factors of PEG-IFN/RBV treatment outcome (table 7).

Discussion

Both host and viral genetic polymorphisms influence the outcome of PEG-IFN/RBV therapy for HCV-infected patients [15]. It has recently been reported that host genetic polymorphisms near or within the IL28B gene on chromosome 19 show a significant impact on the treatment outcome for patients infected with HCV genotype 1 (HCV-1a and -1b) [16–18]. Also, HCV genetic polymorphisms have been known to contribute to differences in the treatment outcome, as demonstrated by the observations that SVR rates for patients infected with HCV genotypes 2 and 3 are higher than those for patients infected with HCV genotype 1 [15]. Moreover, viral genetic polymorphisms, especially in the NS5A (ISDR and IRRDR) and the core regions, among HCV isolates of a given genotype have been linked to the difference in SVR rates [6–9, 19, 20]. In the present study, we compared the impact of IRRDR, ISDR and core polymorphisms of HCV-1b isolates on the clinical outcome of PEG-IFN/RBV therapy. Our results suggest that the degree of IRRDR mutations is more dominant than that of ISDR mutations and core polymorphism for predicting the anti-HCV treatment outcome.

IRRDR corresponds to a region near the C-terminus of NS5A. The obtained result that the IRRDR polymorphism influences the clinical outcome of IFN-based anti-HCV therapy can be linked to a recent experimental observation by Tsai et al. [21]. They reported that an HCV subgenomic RNA replicon containing NS5A of HCV-1b exerted more profound inhibitory effects on IFN activity than the original HCV-2a replicon, and that domain swapping between NS5A sequences of HCV-1b and -2a in the V3 and/or a C-terminus region including IRRDR resulted in a transfer of their anti-IFN activity. Since the C-terminal region of NS5A is among the most variable sequences across the different genotypes and subtypes of HCV [22], the difference in IFN responsiveness among different strains of a given HCV subtype could also be attributable, at least partly, to the genetic polymorphism within this region. The molecular mechanism underling the possible involvement of IRRDR in IFN responsiveness of the virus is still unknown. The significant difference in IRRDR sequence pattern may suggest genetic flexibility of this region and, indeed, the C-terminal portion of NS5A was shown to tolerate sequence insertions and deletions [23, 24]. This means that the C-terminal portion of NS5A is not essential for virus replication in cultured cells. It does not exclude the possibility, however, that the same region plays an important role in modulating the interaction with various host systems, including IFN responsiveness. It is also possible that the genetic flexibility of this region, especially IRRDR, is accompanied by compensatory changes elsewhere in the viral genome and that these compensatory changes affect overall viral fitness and responses to IFN therapy [25].

While we observed significant correlation between the overall number of mutations in IRRDR and PEG-IFN/RBV responsiveness, we also found a particular aa mutation, Ala^{2360}, that was significantly associated with SVR (tables 3, 7; fig. 1). It is possible that Ala or Val at this position confers a certain advantage for interaction between NS5A and the other viral or host proteins, which might affect IFN-induced antiviral responses. This issue needs to be elucidated in further studies.

The ISDR polymorphism was the only virological factor examined that showed a significant correlation with RVR (table 4), with the result being consistent with a recent report by other investigators [26]. This significant correlation, however, disappeared as the treatment went on. In contrast, the IRRDR polymorphism did not correlate significantly with RVR, however, it was the dominant viral genetic factor that was correlated with SVR (tables 3, 7). Interestingly, the combination of IRRDR and ISDR polymorphisms (IRRDR≥6 *plus* ISDR≥2) was significantly correlated with RVR and SVR ($p = 0.0001$ and 0.01, respectively; data not shown). This suggests a possible integrated influence of IRRDR and ISDR polymorphisms, or NS5A as a whole, on the treatment outcome. Further study is needed to clarify the issue.

The core protein polymorphisms (wild-core vs. non-wild-core, and Gln^{70} and non-Gln^{70}) were significantly correlated with the on-treatment HCV clearance kinetics

(fig. 2c, d; tables 4, 6). However, this significant correlation became blurred thereafter and eventually no significant correlation was observed between wild-core (Arg^{70}/Leu^{91}) and the final treatment outcomes (table 3). On the other hand, Gln^{70} was significantly associated with null-response, and almost significantly with non-SVR. This result is consistent, at least partly, with previous reports, including a recent multicenter study in Japan, that identified Gln^{70} as a predictive factor for poor responses to PEG-IFN/RBV treatment [8, 9, 14].

Recently, it was reported that the C-terminal region of NS5A plays a critical role in regulating the early phase of HCV particle formation [27, 28]. Moreover, sequence alteration within this region affected the degree of interaction between NS5A and core protein, which in turn affected the efficiency of progeny virus production [29]. In the present study, we observed a significant correlation between the degree of IRRDR mutations (IRRDR≥6) and the core polymorphism (table 5). Therefore, it would be interesting to investigate the degree of interaction between NS5A with IRRDR of high or low degrees of sequence variation and the wild-type (Arg^{70}/Leu^{91}) or non-wild-type of core protein, and also the impact of these interactions on progeny virus production and IFN sensitivity of the virus.

The present study identified the IRRDR polymorphism as the only viral genetic factor that independently predicted PEG-IFN/RBV treatment outcome (table 7). On the other hand, HCV is likely to utilize an alternative mechanism(s) by which to escape IFN actions through its various structural and non-structural proteins [30]. Also, a different lineage(s) of HCV-1b strains that relies more on the alternative mechanism than on IRRDR may prevail in other regions of the world. It is possible, therefore, that the impact of the IRRDR polymorphism differs with different cohorts. Analysis in a large-scale multicenter study is needed to clarify this issue.

In conclusion, NS5A (IRRDR and ISDR) and core protein polymorphisms are useful viral markers for predicting the outcome of PEG-IFN/RBV therapy for chronic hepatitis C. In particular, IRRDR≥6 is a useful marker for prediction of SVR.

Acknowledgements

This study was supported in part by Health and Labor Sciences Research Grants from the Ministry of Health, Labor and Welfare, Japan. This study was also carried out as part of the Program of Founding Research Centers for Emerging and Reemerging Infectious Diseases, Ministry of Education, Culture, Sports, Science and Technology, Japan, and the Global Center of Excellence (G-COE) Program at Kobe University Graduate School of Medicine.

References

1 Bialek SR, Terrault NA: The changing epidemiology and natural history of hepatitis C virus infection. Clin Liver Dis 2006;10:697–715.
2 Williams R: Global challenges in liver disease. Hepatology 2006;44:521–526.
3 Fried MW, Shiffman ML, Reddy KR, Smith C, Marinos G, Goncales FL Jr, Haussinger D, Diago M, Carosi G, Dhumeaux D, Craxi A, Lin A, Hoffman J, Yu J: Peginterferon alfa-2a plus ribavirin for chronic hepatitis C virus infection. N Engl J Med 2002;347:975–982.
4 Backus LI, Boothroyd DB, Phillips BR, Mole LA: Predictors of response of US veterans to treatment for the hepatitis C virus. Hepatology 2007;46:37–47.
5 Welker MW, Hofmann WP, Welsch C, von Wagner M, Herrmann E, Lengauer T, Zeuzem S, Sarrazin C: Correlation of amino acid variations within nonstructural 4B protein with initial viral kinetics during interferon-α-based therapy in HCV-1b-infected patients. J Viral Hepat 2007;14:338–349.
6 Enomoto N, Sakuma I, Asahina Y, Kurosaki M, Murakami T, Yamamoto C, Ogura Y, Izumi N, Marumo F, Sato C: Mutations in the nonstructural protein 5A gene and response to interferon in patients with chronic hepatitis C virus 1b infection. N Engl J Med 1996;334:77–81.
7 El-Shamy A, Nagano-Fujii M, Sasase N, Imoto S, Kim SR, Hotta H: Sequence variation in hepatitis C virus nonstructural protein 5A predicts clinical outcome of pegylated interferon/ribavirin combination therapy. Hepatology 2008;48:38–47.
8 Akuta N, Suzuki F, Kawamura Y, Yatsuji H, Sezaki H, Suzuki Y, Hosaka T, Kobayashi M, Kobayashi M, Arase Y, Ikeda K, Kumada H: Predictive factors of early and sustained responses to peginterferon plus ribavirin combination therapy in Japanese patients infected with hepatitis C virus genotype 1b: amino acid substitutions in the core region and low-density lipoprotein cholesterol levels. J Hepatol 2007;46:403–410.
9 Akuta N, Suzuki F, Sezaki H, Suzuki Y, Hosaka T, Someya T, Kobayashi M, Saitoh S, Watahiki S, Sato J, Matsuda M, Kobayashi M, Arase Y, Ikeda K, Kumada H: Association of amino acid substitution pattern in core protein of hepatitis C virus genotype 1b high viral load and non-virological response to interferon-ribavirin combination therapy. Intervirology 2005;48:372–380.
10 Okamoto H, Sugiyama Y, Okada S, Kurai K, Akahane Y, Sugai Y, Tanaka T, Sato K, Tsuda F, Miyakawa Y, et al: Typing hepatitis C virus by polymerase chain reaction with type-specific primers: application to clinical surveys and tracing infectious sources. J Gen Virol 1992;73:673–679.
11 El-Shamy A, Sasayama M, Nagano-Fujii M, Sasase N, Imoto S, Kim SR, Hotta H: Prediction of efficient virological response to pegylated interferon/ribavirin combination therapy by NS5A sequences of hepatitis C virus and anti-NS5A antibodies in pretreatment sera. Microbiol Immunol 2007;51:471–482.
12 Ogata S, Nagano-Fujii M, Ku Y, Yoon S, Hotta H: Comparative sequence analysis of the core protein and its frameshift product, the F protein, of hepatitis C virus subtype 1b strains obtained from patients with and without hepatocellular carcinoma. J Clin Microbiol 2002;40:3625–3630.
13 Shirakawa H, Matsumoto A, Joshita S, Komatsu M, Tanaka N, Umemura T, Ichijo T, Yoshizawa K, Kiyosawa K, Tanaka E: Pretreatment prediction of virological response to peginterferon plus ribavirin therapy in chronic hepatitis C patients using viral and host factors. Hepatology 2008;48:1753–1760.
14 Okanoue T, Itoh Y, Hashimoto H, Yasui K, Minami M, Takehara T, Tanaka E, Onji M, Toyota J, Chayama K, Yoshioka K, Izumi N, Akuta N, Kumada H: Predictive values of amino acid sequences of the core and NS5A regions in antiviral therapy for hepatitis C: a Japanese multi-center study. J Gastroenterol 2009;44:952–963.
15 Kau A, Vermehren J, Sarrazin C: Treatment predictors of a sustained virologic response in hepatitis B and C. J Hepatol 2008;49:634–651.
16 Ge D, Fellay J, Thompson AJ, Simon JS, Shianna KV, Urban TJ, Heinzen EL, Qiu P, Bertelsen AH, Muir AJ, Sulkowski M, McHutchison JG, Goldstein DB: Genetic variation in IL28B predicts hepatitis C treatment-induced viral clearance. Nature 2009;461:399–401.
17 Suppiah V, Moldovan M, Ahlenstiel G, Berg T, Weltman M, Abate ML, Bassendine M, Spengler U, Dore GJ, Powell E, Riordan S, Sheridan D, Smedile A, Fragomeli V, Muller T, Bahlo M, Stewart GJ, Booth DR, George J: IL28B is associated with response to chronic hepatitis C interferon-α and ribavirin therapy. Nat Genet 2009;41:1100–1104.
18 Tanaka Y, Nishida N, Sugiyama M, Kurosaki M, Matsuura K, Sakamoto N, Nakagawa M, Korenaga M, Hino K, Hige S, Ito Y, Mita E, Tanaka E, Mochida S, Murawaki Y, Honda M, Sakai A, Hiasa Y, Nishiguchi S, Koike A, Sakaida I, Imamura M, Ito K, Yano K, Masaki N, Sugauchi F, Izumi N, Tokunaga K, Mizokami M: Genome-wide association of IL28B with response to pegylated interferon-α and ribavirin therapy for chronic hepatitis C. Nat Genet 2009;41:1105–1109.
19 Murakami T, Enomoto N, Kurosaki M, Izumi N, Marumo F, Sato C: Mutations in nonstructural protein 5A gene and response to interferon in hepatitis C virus genotype 2 infection. Hepatology 1999;30:1045–1053.
20 Akuta N, Suzuki F, Hirakawa M, Kawamura Y, Yatsuji H, Sezaki H, Suzuki Y, Hosaka T, Kobayashi M, Kobayashi M, Saitoh S, Arase Y, Ikeda K, Kumada H: Association of amino acid substitution pattern in core protein of hepatitis C virus genotype 2a high viral load and virological response to interferon-ribavirin combination therapy. Intervirology 2009;52:301–309.
21 Tsai YH, Kuang WF, Lu TY, Kao JH, Lai MY, Liu CJ, Chen PJ, Hwang LH: The non-structural 5A protein of hepatitis C virus exhibits genotypic differences in interferon antagonism. J Hepatol 2008;49:899–907.
22 Macdonald A, Harris M: Hepatitis C virus NS5A: tales of a promiscuous protein. J Gen Virol 2004;85:2485–2502.
23 Moradpour D, Evans MJ, Gosert R, Yuan Z, Blum HE, Goff SP, Lindenbach BD, Rice CM: Insertion of green fluorescent protein into nonstructural protein 5A allows direct visualization of functional hepatitis C virus replication complexes. J Virol 2004;78:7400–7409.
24 Appel N, Pietschmann T, Bartenschlager R: Mutational analysis of hepatitis C virus nonstructural protein 5A: potential role of differential phosphorylation in RNA replication and identification of a genetically flexible domain. J Virol 2005;79:3187–3194.
25 Yuan HJ, Jain M, Snow KK, Gale Jr M, Lee WM: Evolution of hepatitis C virus NS5A region in breakthrough patients during pegylated interferon and ribavirin therapy. J Viral Hepat 2009;17:208–216.
26 Enomoto N, Maekawa S: HCV genetic elements determining the early response to peginterferon and ribavirin therapy. Intervirology 2010;53:66–69.
27 Hughes M, Griffin S, Harris M: Domain III of NS5A contributes to both RNA replication and assembly of hepatitis C virus particles. J Gen Virol 2009;90:1329–1334.
28 Appel N, Zayas M, Miller S, Krijnse-Locker J, Schaller T, Friebe P, Kallis S, Engel U, Bartenschlager R: Essential role of domain III of nonstructural protein 5A for hepatitis C virus infectious particle assembly. PLoS Pathog 2008;4:e1000035.
29 Masaki T, Suzuki R, Murakami K, Aizaki H, Ishii K, Murayama A, Date T, Matsuura Y, Miyamura T, Wakita T, Suzuki T: Interaction of hepatitis C virus nonstructural protein 5A with core protein is critical for the production of infectious virus particles. J Virol 2008;82:7964–7976.
30 Gale M Jr, Foy EM: Evasion of intracellular host defence by hepatitis C virus. Nature 2005;436:939–945.

JCM
Journals.ASM.org

NS5A Sequence Heterogeneity of Hepatitis C Virus Genotype 4a Predicts Clinical Outcome of Pegylated-Interferon–Ribavirin Therapy in Egyptian Patients

Ahmed El-Shamy,[a,b]* Ikuo Shoji,[a] Wafaa El-Akel,[c] Shymaa E. Bilasy,[d] Lin Deng,[a] Maissa El-Raziky,[c] Da-peng Jiang,[a] Gamal Esmat,[c] and Hak Hotta[a]

Division of Microbiology, Center for Infectious Diseases, Kobe University Graduate School of Medicine, Kobe, Japan[a]; Department of Virology, Suez Canal University Faculty of Veterinary Medicine, Ismalia, Egypt[b]; Department of Tropical Medicine, Cairo University, Cairo, Egypt[c]; and Department of Biochemistry, Suez Canal University Faculty of Pharmacy, Ismalia, Egypt[d]

Hepatitis C virus genotype 4 (HCV-4) is the cause of approximately 20% of the 180 million cases of chronic hepatitis C in the world. HCV-4 infection is common in the Middle East and Africa, with an extraordinarily high prevalence in Egypt. Viral genetic polymorphisms, especially within core and NS5A regions, have been implicated in influencing the response to pegylated-interferon and ribavirin (PEG-IFN/RBV) combination therapy in HCV-1 infection. However, this has not been confirmed in HCV-4 infection. Here, we investigated the impact of heterogeneity of NS5A and core proteins of HCV-4, mostly subtype HCV-4a, on the clinical outcomes of 43 Egyptian patients treated with PEG-IFN/RBV. Sliding window analysis over the carboxy terminus of NS5A protein identified the IFN/RBV resistance-determining region (IRRDR) as the most prominent region associated with sustained virological response (SVR). Indeed, 21 (84%) of 25 patients with SVR, but only 5 (28%) of 18 patients with non-SVR, were infected with HCV having IRRDR with 4 or more mutations (IRRDR ≥ 4) ($P = 0.0004$). Multivariate analysis identified IRRDR ≥ 4 as an independent SVR predictor. The positive predictive value of IRRDR ≥ 4 for SVR was 81% (21/26; $P = 0.002$), while its negative predictive value for non-SVR was 76% (13/17; $P = 0.02$). On the other hand, there was no significant correlation between core protein polymorphisms, either at residue 70 or at residue 91, and treatment outcome. In conclusion, the present results demonstrate for the first time that IRRDR ≥ 4, a viral genetic heterogeneity, would be a useful predictive marker for SVR in HCV-4 infection when treated with PEG-IFN/RBV.

Hepatitis C virus (HCV) is a major cause of chronic liver disease, hepatocellular carcinoma, and deaths from liver disease and is the most common indication for liver transplantation (7, 26–28, 38). HCV has been classified into seven major genotypes and a series of subtypes (35, 36). In general, HCV genotype 4 (HCV-4) is common in the Middle East and Africa, where it is responsible for more than 80% of HCV infections (23). Although HCV-4 is the cause of approximately 20% of the 180 million cases of chronic hepatitis C in the world, it has not been a major subject of research.

Egypt has the highest prevalence of HCV worldwide (15%) and the highest prevalence of HCV-4, which is responsible for 90% of the total HCV infections, with a predominance of the subtype 4a (HCV-4a) (1, 32). This extraordinarily high prevalence results in an increasing incidence of hepatocellular carcinoma in Egypt, which is now the second most frequent cause of cancer and cancer mortality among men (17, 21). More than 2 decades have passed since the discovery of HCV, and yet therapeutic options remain limited. Up to 2011, the standard treatment for chronic hepatitis C consisted of pegylated alpha interferon (PEG-IFN) and ribavirin (RBV) (19); however, by May 2011 two protease inhibitors (telaprevir and boceprevir) were approved by the Food and Drug Administration (FDA) for use in combination with PEG-IFN/RBV for adult chronic hepatitis C patients with HCV genotype 1 (24, 34). Since the approval of these new protease inhibitors for treatment of HCV-1 infection, the response of HCV-4 to the standard regimen of treatment (PEG-IFN/RBV) has lagged behind other genotypes and HCV-4 has become the most resistant genotype to treat. As PEG-IFN/RBV still remains to be used to treat HCV-4-infected patients, exploring the factors that predict the outcome of PEG-IFN/RBV treatment, such as sustained virological response (SVR), for HCV-4 infections is needed to assess more accurately the likelihood of SVR and thus to make more informed treatment decisions.

While the SVR rate for PEG-IFN/RBV treatment hovers at 50 to 60% in HCV-1 and -4 infection, it is up to 80% in HCV-2 and -3 infections (19, 33). This difference in responses among patients infected with different HCV genotypes suggests that viral genetic heterogeneity could affect, at least to some extent, the sensitivity to IFN-based therapy. In this context, the correlation between IFN-based therapy outcome and sequence polymorphisms within the viral core and NS5A proteins has been widely discussed, in particular in regard to Japanese patients with HCV-1b infection. Initially, in the era of IFN monotherapy, it was proposed that sequence variations within a region in NS5A of HCV-1b, called the IFN sensitivity-determining region (ISDR), were correlated with IFN responsiveness (18). Subsequently, in the era of PEG-IFN/RBV combination therapy, we identified a new region near the C terminus of NS5A, referred to as the IFN/RBV resistance-determining region (IRRDR) (13). Recently, we also demonstrated the correlation between IRRDR polymorphism and PEG-IFN/RBV treatment outcome in HCV-2a and -2b infections (15). In addition, HCV core protein polymorphism, in particular at positions 70 and 91, was also proposed as a pretreatment predictor of poor virological response in patients infected with HCV-1b (4–6). To the best of our knowledge, there is no information regarding the correlation between sequence heterogeneity in the NS5A and core proteins of HCV-4 and PEG-IFN/RBV treatment outcome. In the present study, we aimed to investigate this issue in Egyptian patients infected with HCV-4.

Received 8 August 2012 Returned for modification 30 August 2012
Accepted 14 September 2012
Published ahead of print 19 September 2012
Address correspondence to Hak Hotta, hotta@kobe-u.ac.jp.
* Present address: Ahmed El-Shamy, Division of Liver Diseases, Mount Sinai School of Medicine, New York, New York, USA.

doi:10.1128/JCM.02109-12

TABLE 1 Virological responses of HCV-4-infected patients treated with PEG-IFN/RBV

Virological response	Proportion (%) of patients with indicated response (no. of patients/total no.)				
	HCV-4[a]	HCV-4a	HCV-4 m	HCV-4n	HCV-4o
SVR	58 (25/43)	56 (19/34)	100 (3/3)	33 (1/3)	67 (2/3)
Non-SVR	42 (18/43)	44 (15/34)	0 (0/3)	67 (2/3)	33 (1/3)
Null response	30 (13/43)	32 (11/34)	0 (0/3)	67 (2/3)	0 (0/3)
Relapse	12 (5/43)	12 (4/34)	0 (0/3)	0 (0/3)	33 (1/3)

[a] Includes all 43 cases with HCV-4 infection (34 cases with HCV-4a and 3 cases each with HCV-4m, -4n, and -4o).

MATERIALS AND METHODS

Ethics statement. The study protocol, which conforms to the provisions of the Declaration of Helsinki, was approved beforehand by the Ethic Committees in Cairo University Hospital and in Kobe University, and written informed consent was obtained from each patient prior to the treatment.

Patients. A total of 43 previously untreated patients who were chronically infected with HCV-4a (34 patients), HCV-4m (3 patients), HCV-4n (3 patients), or HCV-4o (3 patients) were consecutively evaluated for antiviral treatment at Cairo University Hospital, Cairo, Egypt, between January 2008 and September 2010. The HCV subtype was determined according to the method of Okamoto et al. (31). The patients were treated with PEG-IFN α-2a (180 μg/week, subcutaneously) and RBV (1,000 to 1,200 mg daily, *per os*) for 48 weeks. The quantification of serum HCV RNA titers was performed as previously reported (14). To minimize the therapeutic burdens, including the high cost and possible side effects, therapy was discontinued if HCV RNA titers at week 12 did not drop by 2 log compared with baseline values or if HCV RNA was still detectable at week 24. These were considered a null response (see Results).

Sequence analysis of the NS5A and core regions of the HCV genome. Blood samples were collected using Vacutainer tubes. The sera were separated within 2 h of blood collection, transferred to sterile cryovials, and kept frozen at −80°C until use. HCV RNA was extracted from 140 μl of serum using a commercially available kit (QIAmp viral RNA kit; Qiagen, Tokyo, Japan). The extracted RNA was reverse transcribed and amplified for the HCV genome encoding a carboxy terminus of NS5A (amino acids [aa] 2193 to 2417) and the core protein (aa 1 to 191) using SuperScript III one-step RT-PCR Platinum *Taq* HiFi (Invitrogen, Tokyo, Japan). The resultant reverse transcription (RT)-PCR product was subjected to a second-round PCR by using Platinum *Taq* DNA polymerase high fidelity III (Invitrogen). Primers used for amplification of the 3′ half of the NS5A region of HCV-4 were as follows: NS5A-4/F1 (5′-CTCAAYTCGTTCGT RGTGGGATC-3′; sense) and NS5A-4/R1 (5′-CGAAGGTCACCTTCTT CTGCCG-3′; antisense) for one-step RT-PCR; and NS5A-4/F2 (5′-ATG CGAGCCYGAGCCGGACGT-3′; sense) and NS5A-4/R2 (5′-GCTCAGG GGGYTRATTGGCAGCT-3′; antisense) for the second-round PCR. Primers for amplification of the core region of HCV-4 were 249-F (5′-G CTAGCCGAGTAGTGTTG-3′; sense) and 984-R (5′-GATGTGRTGRTC GGCCTC-3′; antisense) (40) for one-step RT-PCR; and 319-F (5′-GGA GGTCTCGTAGACCGTGC-3′; sense) (40) and primer-186 (5′-ATGTA CCCCATGAGGTCGGC-3′; antisense) (2) for the second-round PCR. RT was performed at 45°C for 30 min and terminated at 94°C for 2 min, followed by the first-round PCR over 35 cycles, with each cycle consisting of denaturation at 94°C for 30 s, annealing at 50°C for 30 s, and extension at 68°C for 90 s. The second-round PCR was performed under the same conditions. The sequences of the amplified fragments were determined by direct sequencing without subcloning. The amino acid sequences were deduced and aligned using Genetyx Win software version 7.0 (Genetyx Corp., Tokyo, Japan). The numbering of amino acid residues for HCV-4 isolates is according to the polyprotein of ED43 isolate (accession no. Y11604) (10). Consensus sequences of the carboxy terminus of NS5A of a given HCV-4 subtype were inferred by alignment of all sequences obtained in this study as well as all available NS5A sequences of HCV-4a (accession no. Y11604, DQ418782 to DQ418789, DQ516084, and DQ988073 to DQ988079), HCV-4m (FJ462433), HCV-4n (FJ462441), and HCV-4o (FJ462440) from the databases.

Statistical analysis. Numerical data were analyzed by Student's *t* test and categorical data by Fisher's exact probability test. To evaluate the optimal threshold of the number of amino acid mutations in IRRDR for prediction of treatment outcomes, the receiver operating characteristic (ROC) curve was constructed. Univariate and multivariate logistic regression analyses were performed to identify independent predictors for treatment outcomes. All statistical analyses were performed using the SPSS version 16 software (SPSS Inc., Chicago, IL). Unless otherwise stated, a P value of <0.05 was considered statistically significant.

Nucleotide sequence accession numbers. The sequence data reported in this paper have been deposited in the DDBJ/EMBL/GenBank nucleotide sequence databases with the accession numbers AB725987 through AB726066.

RESULTS

Patients' responses to PEG-IFN/RBV combination therapy. Among 43 patients enrolled in this study, 30 (70%) patients completed the entire course of PEG-IFN/RBV treatment for 48 weeks and follow-up for 24 weeks. On the other hand, the treatment was discontinued for 13 (30%) patients due to poor virological responses at 12 or 24 weeks after initiation of the therapy. Overall, 25 (58%) patients achieved SVR while 18 (42%) patients had non-SVR (Table 1). When analyzed on the basis of the subtype classification, SVR was achieved by 56% (19/34), 100% (3/3), 33% (1/3), and 67% (2/3) of patients infected with HCV-4a, -4m, -4n, and -4o, respectively.

Non-SVR patients are classified into two groups: (i) patients with null response, who did not achieve >2-log reduction of the initial viral load at week 12 or who had detectable viremia at week 24 of the treatment period; and (ii) patients with relapse, who were negative for HCV-RNA at the end of the treatment period (week 48) followed by a rebound viremia at a certain time point during the follow-up period of 24 weeks. Patients with null response represented 30% (13/43) of all the HCV-4-infected subjects analyzed, while those with relapse represented 12% (5/43). A similar tendency was observed for subtype HCV-4a.

Among various patients' demographic characteristics, SVR patients had a significantly lower average age than that of non-SVR patients (Table 2). Furthermore, a tendency for SVR patients to have a lower average titer of initial viral load than that of non-SVR was noted, although the difference was not statistically significant, due possibly to the small number of patients analyzed ($P = 0.07$).

Downloaded from http://jcm.asm.org/ on December 3, 2012 by KOBE UNIVERSITY

TABLE 2 Demographic characteristics of HCV-4-infected patients with SVR and non-SVR[a]

Factor	SVR	Non-SVR	*P* value
Age	38.47 ± 9.51	45.80 ± 5.65	0.014
Sex (male/female)	18/7	15/3	0.48
BMI	27.36 ± 3.65	27.67 ± 5.28	0.85
Platelets ($\times 10^3/\mu l$)	204.4 ± 40.63	216.7 ± 87.25	0.59
Hemoglobin (g/dl)	14.54 ± 1.38	15.08 ± 1.39	0.25
WBC count	7,041 ± 1,876	7,078 ± 2,977	0.96
Albumin (g/dl)	4.12 ± 0.36	4.328 ± 0.41	0.11
ALT (IU/liter)	78.72 ± 59.68	82.39 ± 41.80	0.83
AST (IU/liter)	64.94 ± 27.63	58.17 ± 23.98	0.44
HCV-RNA (IU/ml)	84,290 ± 186,300	501,800 ± 816,700	0.07

[a] Values are means ± standard deviations. SVR, sustained virological response; BMI, body mass index; WBC, white blood cell; ALT, alanine aminotransferase; AST, aspartate aminotransferase.

Correlation between NS5A sequence heterogeneity and SVR in HCV-4 infection. We and other researchers reported significant correlation between sequence polymorphisms within the C-terminal half of NS5A, including that in ISDR and IRRDR, and PEG-IFN/RBV treatment outcome in HCV-1 and HCV-2 infections (13, 15, 18, 30). However, this information is quite limited in HCV-4 infection. To clarify this issue, part of the HCV-4 genome encoding a carboxy terminus (aa 2193 to 2417) of NS5A in pretreatment sera was amplified and sequenced, and amino acid sequences were deduced. The sequences obtained as well as all available NS5A sequences of HCV-4a, -4m, -4n, and -4o from the databases were aligned, and the consensus sequences for a desired HCV-4 subtype were inferred (see Materials and Methods). Next, to identify an NS5A region(s) that would be significantly correlated with treatment outcome, we carried out a sliding window analysis with a window size of 30 residues over the C-terminal half (aa 2193 to 2417) of NS5A sequences obtained from all SVR (n = 25) and non-SVR (n = 18) patients along with corresponding consensus sequences of each HCV-4 subtype as described previously (30). This analysis revealed that the difference in the overall number of amino acid mutations between SVR and non-SVR isolates exceeded the significant threshold only in a region corresponding to IRRDR of HCV-1b (13), ranging from aa 2331 to 2383, thus being referred to as IRRDR[HCV-4] (Fig. 1). Indeed, the average number of amino acid mutations in IRRDR[HCV-4] was significantly larger in SVR than in non-SVR (P = 0.0005) isolates (Fig. 2A). Sequences of IRRDR of HCV-4a, -4m, -4n, and -4o obtained from SVR and non-SVR patients along with the number of IRRDR mutations of each isolate are shown in Fig. 2B.

Next, we performed ROC curve analysis to estimate the optimal cutoff number of IRRDR[HCV-4] mutations for SVR prediction. This analysis estimated 4 mutations as the optimal number of IRRDR[HCV-4] mutations to predict SVR, since it achieved the highest sensitivity (84%; sensitivity refers to the proportion of SVR patients who were infected with HCV isolates of IRRDR[HCV-4] with 4 or more mutations) and specificity (72%; specificity refers to the proportion of non-SVR patients who were infected with HCV isolates of IRRDR[HCV-4] with 3 or fewer mutations) with an area under the curve (AUC) of 0.82 (Fig. 3). Accordingly, 21 (84%) of 25 patients with SVR, in contrast to only 5 (28%) of 18 patients with non-SVR, had IRRDR[HCV-4] with 4 or more mutations (referred to as IRRDR[HCV-4]≥4), with the difference between the two groups being statistically significant (P = 0.0004) (Table 3). It should be noted that 4 (31%) of 13 patients with null response and only 1 (20%) of 5 patients with relapse had HCV with IRRDR[HCV-4]≥4. These results collectively suggest that IRRDR[HCV-4]≥4 is significantly associated with SVR. In this connection, we also tested the impact of a higher (≥5) and a lower (≥3) degree of IRRDR mutations on treatment outcome. IRRDR[HCV-4]≥5 was significantly associated with SVR, though with a relatively lower sensitivity (64%) than that of IRRDR[HCV-4]≥4 (Table 3). On the other hand, there was no significant correlation between IRRDR[HCV-4]≥3 and SVR.

Correlation between core protein sequence heterogeneity and SVR in HCV-4 infection. A close correlation between core protein sequence patterns at positions 70 and 91 and treatment outcome has been proposed, especially in Japanese patients with HCV-1b infection (4–6). To examine this hypothesis in Egyptian patients infected with HCV-4, core sequences of the viral genome were amplified from the pretreated sera, and the amino acid sequences were deduced. Due to a high degree of sequence homology among core sequences of various HCV-4 subtypes, all sequences obtained were aligned with the prototype sequence, ED43 (10). The residues at positions 70 and 91 were both well conserved among the sequences analyzed, and therefore, no correlation with treatment outcome was observed for these residues (Fig. 4). All but two isolates had arginine at position 70 (Arg^{70}), the residue that has been associated with an IFN-sensitive phenotype as far as the core protein of HCV-1b is concerned (4–6). On the other hand, Pro at position 71 showed a tendency to be more frequent in SVR than in non-SVR patients; however, the frequency was not statistically different between the two groups.

Identification of independent predictive factors for SVR in HCV-4 infection. In order to identify significant independent

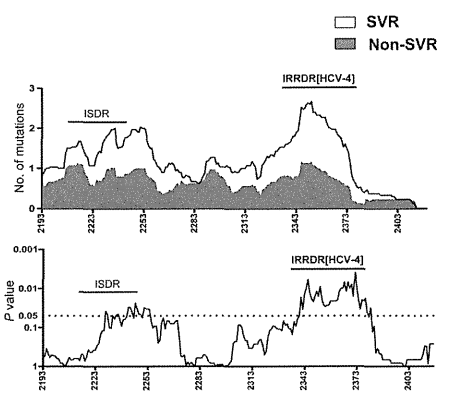

FIG 1 Sliding window analysis over the carboxy terminus (aa 2193 to 2417) of NS5A of HCV-4 obtained from SVR and non-SVR patients.

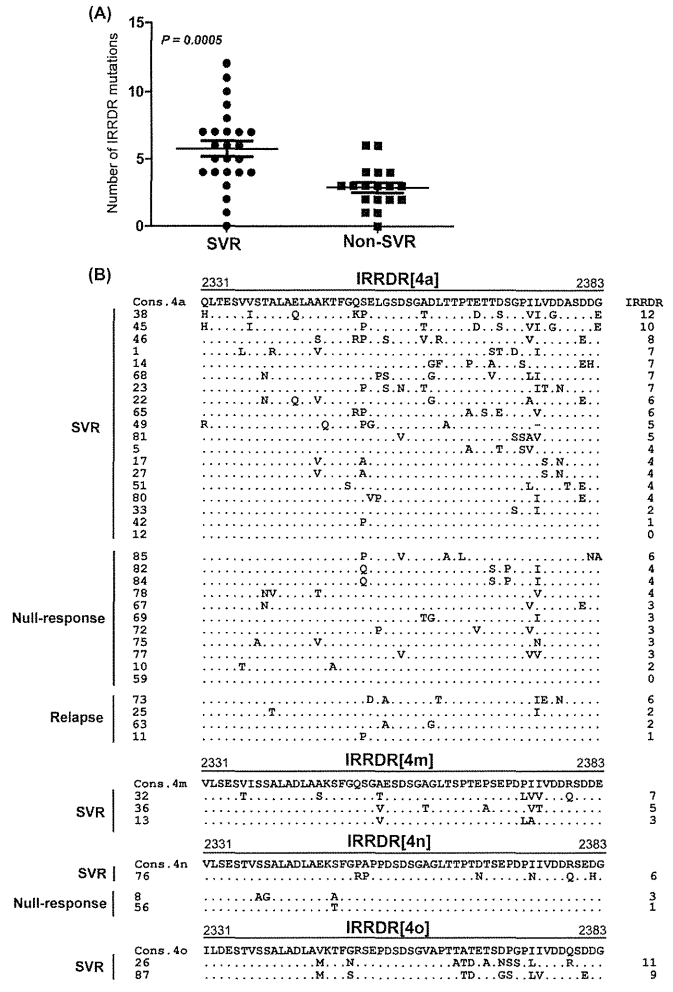

FIG 2 Correlation between *IRRDR*[HCV-4] sequence variations and treatment outcome. (A) Average number of amino acid mutations in *IRRDR*[HCV-4] obtained from SVR and non-SVR patients. (B) Alignment of IRRDR[HCV-4] sequences obtained from SVR and non-SVR patients with HCV-4a, -4m, -4n, and -4o. The consensus sequence (Cons) of each subtype is shown on the top. The numbers along the sequence indicate the amino acid positions. Dots indicate residues identical to those of the Cons sequence. The numbers of the mutations in each IRRDR (4a, 4m, 4n, or 4o) are shown on the right.

predictive factors of SVR for PEG-IFN/RBV treatment outcome in HCV-4 infection, first, all available data of baseline patients' parameters and IRRDR[HCV-4] polymorphism were entered in a univariate logistic analysis. This analysis yielded 3 factors that were correlated or nearly correlated with SVR: IRRDR[HCV-4]≥4 (P = 0.0004), patient's age (<42 years; P = 0.03), and HCV RNA titer (<5,200 IU/ml; P = 0.08). Subsequently, these 3 factors were entered in multivariate logistic regression analysis. This anal-

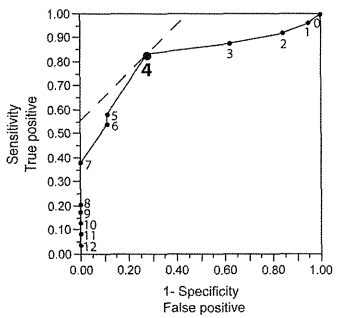

FIG 3 ROC curve analysis of IRRDR[HCV-4] sequence heterogeneity for SVR prediction. The solid line curve shows the AUC. Solid circles with numerals plotted on the curve represent different numbers of IRRDR mutations analyzed. The dashed line in the upper left corner indicates the optimal number of IRRDR[HCV-4] mutations for SVR prediction, which yields the highest sensitivity (84%) and the highest specificity (72%).

ysis revealed that the IRRDR[HCV-4]≥4 was the only independent predictive factor for SVR in HCV-4 infection (Table 4). We then assessed SVR predictability by means of IRRDR[HCV-4]≥4. As shown in Table 5, IRRDR[HCV-4]≥4 would predict SVR with a positive predictive value (PPV) of 81% ($P = 0.002$) and sensitivity of 84%. On the other hand, IRRDR[HCV-4]≤3 would predict non-SVR with a negative predictive value (NPV) of 76% ($P = 0.02$) and specificity of 72%. Thus, the degree of sequence variation in IRRDR[HCV-4] would yield useful positive and negative predictive markers for PEG-IFN/RBV therapy outcome in HCV-4-infected patients.

DISCUSSION

Both host and viral genetic factors have been implicated in influencing the clinical response to PEG-IFN/RBV therapy for HCV infection (22). It has recently been reported that host genetic polymorphisms near or within the IL28B gene on chromosome 19 show a critical impact on the treatment outcome of patients infected with HCV-1 (20, 37, 39). As for the viral factor(s), polymorphisms of NS5A and core regions of a given HCV genotype have been linked to a difference in SVR rates (3, 4, 13, 18, 30). This hypothesis was mostly inferred from studies carried out with Asian populations, in particular Japanese, with HCV-1b infection. However, whether it can be applied to non-Asian populations infected with non-HCV-1 is still unknown. To the best of our knowledge, this is the first study that specifically examines the relationship between HCV genome heterogeneity, in particular in NS5A and core regions, and PEG-IFN/RBV treatment outcome in Egyptian patients infected with HCV-4. In analogy with our previous studies that identified IRRDR as a significant determinant for PEG-IFN/RBV treatment outcome in Japanese patients infected with HCV-1b, -2a, and -2b (12–16), we have demonstrated in the present study that sequence heterogeneity within IRRDR is closely associated with the ultimate treatment outcome in Egyptian patients infected with HCV-4. A high degree of sequence variation in IRRDR[HCV-4], i.e., more than 4 (IRRDR ≥ 4), significantly correlated with SVR, while a low degree of sequence variation in this region (IRRDR ≤ 3) correlated with non-SVR, null response, and relapse. The majority of patients with SVR (84%) had HCV with IRRDR of ≥4. In contrast, nearly two-thirds (72%) of the patients with non-SVR had HCV with IRRDR ≤ 3 ($P = 0.0004$) (Table 3). Notably, 21 of the 26 patients infected with HCV with IRRDR[HCV-4]≥4 achieved SVR. Accordingly, the PPV and NPV of IRRDR[HCV-4]≥4 for SVR and non-SVR patients were 81% ($P = 0.002$) and 76% ($P = 0.02$), respectively (Table 5). Our present results thus strongly suggest that the degree of sequence heterogeneity within IRRDR[HCV-4] would be a useful marker for prediction of treatment outcome in HCV-4 infection.

The molecular mechanism underlying the possible involvement of this region in IFN responsiveness of the virus is still unknown. The significant difference among IRRDR sequence patterns may suggest genetic flexibility of this region. Indeed, the C-terminal portion of NS5A was shown to tolerate sequence insertions and deletions (29). This flexibility might play an important role in modulating the interaction with various host systems, including IFN-induced antiviral machineries. It is also possible that the genetic flexibility of IRRDR is accompanied by compensatory changes elsewhere in the viral genome and that these compensatory changes affect overall viral fitness and responses to IFN-based therapy (8, 29, 41). Also, it is worth noting that IRRDR is among the most variable sequences across the different genotypes and subtypes of HCV (25) whereas its upstream and downstream sequences show a higher degree of sequence conservation (15). This may suggest that whereas the upstream and downstream sequences have a conserved function(s) across all the HCV genotypes, IRRDR sequences have a genotype-dependent or even a strain-dependent function(s).

A mutation at position 70 of the core protein of HCV-1b has been reported to be correlated with PEG-IFN/RBV treatment outcome (4, 12). In the present study, however, we found no significant correlation between core protein polymorphism and treatment outcome in HCV-4 infection. The residue at position 70 of the core protein of all but two HCV-4 isolates analyzed in this study was Arg (Fig. 4), which is known to be associated with SVR in HCV-1b infection (4, 12). This high degree of sequence conservation at position 70 might be the reason for the lack of significant correlation between core protein polymorphism and treatment outcome in HCV-4 infection.

Single nucleotide polymorphisms (SNPs) near the IL28B region have been identified as the strongest baseline predictors of SVR to PEG-IFN/RBV in patients with HCV-1 infection. More recently, in two major studies that were carried out exclusively with HCV-4-infected patients (9, 11), the CC genotype of rs12979860 IL28B SNP was also strongly associated with SVR. It is worth noting that although the SVR rate was more than 80% among the patients with the CC genotype, these patients represented only around 40% of total SVR cases in both studies. Furthermore, the CC genotype was found in only 34% of all Egyptian patients analyzed (9). Taken together, those observations support the idea that in addition to IL28B polymorphism, there should be an additional factor(s) that influences SVR. In this context, an interplay between IRRDR and IL28B polymorphisms might explain why some patients with undesirable IL28B genotype achieve SVR and why some patients infected with HCV isolates with IRRDR[HCV-4]≥4 do not achieve SVR. Further comprehensive study is needed to validate the importance of IRRDR and IL28B polymorphisms in predicting the treatment outcome of HCV-4-infected patients.

In conclusion, the present study emphasizes the importance of IRRDR sequence heterogeneity in the prediction of PEG-IFN/RBV treatment outcome for different HCV genotype infections in

TABLE 3 Correlation between NS5A sequence heterogeneity and virological responses in HCV-4 infection

Factor	No. of isolates/total no. (%)				*P* value for SVR versus:		
	SVR	Non-SVR	Null response	Relapse	Non-SVR	Null response	Relapse
IRRDR ≥ 4	21/25 (84)[a]	5/18 (28)	4/13 (31)	1/5 (20)	0.0004	0.003	0.01
IRRDR ≤ 3	4/25 (16)	13/18 (72)[b]	9/13 (69)	4/5 (80)			
IRRDR ≥ 5	16/25 (64)[a]	2/18 (11)	1/13 (8)	1/5 (20)	0.0006	0.002	0.14
IRRDR ≤ 4	9/25 (36)	16/18 (89)[b]	12/13 (92)	4/5 (80)			
IRRDR ≥ 3	22/25 (88)[a]	11/18 (61)	10/13 (77)	1/5 (20)	0.066	0.39	0.006
IRRDR ≤ 2	3/25 (12)	7/18 (39)[b]	3/13 (23)	4/5 (80)			

[a] Sensitivity (proportion of SVR patients with the favorable factor).
[b] Specificity (proportion of non-SVR patients with the unfavorable factor).

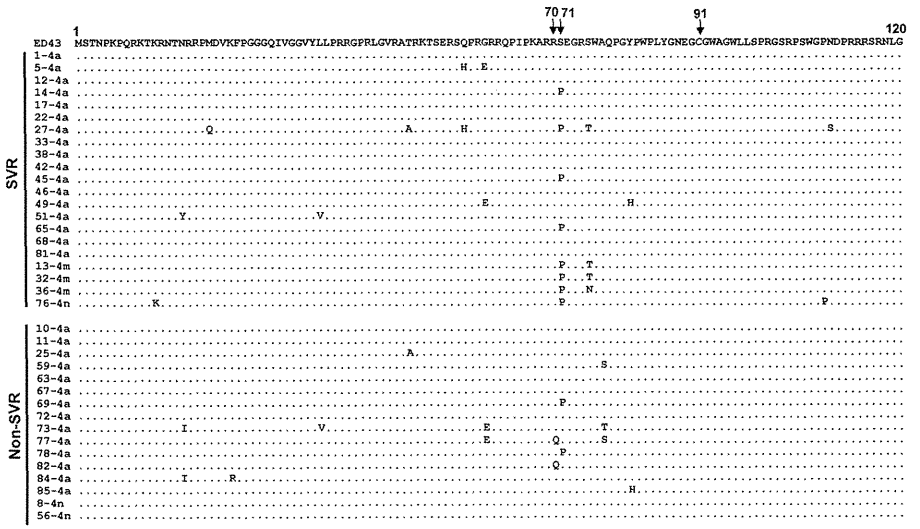

FIG 4 Sequence alignment of the core protein of HCV-4 isolates. Core protein sequences (aa 1 to 120) of HCV-4 obtained from SVR and non-SVR patients are aligned. The prototype sequence of ED43 (10) is shown on the top. The numbers along the sequence indicate the amino acid positions. Dots indicate residues identical to those of the prototype sequence.

TABLE 4 Univariate and multivariate analyses for identification of independent predictive factors for SVR in HCV-4-infected patients treated with PEG-IFN/RBV therapy

Univariate analysis		Multivariate analysis	
Variable	*P* value	Odds ratio (95% CI)	*P* value
IRRDR mutations (IRRDR ≥ 4 versus IRRDR ≤ 3)	0.0004	10.5 (1.12–98.91)	0.04
Age (<42 years)	0.03		
HCV-RNA (<5,200 IU/ml)	0.08		

TABLE 5 PPV, NPV, sensitivity, and specificity of IRRDR sequence heterogeneity on the likelihood of achieving SVR and non-SVR in HCV-4 infection

Factor	PPV	NPV	Sensitivity[c]	Specificity[d]
IRRDR ≥ 4	81% (21/26)[a]		84% (21/25)	
IRRDR ≤ 3		76% (13/17)[b]		72% (13/18)

[a] $P = 0.002$.
[b] $P = 0.02$.
[c] Proportion of SVR patients who were infected with HCV isolates with IRRDR of ≥4.
[d] Proportion of non-SVR patients who were infected with HCV isolates with IRRDR of ≤3.

Downloaded from http://jcm.asm.org/ on December 3, 2012 by KOBE UNIVERSITY

different ethnic groups, including Egyptian patients infected with HCV-4.

ACKNOWLEDGMENTS

This study was supported in part by Health and Labor Sciences Research Grants from the Ministry of Health, Labor and Welfare, Japan, and a SATREPS Grant from Japan Science and Technology Agency (JST) and Japan International Cooperation Agency (JICA).

This study was also carried out as part of Japan Initiative for Global Research Network on Infectious Diseases (J-GRID), Ministry of Education, Culture, Sports, Science and Technology, Japan, and the Global Center of Excellence (G-COE) Program at Kobe University Graduate School of Medicine.

No conflicts of interest exist.

REFERENCES

1. Abdel-Aziz F, et al. 2000. Hepatitis C virus (HCV) infection in a community in the Nile Delta: population description and HCV prevalence. Hepatology 32:111–115.
2. Abdel-Hamid M, et al. 2007. Genetic diversity in hepatitis C virus in Egypt and possible association with hepatocellular carcinoma. J. Gen. Virol. 88:1526–1531.
3. Akuta N, et al. 2009. Association of amino acid substitution pattern in core protein of hepatitis C virus genotype 2a high viral load and virological response to interferon-ribavirin combination therapy. Intervirology 52: 301–309.
4. Akuta N, et al. 2007. Predictive factors of early and sustained responses to peginterferon plus ribavirin combination therapy in Japanese patients infected with hepatitis C virus genotype 1b: amino acid substitutions in the core region and low-density lipoprotein cholesterol levels. J. Hepatol. 46: 403–410.
5. Akuta N, et al. 2007. Prediction of response to pegylated interferon and ribavirin in hepatitis C by polymorphisms in the viral core protein and very early dynamics of viremia. Intervirology 50:361–368.
6. Akuta N, et al. 2005. Association of amino acid substitution pattern in core protein of hepatitis C virus genotype 1b high viral load and non-virological response to interferon-ribavirin combination therapy. Intervirology 48:372–380.
7. Amoroso P, et al. 1998. Correlation between virus genotype and chronicity rate in acute hepatitis C. J. Hepatol. 28:939–944.
8. Appel N, Pietschmann T, Bartenschlager R. 2005. Mutational analysis of hepatitis C virus nonstructural protein 5A: potential role of differential phosphorylation in RNA replication and identification of a genetically flexible domain. J. Virol. 79:3187–3194.
9. Asselah T, et al. 2012. IL28B polymorphism is associated with treatment response in patients with genotype 4 chronic hepatitis C. J. Hepatol. 56: 527–532.
10. Chamberlain RW, Adams N, Saeed AA, Simmonds P, Elliott RM. 1997. Complete nucleotide sequence of a type 4 hepatitis C virus variant, the predominant genotype in the Middle East. J. Gen. Virol. 78(Pt 6):1341–1347.
11. De Nicola S, et al. 2012. Interleukin 28B polymorphism predicts pegylated interferon plus ribavirin treatment outcome in chronic hepatitis C genotype 4. Hepatology 55:336–342.
12. El-Shamy A, et al. 2012. Polymorphisms of hepatitis C virus nonstructural protein 5A and core protein and clinical outcome of pegylated-interferon/ribavirin combination therapy. Intervirology 55:1–11.
13. El-Shamy A, et al. 2008. Sequence variation in hepatitis C virus nonstructural protein 5A predicts clinical outcome of pegylated interferon/ribavirin combination therapy. Hepatology 48:38–47.
14. El-Shamy A, et al. 2007. Prediction of efficient virological response to pegylated interferon/ribavirin combination therapy by NS5A sequences of hepatitis C virus and anti-NS5A antibodies in pre-treatment sera. Microbiol. Immunol. 51:471–482.
15. El-Shamy A, et al. 2012. Sequence heterogeneity in NS5A of hepatitis C virus genotypes 2a and 2b and clinical outcome of pegylated-interferon/ribavirin therapy. PLoS One 7:e30513. doi:10.1371/journal.pone.0030513.
16. El-Shamy A, et al. 2011. Sequence heterogeneity of NS5A and core proteins of hepatitis C virus and virological responses to pegylated-interferon/ribavirin combination therapy. Microbiol. Immunol. 55:418–426.
17. el-Zayadi AR, et al. 2005. Hepatocellular carcinoma in Egypt: a single center study over a decade. World J. Gastroenterol. 11:5193–5198.
18. Enomoto N, et al. 1996. Mutations in the nonstructural protein 5A gene and response to interferon in patients with chronic hepatitis C virus 1b infection. N. Engl. J. Med. 334:77–81.
19. Fried MW, et al. 2002. Peginterferon alfa-2a plus ribavirin for chronic hepatitis C virus infection. N. Engl. J. Med. 347:975–982.
20. Ge D, et al. 2009. Genetic variation in IL28B predicts hepatitis C treatment-induced viral clearance. Nature 461:399–401.
21. Hassan MM, et al. 2001. The role of hepatitis C in hepatocellular carcinoma: a case control study among Egyptian patients. J. Clin. Gastroenterol. 33:123–126.
22. Kau A, Vermehren J, Sarrazin C. 2008. Treatment predictors of a sustained virologic response in hepatitis B and C. J. Hepatol. 49:634–651.
23. Khattab MA, et al. 2011. Management of hepatitis C virus genotype 4: recommendations of an international expert panel. J. Hepatol. 54:1250–1262.
24. Limaye AR, Draganov PV, Cabrera R. 2011. Boceprevir for chronic HCV genotype 1 infection. N. Engl. J. Med. 365:176, 177–178.
25. Macdonald A, Harris M. 2004. Hepatitis C virus NS5A: tales of a promiscuous protein. J. Gen. Virol. 85:2485–2502.
26. Maekawa S, Enomoto N. 2009. Viral factors influencing the response to the combination therapy of peginterferon plus ribavirin in chronic hepatitis C. J. Gastroenterol. 44:1009–1015.
27. Mattsson L, Sonnerborg A, Weiland O. 1993. Outcome of acute symptomatic non-A, non-B hepatitis: a 13-year follow-up study of hepatitis C virus markers. Liver 13:274–278.
28. Micallef JM, Kaldor JM, Dore GJ. 2006. Spontaneous viral clearance following acute hepatitis C infection: a systematic review of longitudinal studies. J. Viral Hepat. 13:34–41.
29. Moradpour D, et al. 2004. Insertion of green fluorescent protein into nonstructural protein 5A allows direct visualization of functional hepatitis C virus replication complexes. J. Virol. 78:7400–7409.
30. Murakami T, et al. 1999. Mutations in nonstructural protein 5A gene and response to interferon in hepatitis C virus genotype 2 infection. Hepatology 30:1045–1053.
31. Okamoto H, et al. 1992. Typing hepatitis C virus by polymerase chain reaction with type-specific primers: application to clinical surveys and tracing infectious sources. J. Gen. Virol. 73(Pt 3):673–679.
32. Ray SC, Arthur RR, Carella A, Bukh J, Thomas DL. 2000. Genetic epidemiology of hepatitis C virus throughout Egypt. J. Infect. Dis. 182: 698–707.
33. Sarasin-Filipowicz M. 2010. Interferon therapy of hepatitis C: molecular insights into success and failure. Swiss Med. Wkly. 140:3–11.
34. Sherman KE, et al. 2011. Response-guided telaprevir combination treatment for hepatitis C virus infection. N. Engl. J. Med. 365:1014–1024.
35. Simmonds P, et al. 2005. Consensus proposals for a unified system of nomenclature of hepatitis C virus genotypes. Hepatology 42:962–973.
36. Simmonds P, et al. 1993. Classification of hepatitis C virus into six major genotypes and a series of subtypes by phylogenetic analysis of the NS-5 region. J. Gen. Virol. 74(Pt 11):2391–2399.
37. Suppiah V, et al. 2009. IL28B is associated with response to chronic hepatitis C interferon-alpha and ribavirin therapy. Nat. Genet. 41:1100–1104.
38. Tanaka E, Kiyosawa K. 2000. Natural history of acute hepatitis C. J. Gastroenterol. Hepatol. 15(Suppl):E97–E104.
39. Tanaka Y, et al. 2009. Genome-wide association of IL28B with response to pegylated interferon-alpha and ribavirin therapy for chronic hepatitis C. Nat. Genet. 41:1105–1109.
40. Timm J, et al. 2007. Characterization of full-length hepatitis C virus genotype 4 sequences. J. Viral Hepat. 14:330–337.
41. Yuan HJ, Jain M, Snow KK, Gale M, Jr, Lee WM. 2010. Evolution of hepatitis C virus NS5A region in breakthrough patients during pegylated interferon and ribavirin therapy. J. Viral Hepat. 17:208–216.

JCM Journals.ASM.org

NS5A Sequence Heterogeneity of Hepatitis C Virus Genotype 4a Predicts Clinical Outcome of Pegylated-Interferon–Ribavirin Therapy in Egyptian Patients

Ahmed El-Shamy,[a,b]* Ikuo Shoji,[a] Wafaa El-Akel,[c] Shymaa E. Bilasy,[d] Lin Deng,[a] Maissa El-Raziky,[c] Da-peng Jiang,[a] Gamal Esmat,[c] and Hak Hotta[a]

Division of Microbiology, Center for Infectious Diseases, Kobe University Graduate School of Medicine, Kobe, Japan[a]; Department of Virology, Suez Canal University Faculty of Veterinary Medicine, Ismalia, Egypt[b]; Department of Tropical Medicine, Cairo University, Cairo, Egypt[c]; and Department of Biochemistry, Suez Canal University Faculty of Pharmacy, Ismalia, Egypt[d]

Hepatitis C virus genotype 4 (HCV-4) is the cause of approximately 20% of the 180 million cases of chronic hepatitis C in the world. HCV-4 infection is common in the Middle East and Africa, with an extraordinarily high prevalence in Egypt. Viral genetic polymorphisms, especially within core and NS5A regions, have been implicated in influencing the response to pegylated-interferon and ribavirin (PEG-IFN/RBV) combination therapy in HCV-1 infection. However, this has not been confirmed in HCV-4 infection. Here, we investigated the impact of heterogeneity of NS5A and core proteins of HCV-4, mostly subtype HCV-4a, on the clinical outcomes of 43 Egyptian patients treated with PEG-IFN/RBV. Sliding window analysis over the carboxy terminus of NS5A protein identified the IFN/RBV resistance-determining region (IRRDR) as the most prominent region associated with sustained virological response (SVR). Indeed, 21 (84%) of 25 patients with SVR, but only 5 (28%) of 18 patients with non-SVR, were infected with HCV having IRRDR with 4 or more mutations (IRRDR ≥ 4) ($P = 0.0004$). Multivariate analysis identified IRRDR ≥ 4 as an independent SVR predictor. The positive predictive value of IRRDR ≥ 4 for SVR was 81% (21/26; $P = 0.002$), while its negative predictive value for non-SVR was 76% (13/17; $P = 0.02$). On the other hand, there was no significant correlation between core protein polymorphisms, either at residue 70 or at residue 91, and treatment outcome. In conclusion, the present results demonstrate for the first time that IRRDR ≥ 4, a viral genetic heterogeneity, would be a useful predictive marker for SVR in HCV-4 infection when treated with PEG-IFN/RBV.

Hepatitis C virus (HCV) is a major cause of chronic liver disease, hepatocellular carcinoma, and deaths from liver disease and is the most common indication for liver transplantation (7, 26–28, 38). HCV has been classified into seven major genotypes and a series of subtypes (35, 36). In general, HCV genotype 4 (HCV-4) is common in the Middle East and Africa, where it is responsible for more than 80% of HCV infections (23). Although HCV-4 is the cause of approximately 20% of the 180 million cases of chronic hepatitis C in the world, it has not been a major subject of research.

Egypt has the highest prevalence of HCV worldwide (15%) and the highest prevalence of HCV-4, which is responsible for 90% of the total HCV infections, with a predominance of the subtype 4a (HCV-4a) (1, 32). This extraordinarily high prevalence results in an increasing incidence of hepatocellular carcinoma in Egypt, which is now the second most frequent cause of cancer and cancer mortality among men (17, 21). More than 2 decades have passed since the discovery of HCV, and yet therapeutic options remain limited. Up to 2011, the standard treatment for chronic hepatitis C consisted of pegylated alpha interferon (PEG-IFN) and ribavirin (RBV) (19); however, by May 2011 two protease inhibitors (telaprevir and boceprevir) were approved by the Food and Drug Administration (FDA) for use in combination with PEG-IFN/RBV for adult chronic hepatitis C patients with HCV genotype 1 (24, 34). Since the approval of these new protease inhibitors for treatment of HCV-1 infection, the response of HCV-4 to the standard regimen of treatment (PEG-IFN/RBV) has lagged behind other genotypes and HCV-4 has become the most resistant genotype to treat. As PEG-IFN/RBV still remains to be used to treat HCV-4-infected patients, exploring the factors that predict the outcome of PEG-IFN/RBV treatment, such as sustained virological response (SVR), for HCV-4 infections is needed to assess more accurately the likelihood of SVR and thus to make more informed treatment decisions.

While the SVR rate for PEG-IFN/RBV treatment hovers at 50 to 60% in HCV-1 and -4 infection, it is up to 80% in HCV-2 and -3 infections (19, 33). This difference in responses among patients infected with different HCV genotypes suggests that viral genetic heterogeneity could affect, at least to some extent, the sensitivity to IFN-based therapy. In this context, the correlation between IFN-based therapy outcome and sequence polymorphisms within the viral core and NS5A proteins has been widely discussed, in particular in regard to Japanese patients with HCV-1b infection. Initially, in the era of IFN monotherapy, it was proposed that sequence variations within a region in NS5A of HCV-1b, called the IFN sensitivity-determining region (ISDR), were correlated with IFN responsiveness (18). Subsequently, in the era of PEG-IFN/

Received 8 August 2012 Returned for modification 30 August 2012
Accepted 14 September 2012
Published ahead of print 19 September 2012
Address correspondence to Hak Hotta, hotta@kobe-u.ac.jp.
* Present address: Ahmed El-Shamy, Division of Liver Diseases, Mount Sinai School of Medicine, New York, New York, USA.

doi:10.1128/JCM.02109-12

RBV combination therapy, we identified a new region near the C terminus of NS5A, referred to as the IFN/RBV resistance-determining region (IRRDR) (13). Recently, we also demonstrated the correlation between IRRDR polymorphism and PEG-IFN/RBV treatment outcome in HCV-2a and -2b infections (15). In addition, HCV core protein polymorphism, in particular at positions 70 and 91, was also proposed as a pretreatment predictor of poor virological response in patients infected with HCV-1b (4–6). To the best of our knowledge, there is no information regarding the correlation between sequence heterogeneity in the NS5A and core proteins of HCV-4 and PEG-IFN/RBV treatment outcome. In the present study, we aimed to investigate this issue in Egyptian patients infected with HCV-4.

MATERIALS AND METHODS

Ethics statement. The study protocol, which conforms to the provisions of the Declaration of Helsinki, was approved beforehand by the Ethic Committees in Cairo University Hospital and in Kobe University, and written informed consent was obtained from each patient prior to the treatment.

Patients. A total of 43 previously untreated patients who were chronically infected with HCV-4a (34 patients), HCV-4m (3 patients), HCV-4n (3 patients), or HCV-4o (3 patients) were consecutively evaluated for antiviral treatment at Cairo University Hospital, Cairo, Egypt, between January 2008 and September 2010. The HCV subtype was determined according to the method of Okamoto et al. (31). The patients were treated with PEG-IFN α-2a (180 μg/week, subcutaneously) and RBV (1,000 to 1,200 mg daily, *per os*) for 48 weeks. The quantification of serum HCV RNA titers was performed as previously reported (14). To minimize the therapeutic burdens, including the high cost and possible side effects, therapy was discontinued if HCV RNA titers at week 12 did not drop by 2 log compared with baseline values or if HCV RNA was still detectable at week 24. These were considered a null response (see Results).

Sequence analysis of the NS5A and core regions of the HCV genome. Blood samples were collected using Vacutainer tubes. The sera were separated within 2 h of blood collection, transferred to sterile cryovials, and kept frozen at −80°C until use. HCV RNA was extracted from 140 μl of serum using a commercially available kit (QIAmp viral RNA kit; Qiagen, Tokyo, Japan). The extracted RNA was reverse transcribed and amplified for the HCV genome encoding a carboxy terminus of NS5A (amino acids [aa] 2193 to 2417) and the core protein (aa 1 to 191) using SuperScript III one-step RT-PCR Platinum *Taq* HiFi (Invitrogen, Tokyo, Japan). The resultant reverse transcription (RT)-PCR product was subjected to a second-round PCR by using Platinum *Taq* DNA polymerase high fidelity III (Invitrogen). Primers used for amplification of the 3′ half of the NS5A region of HCV-4 were as follows: NS5A-4/F1 (5′-CTCAAYTCGTTCGT RGTGGGATC-3′; sense) and NS5A-4/R1 (5′-CGAAGGTCACCTTCTT CTGCCG-3′; antisense) for one-step RT-PCR; and NS5A-4/F2 (5′-ATG CGAGCCYGAGCCGGACGT-3′; sense) and NS5A-4/R2 (5′-GCTCAGG GGGYTRATTGGCAGCT-3′; antisense) for the second-round PCR. Primers for amplification of the core region of HCV-4 were 249-F (5′-G CTAGCCGAGTAGTGTTG-3′; sense) and 984-R (5′-GATGTGRTGRTC GGCCTC-3′; antisense) (40) for one-step RT-PCR; and 319-F (5′-GGA GGTCTCGTAGACCGTGC-3′; sense) (40) and primer-186 (5′-ATGTA CCCCATGAGGTCGGC-3′; antisense) (2) for the second-round PCR. RT was performed at 45°C for 30 min and terminated at 94°C for 2 min, followed by the first-round PCR over 35 cycles, with each cycle consisting of denaturation at 94°C for 30 s, annealing at 50°C for 30 s, and extension at 68°C for 90 s. The second-round PCR was performed under the same conditions. The sequences of the amplified fragments were determined by direct sequencing without subcloning. The amino acid sequences were deduced and aligned using Genetyx Win software version 7.0 (Genetyx Corp., Tokyo, Japan). The numbering of amino acid residues for HCV-4 isolates is according to the polyprotein of ED43 isolate (accession no. Y11604) (10). Consensus sequences of the carboxy terminus of NS5A of a given HCV-4 subtype were inferred by alignment of all sequences obtained in this study as well as all available NS5A sequences of HCV-4a (accession no. Y11604, DQ418782 to DQ418789, DQ516084, and DQ988073 to DQ988079), HCV-4m (FJ462433), HCV-4n (FJ462441), and HCV-4o (FJ462440) from the databases.

TABLE 1 Virological responses of HCV-4-infected patients treated with PEG-IFN/RBV

Virological response	Proportion (%) of patients with indicated response (no. of patients/total no.)				
	HCV-4[a]	HCV-4a	HCV-4 m	HCV-4n	HCV-4o
SVR	58 (25/43)	56 (19/34)	100 (3/3)	33 (1/3)	67 (2/3)
Non-SVR	42 (18/43)	44 (15/34)	0 (0/3)	67 (2/3)	33 (1/3)
Null response	30 (13/43)	32 (11/34)	0 (0/3)	67 (2/3)	0 (0/3)
Relapse	12 (5/43)	12 (4/34)	0 (0/3)	0 (0/3)	33 (1/3)

[a] Includes all 43 cases with HCV-4 infection (34 cases with HCV-4a and 3 cases each with HCV-4m, -4n, and -4o).

Statistical analysis. Numerical data were analyzed by Student's *t* test and categorical data by Fisher's exact probability test. To evaluate the optimal threshold of the number of amino acid mutations in IRRDR for prediction of treatment outcomes, the receiver operating characteristic (ROC) curve was constructed. Univariate and multivariate logistic regression analyses were performed to identify independent predictors for treatment outcomes. All statistical analyses were performed using the SPSS version 16 software (SPSS Inc., Chicago, IL). Unless otherwise stated, a P value of <0.05 was considered statistically significant.

Nucleotide sequence accession numbers. The sequence data reported in this paper have been deposited in the DDBJ/EMBL/GenBank nucleotide sequence databases with the accession numbers AB725987 through AB726066.

RESULTS

Patients' responses to PEG-IFN/RBV combination therapy. Among 43 patients enrolled in this study, 30 (70%) patients completed the entire course of PEG-IFN/RBV treatment for 48 weeks and follow-up for 24 weeks. On the other hand, the treatment was discontinued for 13 (30%) patients due to poor virological responses at 12 or 24 weeks after initiation of the therapy. Overall, 25 (58%) patients achieved SVR while 18 (42%) patients had non-SVR (Table 1). When analyzed on the basis of the subtype classification, SVR was achieved by 56% (19/34), 100% (3/3), 33% (1/3), and 67% (2/3) of patients infected with HCV-4a, -4m, -4n, and -4o, respectively.

Non-SVR patients are classified into two groups: (i) patients with null response, who did not achieve >2-log reduction of the initial viral load at week 12 or who had detectable viremia at week 24 of the treatment period; and (ii) patients with relapse, who were negative for HCV-RNA at the end of the treatment period (week 48) followed by a rebound viremia at a certain time point during the follow-up period of 24 weeks. Patients with null response represented 30% (13/43) of all the HCV-4-infected subjects analyzed, while those with relapse represented 12% (5/43). A similar tendency was observed for subtype HCV-4a.

Among various patients' demographic characteristics, SVR patients had a significantly lower average age than that of non-SVR patients (Table 2). Furthermore, a tendency for SVR patients to have a lower average titer of initial viral load than that of non-SVR was noted, although the difference was not statistically significant, due possibly to the small number of patients analyzed ($P = 0.07$).

TABLE 2 Demographic characteristics of HCV-4-infected patients with SVR and non-SVR[a]

Factor	SVR	Non-SVR	*P* value
Age	38.47 ± 9.51	45.80 ± 5.65	0.014
Sex (male/female)	18/7	15/3	0.48
BMI	27.36 ± 3.65	27.67 ± 5.28	0.85
Platelets ($\times 10^3/\mu l$)	204.4 ± 40.63	216.7 ± 87.25	0.59
Hemoglobin (g/dl)	14.54 ± 1.38	15.08 ± 1.39	0.25
WBC count	7,041 ± 1,876	7,078 ± 2,977	0.96
Albumin (g/dl)	4.12 ± 0.36	4.328 ± 0.41	0.11
ALT (IU/liter)	78.72 ± 59.68	82.39 ± 41.80	0.83
AST (IU/liter)	64.94 ± 27.63	58.17 ± 23.98	0.44
HCV-RNA (IU/ml)	84,290 ± 186,300	501,800 ± 816,700	0.07

[a] Values are means ± standard deviations. SVR, sustained virological response; BMI, body mass index; WBC, white blood cell; ALT, alanine aminotransferase; AST, aspartate aminotransferase.

Correlation between NS5A sequence heterogeneity and SVR in HCV-4 infection. We and other researchers reported significant correlation between sequence polymorphisms within the C-terminal half of NS5A, including that in ISDR and IRRDR, and PEG-IFN/RBV treatment outcome in HCV-1 and HCV-2 infections (13, 15, 18, 30). However, this information is quite limited in HCV-4 infection. To clarify this issue, part of the HCV-4 genome encoding a carboxy terminus (aa 2193 to 2417) of NS5A in pretreatment sera was amplified and sequenced, and amino acid sequences were deduced. The sequences obtained as well as all available NS5A sequences of HCV-4a, -4m, -4n, and -4o from the databases were aligned, and the consensus sequences for a desired HCV-4 subtype were inferred (see Materials and Methods). Next, to identify an NS5A region(s) that would be significantly correlated with treatment outcome, we carried out a sliding window analysis with a window size of 30 residues over the C-terminal half (aa 2193 to 2417) of NS5A sequences obtained from all SVR ($n = 25$) and non-SVR ($n = 18$) patients along with corresponding consensus sequences of each HCV-4 subtype as described previously (30). This analysis revealed that the difference in the overall number of amino acid mutations between SVR and non-SVR isolates exceeded the significant threshold only in a region corresponding to IRRDR of HCV-1b (13), ranging from aa 2331 to 2383, thus being referred to as IRRDR[HCV-4] (Fig. 1). Indeed, the average number of amino acid mutations in IRRDR[HCV-4] was significantly larger in SVR than in non-SVR ($P = 0.0005$) isolates (Fig. 2A). Sequences of IRRDR of HCV-4a, -4m, -4n, and -4o obtained from SVR and non-SVR patients along with the number of IRRDR mutations of each isolate are shown in Fig. 2B.

Next, we performed ROC curve analysis to estimate the optimal cutoff number of IRRDR[HCV-4] mutations for SVR prediction. This analysis estimated 4 mutations as the optimal number of IRRDR[HCV-4] mutations to predict SVR, since it achieved the highest sensitivity (84%; sensitivity refers to the proportion of SVR patients who were infected with HCV isolates of IRRDR[HCV-4] with 4 or more mutations) and specificity (72%; specificity refers to the proportion of non-SVR patients who were infected with HCV isolates of IRRDR[HCV-4] with 3 or fewer mutations) with an area under the curve (AUC) of 0.82 (Fig. 3). Accordingly, 21 (84%) of 25 patients with SVR, in contrast to only 5 (28%) of 18 patients with non-SVR, had IRRDR[HCV-4] with 4 or more mutations (referred to as IRRDR[HCV-4]≥4), with the difference between the two groups being statistically significant ($P = 0.0004$) (Table 3). It should be noted that 4 (31%) of 13 patients with null response and only 1 (20%) of 5 patients with relapse had HCV with IRRDR[HCV-4]≥4. These results collectively suggest that IRRDR[HCV-4]≥4 is significantly associated with SVR. In this connection, we also tested the impact of a higher (≥5) and a lower (≥3) degree of IRRDR mutations on treatment outcome. IRRDR[HCV-4]≥5 was significantly associated with SVR, though with a relatively lower sensitivity (64%) than that of IRRDR[HCV-4]≥4 (Table 3). On the other hand, there was no significant correlation between IRRDR[HCV-4]≥3 and SVR.

Correlation between core protein sequence heterogeneity and SVR in HCV-4 infection. A close correlation between core protein sequence patterns at positions 70 and 91 and treatment outcome has been proposed, especially in Japanese patients with HCV-1b infection (4–6). To examine this hypothesis in Egyptian patients infected with HCV-4, core sequences of the viral genome were amplified from the pretreated sera, and the amino acid sequences were deduced. Due to a high degree of sequence homology among core sequences of various HCV-4 subtypes, all sequences obtained were aligned with the prototype sequence, ED43 (10). The residues at positions 70 and 91 were both well conserved among the sequences analyzed, and therefore, no correlation with treatment outcome was observed for these residues (Fig. 4). All but two isolates had arginine at position 70 (Arg^{70}), the residue that has been associated with an IFN-sensitive phenotype as far as the core protein of HCV-1b is concerned (4–6). On the other hand, Pro at position 71 showed a tendency to be more frequent in SVR than in non-SVR patients; however, the frequency was not statistically different between the two groups.

Identification of independent predictive factors for SVR in HCV-4 infection. In order to identify significant independent

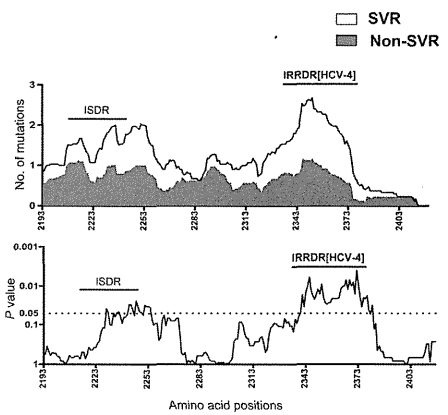

FIG 1 Sliding window analysis over the carboxy terminus (aa 2193 to 2417) of NS5A of HCV-4 obtained from SVR and non-SVR patients.

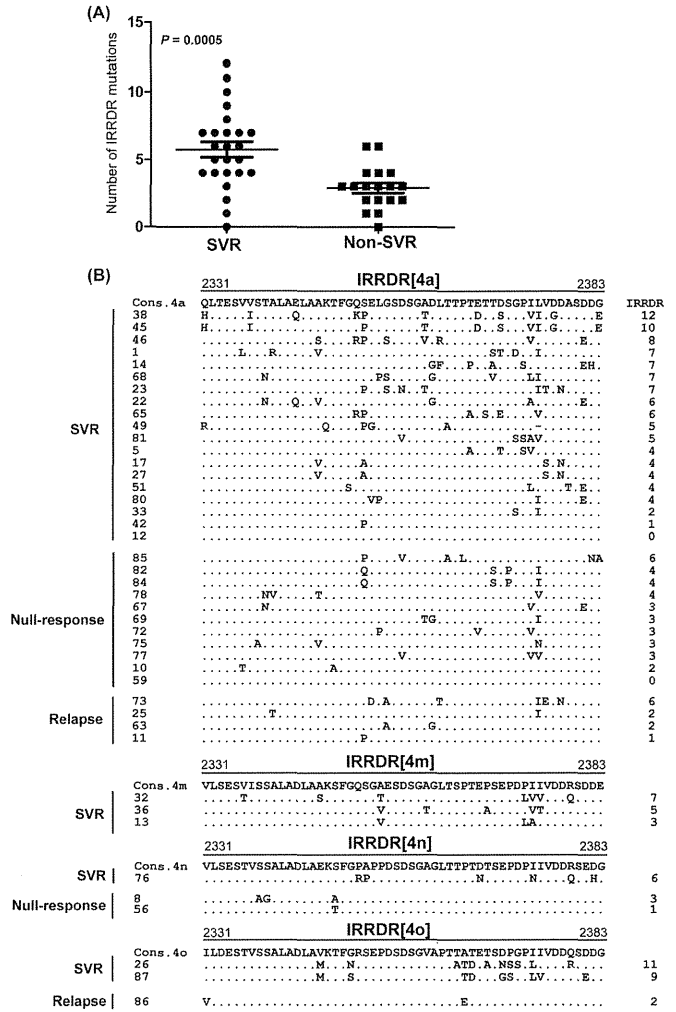

FIG 2 Correlation between *IRRDR*[HCV-4] sequence variations and treatment outcome. (A) Average number of amino acid mutations in *IRRDR*[HCV-4] obtained from SVR and non-SVR patients. (B) Alignment of IRRDR[HCV-4] sequences obtained from SVR and non-SVR patients with HCV-4a, -4m, -4n, and -4o. The consensus sequence (Cons) of each subtype is shown on the top. The numbers along the sequence indicate the amino acid positions. Dots indicate residues identical to those of the Cons sequence. The numbers of the mutations in each IRRDR (4a, 4m, 4n, or 4o) are shown on the right.

predictive factors of SVR for PEG-IFN/RBV treatment outcome in HCV-4 infection, first, all available data of baseline patients' parameters and IRRDR[HCV-4] polymorphism were entered in a univariate logistic analysis. This analysis yielded 3 factors that were correlated or nearly correlated with SVR: IRRDR[HCV-4]≥4 ($P = 0.0004$), patient's age (<42 years; $P = 0.03$), and HCV RNA titer (<5,200 IU/ml; $P = 0.08$). Subsequently, these 3 factors were entered in multivariate logistic regression analysis. This analysis revealed that the IRRDR[HCV-4]≥4 was the only independent predictive factor for SVR in HCV-4 infection (Table 4). We then assessed SVR predictability by means of IRRDR[HCV-4]≥4. As shown in Table 5, IRRDR[HCV-4]≥4 would predict SVR with a positive predictive value (PPV) of 81% ($P = 0.002$) and sensitivity of 84%. On the other hand, IRRDR[HCV-4]≤3 would predict non-SVR with a negative predictive value (NPV) of 76% ($P = 0.02$) and specificity of 72%. Thus, the degree of sequence variation in IRRDR[HCV-4] would yield useful positive and negative predictive markers for PEG-IFN/RBV therapy outcome in HCV-4-infected patients.

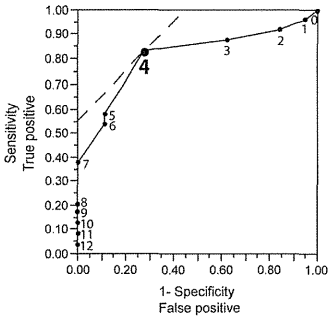

FIG 3 ROC curve analysis of IRRDR[HCV-4] sequence heterogeneity for SVR prediction. The solid line curve shows the AUC. Solid circles with numerals plotted on the curve represent different numbers of IRRDR mutations analyzed. The dashed line in the upper left corner indicates the optimal number of IRRDR[HCV-4] mutations for SVR prediction, which yields the highest sensitivity (84%) and the highest specificity (72%).

DISCUSSION

Both host and viral genetic factors have been implicated in influencing the clinical response to PEG-IFN/RBV therapy for HCV infection (22). It has recently been reported that host genetic polymorphisms near or within the IL28B gene on chromosome 19 show a critical impact on the treatment outcome of patients infected with HCV-1 (20, 37, 39). As for the viral factor(s), polymorphisms of NS5A and core regions of a given HCV genotype have been linked to a difference in SVR rates (3, 4, 13, 18, 30). This hypothesis was mostly inferred from studies carried out with Asian populations, in particular Japanese, with HCV-1b infection. However, whether it can be applied to non-Asian populations infected with non-HCV-1 is still unknown. To the best of our knowledge, this is the first study that specifically examines the relationship between HCV genome heterogeneity, in particular in NS5A and core regions, and PEG-IFN/RBV treatment outcome in Egyptian patients infected with HCV-4. In analogy with our previous studies that identified IRRDR as a significant determinant for PEG-IFN/RBV treatment outcome in Japanese patients infected with HCV-1b, -2a, and -2b (12–16), we have demonstrated in the present study that sequence heterogeneity within IRRDR is closely associated with the ultimate treatment outcome in Egyptian patients infected with HCV-4. A high degree of sequence variation in IRRDR[HCV-4], i.e., more than 4 (IRRDR ≥ 4), significantly correlated with SVR, while a low degree of sequence variation in this region (IRRDR ≤ 3) correlated with non-SVR, null response, and relapse. The majority of patients with SVR (84%) had HCV with IRRDR of ≥4. In contrast, nearly two-thirds (72%) of the patients with non-SVR had HCV with IRRDR ≤ 3 ($P = 0.0004$) (Table 3). Notably, 21 of the 26 patients infected with HCV with IRRDR[HCV-4]≥4 achieved SVR. Accordingly, the PPV and NPV of IRRDR[HCV-4]≥4 for SVR and non-SVR patients were 81% ($P = 0.002$) and 76% ($P = 0.02$), respectively (Table 5). Our present results thus strongly suggest that the degree of sequence heterogeneity within IRRDR[HCV-4] would be a useful marker for prediction of treatment outcome in HCV-4 infection.

The molecular mechanism underlying the possible involvement of this region in IFN responsiveness of the virus is still unknown. The significant difference among IRRDR sequence patterns may suggest genetic flexibility of this region. Indeed, the C-terminal portion of NS5A was shown to tolerate sequence insertions and deletions (29). This flexibility might play an important role in modulating the interaction with various host systems, including IFN-induced antiviral machineries. It is also possible that the genetic flexibility of IRRDR is accompanied by compensatory changes elsewhere in the viral genome and that these compensatory changes affect overall viral fitness and responses to IFN-based therapy (8, 29, 41). Also, it is worth noting that IRRDR is among the most variable sequences across the different genotypes and subtypes of HCV (25) whereas its upstream and downstream sequences show a higher degree of sequence conservation (15). This may suggest that whereas the upstream and downstream sequences have a conserved function(s) across all the HCV genotypes, IRRDR sequences have a genotype-dependent or even a strain-dependent function(s).

A mutation at position 70 of the core protein of HCV-1b has been reported to be correlated with PEG-IFN/RBV treatment out-

TABLE 3 Correlation between NS5A sequence heterogeneity and virological responses in HCV-4 infection

Factor	No. of isolates/total no. (%)				*P* value for SVR versus:		
	SVR	Non-SVR	Null response	Relapse	Non-SVR	Null response	Relapse
IRRDR ≥ 4	21/25 (84)[a]	5/18 (28)	4/13 (31)	1/5 (20)	0.0004	0.003	0.01
IRRDR ≤ 3	4/25 (16)	13/18 (72)[b]	9/13 (69)	4/5 (80)			
IRRDR ≥ 5	16/25 (64)[a]	2/18 (11)	1/13 (8)	1/5 (20)	0.0006	0.002	0.14
IRRDR ≤ 4	9/25 (36)	16/18 (89)[b]	12/13 (92)	4/5 (80)			
IRRDR ≥ 3	22/25 (88)[a]	11/18 (61)	10/13 (77)	1/5 (20)	0.066	0.39	0.006
IRRDR ≤ 2	3/25 (12)	7/18 (39)[b]	3/13 (23)	4/5 (80)			

[a] Sensitivity (proportion of SVR patients with the favorable factor).
[b] Specificity (proportion of non-SVR patients with the unfavorable factor).

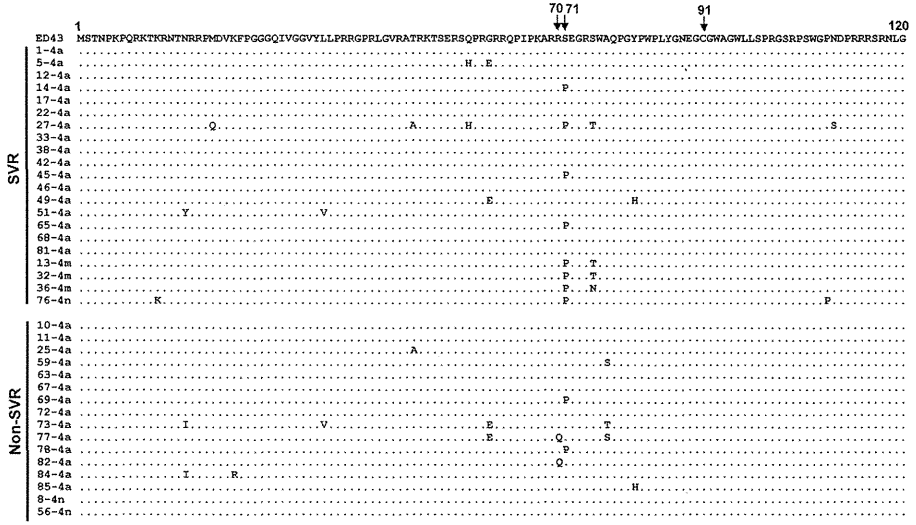

FIG 4 Sequence alignment of the core protein of HCV-4 isolates. Core protein sequences (aa 1 to 120) of HCV-4 obtained from SVR and non-SVR patients are aligned. The prototype sequence of ED43 (10) is shown on the top. The numbers along the sequence indicate the amino acid positions. Dots indicate residues identical to those of the prototype sequence.

come (4, 12). In the present study, however, we found no significant correlation between core protein polymorphism and treatment outcome in HCV-4 infection. The residue at position 70 of the core protein of all but two HCV-4 isolates analyzed in this study was Arg (Fig. 4), which is known to be associated with SVR in HCV-1b infection (4, 12). This high degree of sequence conservation at position 70 might be the reason for the lack of significant correlation between core protein polymorphism and treatment outcome in HCV-4 infection.

Single nucleotide polymorphisms (SNPs) near the IL28B region have been identified as the strongest baseline predictors of SVR to PEG-IFN/RBV in patients with HCV-1 infection. More recently, in two major studies that were carried out exclusively with HCV-4-infected patients (9, 11), the CC genotype of rs12979860 IL28B SNP was also strongly associated with SVR. It is worth noting that although the SVR rate was more than 80% among the patients with the CC genotype, these patients represented only around 40% of total SVR cases in both studies. Furthermore, the CC genotype was found in only 34% of all Egyptian patients analyzed (9). Taken together, those observations support the idea that in addition to IL28B polymorphism, there should be an additional factor(s) that influences SVR. In this context, an interplay between IRRDR and IL28B polymorphisms might explain why some patients with undesirable IL28B genotype achieve SVR and why some patients infected with HCV isolates with IRRDR[HCV-4]≥4 do not achieve SVR. Further comprehensive study is needed to validate the importance of IRRDR and IL28B polymorphisms in predicting the treatment outcome of HCV-4-infected patients.

In conclusion, the present study emphasizes the importance of IRRDR sequence heterogeneity in the prediction of PEG-IFN/RBV treatment outcome for different HCV genotype infections in

TABLE 4 Univariate and multivariate analyses for identification of independent predictive factors for SVR in HCV-4-infected patients treated with PEG-IFN/RBV therapy

Univariate analysis		Multivariate analysis	
Variable	*P* value	Odds ratio (95% CI)	*P* value
IRRDR mutations (IRRDR ≥ 4 versus IRRDR ≤ 3)	0.0004	10.5 (1.12–98.91)	0.04
Age (<42 years)	0.03		
HCV-RNA (<5,200 IU/ml)	0.08		

TABLE 5 PPV, NPV, sensitivity, and specificity of IRRDR sequence heterogeneity on the likelihood of achieving SVR and non-SVR in HCV-4 infection

Factor	PPV	NPV	Sensitivity[c]	Specificity[d]
IRRDR ≥ 4	81% (21/26)[a]		84% (21/25)	
IRRDR ≤ 3		76% (13/17)[b]		72% (13/18)

[a] $P = 0.002$.
[b] $P = 0.02$.
[c] Proportion of SVR patients who were infected with HCV isolates with IRRDR of ≥4.
[d] Proportion of non-SVR patients who were infected with HCV isolates with IRRDR of ≤3.

different ethnic groups, including Egyptian patients infected with HCV-4.

ACKNOWLEDGMENTS

This study was supported in part by Health and Labor Sciences Research Grants from the Ministry of Health, Labor and Welfare, Japan, and a SATREPS Grant from Japan Science and Technology Agency (JST) and Japan International Cooperation Agency (JICA).

This study was also carried out as part of Japan Initiative for Global Research Network on Infectious Diseases (J-GRID), Ministry of Education, Culture, Sports, Science and Technology, Japan, and the Global Center of Excellence (G-COE) Program at Kobe University Graduate School of Medicine.

No conflicts of interest exist.

REFERENCES

1. **Abdel-Aziz F, et al.** 2000. Hepatitis C virus (HCV) infection in a community in the Nile Delta: population description and HCV prevalence. Hepatology 32:111–115.
2. **Abdel-Hamid M, et al.** 2007. Genetic diversity in hepatitis C virus in Egypt and possible association with hepatocellular carcinoma. J. Gen. Virol. 88:1526–1531.
3. **Akuta N, et al.** 2009. Association of amino acid substitution pattern in core protein of hepatitis C virus genotype 2a high viral load and virological response to interferon-ribavirin combination therapy. Intervirology 52: 301–309.
4. **Akuta N, et al.** 2007. Predictive factors of early and sustained responses to peginterferon plus ribavirin combination therapy in Japanese patients infected with hepatitis C virus genotype 1b: amino acid substitutions in the core region and low-density lipoprotein cholesterol levels. J. Hepatol. 46: 403–410.
5. **Akuta N, et al.** 2007. Prediction of response to pegylated interferon and ribavirin in hepatitis C by polymorphisms in the viral core protein and very early dynamics of viremia. Intervirology 50:361–368.
6. **Akuta N, et al.** 2005. Association of amino acid substitution pattern in core protein of hepatitis C virus genotype 1b high viral load and non-virological response to interferon-ribavirin combination therapy. Intervirology 48:372–380.
7. **Amoroso P, et al.** 1998. Correlation between virus genotype and chronicity rate in acute hepatitis C. J. Hepatol. 28:939–944.
8. **Appel N, Pietschmann T, Bartenschlager R.** 2005. Mutational analysis of hepatitis C virus nonstructural protein 5A: potential role of differential phosphorylation in RNA replication and identification of a genetically flexible domain. J. Virol. 79:3187–3194.
9. **Asselah T, et al.** 2012. IL28B polymorphism is associated with treatment response in patients with genotype 4 chronic hepatitis C. J. Hepatol. 56: 527–532.
10. **Chamberlain RW, Adams N, Saeed AA, Simmonds P, Elliott RM.** 1997. Complete nucleotide sequence of a type 4 hepatitis C virus variant, the predominant genotype in the Middle East. J. Gen. Virol. 78(Pt 6):1341–1347.
11. **De Nicola S, et al.** 2012. Interleukin 28B polymorphism predicts pegylated interferon plus ribavirin treatment outcome in chronic hepatitis C genotype 4. Hepatology 55:336–342.
12. **El-Shamy A, et al.** 2012. Polymorphisms of hepatitis C virus nonstructural protein 5A and core protein and clinical outcome of pegylated-interferon/ribavirin combination therapy. Intervirology 55:1–11.
13. **El-Shamy A, et al.** 2008. Sequence variation in hepatitis C virus nonstructural protein 5A predicts clinical outcome of pegylated interferon/ribavirin combination therapy. Hepatology 48:38–47.
14. **El-Shamy A, et al.** 2007. Prediction of efficient virological response to pegylated interferon/ribavirin combination therapy by NS5A sequences of hepatitis C virus and anti-NS5A antibodies in pre-treatment sera. Microbiol. Immunol. 51:471–482.
15. **El-Shamy A, et al.** 2012. Sequence heterogeneity in NS5A of hepatitis C virus genotypes 2a and 2b and clinical outcome of pegylated-interferon/ribavirin therapy. PLoS One 7:e30513. doi:10.1371/journal.pone.0030513.
16. **El-Shamy A, et al.** 2011. Sequence heterogeneity of NS5A and core proteins of hepatitis C virus and virological responses to pegylated-interferon/ribavirin combination therapy. Microbiol. Immunol. 55:418–426.
17. **el-Zayadi AR, et al.** 2005. Hepatocellular carcinoma in Egypt: a single center study over a decade. World J. Gastroenterol. 11:5193–5198.
18. **Enomoto N, et al.** 1996. Mutations in the nonstructural protein 5A gene and response to interferon in patients with chronic hepatitis C virus 1b infection. N. Engl. J. Med. 334:77–81.
19. **Fried MW, et al.** 2002. Peginterferon alfa-2a plus ribavirin for chronic hepatitis C virus infection. N. Engl. J. Med. 347:975–982.
20. **Ge D, et al.** 2009. Genetic variation in IL28B predicts hepatitis C treatment-induced viral clearance. Nature 461:399–401.
21. **Hassan MM, et al.** 2001. The role of hepatitis C in hepatocellular carcinoma: a case control study among Egyptian patients. J. Clin. Gastroenterol. 33:123–126.
22. **Kau A, Vermehren J, Sarrazin C.** 2008. Treatment predictors of a sustained virologic response in hepatitis B and C. J. Hepatol. 49:634–651.
23. **Khattab MA, et al.** 2011. Management of hepatitis C virus genotype 4: recommendations of an international expert panel. J. Hepatol. 54:1250–1262.
24. **Limaye AR, Draganov PV, Cabrera R.** 2011. Boceprevir for chronic HCV genotype 1 infection. N. Engl. J. Med. 365:176, 177–178.
25. **Macdonald A, Harris M.** 2004. Hepatitis C virus NS5A: tales of a promiscuous protein. J. Gen. Virol. 85:2485–2502.
26. **Maekawa S, Enomoto N.** 2009. Viral factors influencing the response to the combination therapy of peginterferon plus ribavirin in chronic hepatitis C. J. Gastroenterol. 44:1009–1015.
27. **Mattsson L, Sonnerborg A, Weiland O.** 1993. Outcome of acute symptomatic non-A, non-B hepatitis: a 13-year follow-up study of hepatitis C virus markers. Liver 13:274–278.
28. **Micallef JM, Kaldor JM, Dore GJ.** 2006. Spontaneous viral clearance following acute hepatitis C infection: a systematic review of longitudinal studies. J. Viral Hepat. 13:34–41.
29. **Moradpour D, et al.** 2004. Insertion of green fluorescent protein into nonstructural protein 5A allows direct visualization of functional hepatitis C virus replication complexes. J. Virol. 78:7400–7409.
30. **Murakami T, et al.** 1999. Mutations in nonstructural protein 5A gene and response to interferon in hepatitis C virus genotype 2 infection. Hepatology 30:1045–1053.
31. **Okamoto H, et al.** 1992. Typing hepatitis C virus by polymerase chain reaction with type-specific primers: application to clinical surveys and tracing infectious sources. J. Gen. Virol. 73(Pt 3):673–679.
32. **Ray SC, Arthur RR, Carella A, Bukh J, Thomas DL.** 2000. Genetic epidemiology of hepatitis C virus throughout Egypt. J. Infect. Dis. 182: 698–707.
33. **Sarasin-Filipowicz M.** 2010. Interferon therapy of hepatitis C: molecular insights into success and failure. Swiss Med. Wkly. 140:3–11.
34. **Sherman KE, et al.** 2011. Response-guided telaprevir combination treatment for hepatitis C virus infection. N. Engl. J. Med. 365:1014–1024.
35. **Simmonds P, et al.** 2005. Consensus proposals for a unified system of nomenclature of hepatitis C virus genotypes. Hepatology 42:962–973.
36. **Simmonds P, et al.** 1993. Classification of hepatitis C virus into six major genotypes and a series of subtypes by phylogenetic analysis of the NS-5 region. J. Gen. Virol. 74(Pt 11):2391–2399.
37. **Suppiah V, et al.** 2009. IL28B is associated with response to chronic hepatitis C interferon-alpha and ribavirin therapy. Nat. Genet. 41:1100–1104.
38. **Tanaka E, Kiyosawa K.** 2000. Natural history of acute hepatitis C. J. Gastroenterol. Hepatol. 15(Suppl):E97–E104.
39. **Tanaka Y, et al.** 2009. Genome-wide association of IL28B with response to pegylated interferon-alpha and ribavirin therapy for chronic hepatitis C. Nat. Genet. 41:1105–1109.
40. **Timm J, et al.** 2007. Characterization of full-length hepatitis C virus genotype 4 sequences. J. Viral Hepat. 14:330–337.
41. **Yuan HJ, Jain M, Snow KK, Gale M, Jr, Lee WM.** 2010. Evolution of hepatitis C virus NS5A region in breakthrough patients during pegylated interferon and ribavirin therapy. J. Viral Hepat. 17:208–216.

Mutations in non-structural 5A and rapid viral response to pegylated interferon-α-2b plus ribavirin therapy are associated with therapeutic efficacy in patients with genotype 1b chronic hepatitis C

YOSHIHIKO YANO[1,2], YASUSHI SEO[1], AKIRA MIKI[1], MASAYA SAITO[1], HIROTAKA KATO[4], KEN-ICHI HAMANO[5], MANABU OYA[6], SACHIKO OUCHI[7,8], TAKASHI FUJISAWA[8], HAJIME YAMADA[9], YUKIMASA YAMASHITA[10], SATOSHI TANI[11], SHIGEYA HIROHATA[12], SEITETSU YOON[12], NAOTO KITAJIMA[13], KAZUNARI KITAGAKI[14], AKIRA KAWARA[15], TAKATOSHI NAKASHIMA[16], HOSAI YU[17], TETSUO MAEDA[18], TAKESHI AZUMA[1], AHMED EL-SHAMY[3], HAK HOTTA[3] and YOSHITAKE HAYASHI[2]; Kobe Hepatitis Therapeutic Group

[1]Department of Gastroenterology, [2]Center for Infectious Diseases, and [3]Department of Microbiology, Kobe University Graduate School of Medicine; [4]Kato Clinic; [5]Hamano Clinic; [6]Division of Internal Medicine, Shin-Suma Hospital; [7]Division of Internal Medicine, Steel Memorial Hirohata Hospital; [8]Division of Internal Medicine, Kakogawa West City Hospital; [9]Department of Gastroenterology, Shinko Hospital; [10]Department of Gastroenterology, Kobe City Hospital Organization, Kobe City Medical Center West Hospital; [11]Division of Internal Medicine, Konan Hospital; [12]Department of Gastroenterology, Hyogo Prefectural Kakogawa Medical Center; [13]Division of Internal Medicine, Kasai City Hospital; [14]Division of Internal Medicine, Rokko-Island Hospital; [15]Kawara Clinic; [16]Department of Gastroenterology, Akashi Medical Center; [17]Division of Internal Medicine, National Hospital Organization, Kobe Medical Center; [18]Division of Internal Medicine, Kawasaki Hospital, Kobe, Japan

Received March 30, 2012; Accepted July 6, 2012

DOI: 10.3892/ijmm.2012.1093

Abstract. For patients chronically infected with hepatitis C virus (HCV), mutations in the non-structural 5A (NS5A) gene are important predictive factors for the response to interferon (IFN) therapy. In the present study, factor analysis of the therapeutic response of patients following pegylated IFN and ribavirin combination therapy was assessed in a multicenter study. Chronic HCV-infected patients with genotype 1b and high viral load (n=96, mean age 56.5 years; 59 males, 68 females) treated with pegylated IFN-α-2b and ribavirin combination therapy were enrolled. This study was conducted at Kobe University Hospital and 25 affiliated hospitals in Hyogo prefecture. Sixty-five patients (68%) completed treatment with both pegylated IFN and ribavirin at >80% of the weight-based scheduled dosages. Patients who reduced or terminated therapy were frequently aged women (mean age 60.8 years; 11 males, 17 females). Overall, a sustained viral response (SVR) was achieved in 42 (44%) patients out of 96. Based on per-protocol-based (PPB) analysis, the SVR rate in patients with ≥6 amino acid (aa) mutations in the IFN resistance-determining region (IRRDR) (75%) or ≥1 aa mutation in the IFN sensitivity-determining region (ISDR) (61%) was significantly higher than that in patients with <5 aa mutations in IRRDR (30%) or no mutation in ISDR (29%). Multivariate analysis revealed that rapid viral response (RVR) (odds ratio, 18.1) and mutations of ≥6 in IRRDR (odds ratio, 15.5) were significantly associated with SVR. In conclusion, mutations in the NS5A region, particularly in patients with ≥6 aa mutations in IRRDR were strongly associated with a therapeutic response to pegylated IFN and ribavirin combination therapy.

Correspondence to: Dr Yoshihiko Yano, Center for Infectious Diseases, Kobe University Graduate School of Medicine, 7-5-1 Kusunoki-cho, Chuo-ku, Kobe 650-0017, Japan
E-mail: yanoyo@med.kobe-u.ac.jp

Key words: chronic hepatitis C, pegylated IFN and ribavirin therapy, non-structural 5A

Introduction

Hepatitis C virus (HCV) is a major cause of chronic liver disease, with an estimated 170 million people infected worldwide. In Japan, the carrier rate is estimated to be approximately 1% of the general population. This rate increases depending on age and reaches approximately 5% in individuals over 70 years of age. The main goal of treatment for chronic hepatitis C is prevention of cirrhosis and hepatocellular carcinoma by eradication of the virus. Interferon (IFN)-based therapy was initiated in 1992, and efficacy of treatment regimens has improved year by year. Although the HCV viral eradication rate is approximately 5% following 24 weeks of treatment with conventional IFN therapy, the therapeutic result of combined pegylated IFN and ribavirin is ~55%. However, approximately half of patients treated with pegylated-IFN do not achieve a sustained viral response (1-3).

Due to the numerous side effects and the high cost of treatment, it is important to understand the individual mechanisms involved in non-response to treatment and to predict therapeutic efficacy prior to treatment. It has been reported that various viral and host factors are associated with the therapeutic response.

The role of amino acid (aa) mutations within the functional regions of non-structural 5A (NS5A) in relation to therapeutic response has been reported by several researchers. In 1996, it was reported that a high number of mutations in the IFN-sensitivity-determining region (ISDR) (aa 2209-2248) was strongly related to the sustained viral response (SVR) to IFN monotherapy in genotype 1b Japanese patients (4,5). In 2008, high mutations in the IFN-ribavirin resistance-determining region (IRRDR) (aa 2334-2379) were also related to the SVR to combined pegylated-IFN and ribavirin therapy (6). The significance of these mutations was also confirmed by studies carried out in different populations in different countries (7).

Based on previous studies, factor analysis and determination of NS5A viral mutations in relation to SVR of patients treated with pegylated-IFN and ribavirin combination therapy for HCV genotype 1b and a high viral load was carried out in a collaborative study in Kobe, Japan.

Materials and methods

Sample collection. Serum samples were collected from chronic hepatitis C patients with genotype 1b and a high viral load. A total of 96 patients (age 57.7±8.3 years; 45 males, 51 females) who were treated by subcutaneous injections of pegylated-IFN-α-2b once every week (1.5 μg/kg) (Pegintron; Schering-Plough, Innishannon, Country Cork, Ireland) in combination with oral ribavirin (400-800 mg) daily for 48 weeks between September, 2006 and June, 2008 were enrolled. HCV-RNA in serum samples was examined at 4 weeks, at the end of treatment and 6 months after the end of treatment. Serum samples were collected and stored at -80°C until virological examination. The rapid virological response (RVR) was defined as undetectable HCV-RNA at 4 weeks. Patients who had persistent undetectable serum HCV-RNA and normal serum alanine aminotransferase (ALT) levels 6 months after the end of treatment were considered to have an SVR.

The standard dosage of PEG-IFN (1.5 μg/kg) and ribavirin (12 mg/kg) was determined depending on the weight-based dose. Patients treated with >80% of the standard dosage were considered as high drug adherence and patients treated with at least one drug at <80% of the standard dosage were categorized as a low drug adherence group.

This study was conducted by Kobe University Hospital and 25 affiliated hospitals in Hyogo prefecture. The study protocol was approved by the Ethics Committee of Kobe University Hospital, and written informed consent was obtained from each patient before treatment.

Table I. Comparison of the base characteristics of the SVR and the non-SVR groups.

Factor	SVR	Non-SVR	P-value
No. of patients (%)	42 (44%)	54 (56%)	
Age, years	55.1±8.6	59.7±7.5	0.005
Males:Females	22:20	23:31	
BMI (kg/m^2)	24.0±3.4	23.2±3.4	0.85
ALT (IU/l)	72.3±69.4	75.8±61.8	0.66
PLT (x10^4/mm^3)	17.7±4.9	17.0±5.3	0.68
RVR	15/38	3/49	<0.001
PPB/ITT	30/41 (73%)	25/54 (46%)	0.03

SRV, sustained viral response; BMI, body mass index; PLT, platelets; ALT, alanine aminotransferase; RVR, rapid viral response; PPB, per-protocol-based analysis; ITT, intention-to-treat analysis.

Table II. Drug adherence of patients to pegylated-interferon and ribavirin therapy.

	High drug adherence	Low drug adherence	P-value
No. of patients (%)	65 (68%)	31 (32%)	
Age, years	57.4±8.2	59.3±7.2	0.25
Male:Female	33:32	13:18	
BMI (kg/m^2)	23.6±2.8	23.5±4.3	NS
ALT (IU/l)	78.2±54.5	72.7±68.5	0.7
PLT (x10^4/mm^3)	16.3±5.6	16.7±4.6	0.8
SVR	30/65 (46%)	11/31 (35%)	NS
ISDR ≥1	26/50 (52%)	12/26 (46%)	NS
IRRDR ≥6	18/50 (36%)	11/26 (42%)	NS

BMI, body mass index; ALT, alanine aminotransferase; PLT, platelets; SRV, sustained viral response; ISDR, IFN sensitivity-determining region; IRRDR, IFN resistance-determining region.

NS5A sequence analysis. HCV-RNA was extracted from 140 μl serum using a commercial kit according to the manufacturer's protocol (QIAmp Viral RNA kit; Qiagen, Tokyo, Japan). The NS5A region of the HCV genome was amplified and sequenced by nested RT-PCR using primer sets (6). The aa sequences were deduced and aligned using GENETYX Win software version 7.0 (Genetyx Corp., Tokyo, Japan).

Statistical analysis. Differences in parameters, including all available patient demographic, biochemical, hematological, and virological data, as well as ISDR and IRRDR sequence variations factors, were determined between the different patient groups by the Student's t-test for numerical variables, and Fisher's exact probability test for categorical variables.

Subsequently, univariate and multivariate logistic analyses were performed to identify variables that independently predict SVR. The odds ratios (OR) and 95% confidence intervals

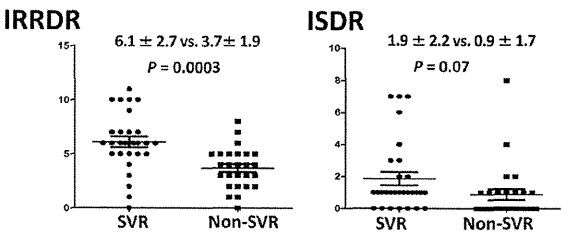

Figure 1. The number of mutations in IRRDR and ISDR. The number of mutations in IRRDR and ISDR was higher in the SVR group than in the non-SVR group.

Table III. Number of mutations in the NS5A region in relation to sustained viral response (SVR).

NS5A	Factor	SVR n (%)	Non-SVR n (%)	P-value
IRRDR	≥6	9/15 (60)[a]	3/17 (18)[a]	0.02[a]
	≥4	13/15 (87)	9/17 (53)	0.05
ISDR	≥4	3/15 (20)	1/17 (6)	0.25
	≥2	5/15 (33)	3/17 (18)	0.22
	≥1	11/15 (73)	7/17 (41)	0.06

[a]Statistically significant result. ISDR, IFN sensitivity-determining region; IRRDR, IFN resistance-determining region.

Table IV. Univariate and multivariate analyses in relation to the sustained viral response (SVR).

Univariate analysis		Multivariate analysis	
Factor	P-value	Odds ratio (95% CI)	P-value
IRRDR (IRRDR ≥6 vs. IRRDR ≤5)	0.000	18.1 (3.5-94.4)	0.001
ISDR (ISDR ≥1 vs. ISDR =0)	0.000		
RVR	0.017	15.5 (1.3-179.1)	0.028
LVR	0.001		
HCV-RNA titer (≥1000 vs. <1000)	0.099		
Age (≥60 vs. <60)	0.072		
Gender (male)	1.000		
PLT (≥15 vs. <15)	0.427		

ISDR, IFN sensitivity-determining region; IRRDR, IFN resistance-determining region; RVR, rapid viral response; LVR, late viral response.

(CIs) were also calculated. Positive and negative predictive values of SVR were computed, and their significance levels were evaluated using the sign test. All statistical analyses were performed using the SPSS version 16 software (SPSS Inc., Chicago, IL). Unless otherwise stated, a P-value of <0.05 was considered to indicate a statistically significant result.

Results

Baseline characteristics and on-treatment response in association with SVR. Baseline characteristics and on-treatment response are summarized in Table I. Overall, 42 cases out of 96 (44%) achieved an SVR. SVR patients were significantly younger in age and had a higher rate of RVR than the non-SVR patients. The prevalence of high drug adherence in SVR patients (73%) was significantly higher than that in non-SVR patients (46%) (P=0.03).

Drug adherence to pegylated interferon and ribavirin therapy. Due to various side effects, 31 patients were not treated with a sufficiently high dosage. Table II summarizes the patient groups with low and high drug adherence. Sixty-five (68%) patients had high drug adherence to the therapy. Older age women tended to require dose reductions. The SVR rate (35%) in patients with low drug adherence was significantly lower than those (46%) with high drug adherence.

Mutations in the NS5A region and predictive indicators for SVR. Factor analysis in association with the SVR was performed by per-protocol-based (PPB) analysis. The average number of mutations in IRRDR was significantly higher in the SVR group (6.1±2.7) than that in the non-SVR group (3.7±1.9) (P=0.0003). The average number of mutations in ISDR was also higher in the SVR group (1.9±2.2) than that in the non-SVR group (0.9±1.7), but this difference did not achieve statistical significance (Fig. 1). The SVR group and the non-SVR group were compared based on the number of mutations in the NS5A region. The prevalence of patients with ≥6 aa mutations within IRRDR in the SVR group (60%) was significantly higher than that in the non-SVR group (18%) (P=0.02). Similarly, the prevalence of patients with ≥1 aa mutation within ISDR in the SVR group (73%) was higher than that in the non-SVR group (41%), but this difference was not statistically significant (P=0.06). All patients with ≥6 aa mutations in IRRDR and ≥1 aa mutation in ISDR achieved an SVR (Table III). The positive predictive values of SVR in patients with ≥6 aa mutations in IRRDR was 78%. The sensitivity and specificity were 64 and 86%, respectively.

Factor analysis in association with the SVR. Univariate and multivariate analyses are summarized in Table IV. Univariate analysis showed that ≥6 aa mutations in IRRDR and ≥1 aa mutation in ISDR were strongly associated with an SVR. In addition, RVR and LVR were also significant between the two groups. Multivariate analysis revealed that ≥6 aa mutations in IRRDR (odds ratio 18.1) and RVR (odds ratio 15.5) were significantly related to the SVR.

Discussion

Pegylated-IFN and ribavirin combination therapy has been a standard treatment for patients with chronic hepatitis C. However, HCV genotype 1 is more resistant to IFN treatment than genotypes 2 or 3. In Japan, genotype 1b is the most prevalent and it is important to predict the therapeutic response for these patients prior to therapy (7-9). In general, approximately 50% of patients with genotype 1b do not achieve SVR even when using a combination of pegylated-IFN plus ribavirin treatment (10). In the present study, the overall SVR rate was 44% and this value was slightly lower than that in a previous study (8). The reason for this is possibly related to the patient age and drug adherence. The present study showed that age, drug adherence and RVR in the SVR group were significantly different than these values in the non-SVR group. The SVR rate in patients younger than 65 years was 52% and was significantly higher than that in patients over 65. In addition, the SVR rate (46%) in patients with high drug adherence was higher than that (35%) in patients with low drug adherence. There is no doubt that elder patients have difficulties continuing therapy and are forced to reduce the dosage or terminate treatment because of side effects. In the present study, the percentage of patients having low drug adherence was 32%, and the majority of patients in this group were aged women. Physically and mentally, it is frequently difficult to continue therapy for elder patients. The average age of patients in Japan is older than that in most other European countries and this is one of the important reasons for the therapeutic difference among Japanese studies and those carried out in other countries.

On-treatment response is an important factor for predicting SVR; RVR 4 weeks following the initiation of treatment has been reported to be a good predictor of SVR (11-13). In this study, RVR was an important factor for predicting SVR by multivariate analysis. The positive predictive value was 82% and RVR was confirmed to be a good predictor in this study. However, even when patients are predicted as good responders for IFN/RBV therapy, they do not always achieve SVR as side effects result in dose reduction or termination of the planned IFN/RBV treatment. It was also reported that drug adherence is related to SVR (14). In this study, 3 patients relapsed after achieving RVR. The first case was over 65 years of age, the second case had low drug adherence, and the third was an older patient over 65 years with low drug adherence. Incomplete treatment is an important factor contributing to the failure of achieving SVR. This result suggests the necessity for prolonged therapy or therapeutic modification in patients with RVR receiving a dosage reduction.

Mutations in several amino acids in the NS5A protein have been described and are thought to play an important role in response to IFN treatment. It has been reported that a high number of mutations in ISDR and IRRDR are significantly associated with SVR (6). In the present study, patients with ≥1 aa mutation in ISDR and ≥6 aa mutations in IRRDR tended to achieve SVR, which was supported by previous data (6). For ISDR, the mutation results are similar to previous studies (4,5). Compared with ISDR, IRRDR was more strongly associated with SVR in this study. Based on the multivariate analysis, only IRRDR was associated with an SVR. Patients with more than 6 IRRDR mutations had a higher SVR rate and it was the same as previous studies (6). The positive predictive value and sensitivity was >80%, suggesting it to be a good predictive marker. All patients with ≥6 aa mutations and ≥1 aa mutation in ISDR achieved SVR following pegylated-IFN and ribavirin combination therapy. The importance of the NS5A mutation is still controversial. It has been reported that a mutation in NS5A is not related to the IFN response in European and American HCV strains (15-18). However, the importance of NS5A was reported in Asian HCV strains including Taiwan and Chinese strains (19,20). To date, this inconsistency is unclear but is partly related to the fact that HCV strains are different depending on geographic distribution (21). Meta-analysis revealed that the prevalence of a mutation in ISDR was 44.1% in Japanese and 24.8% in European patients, respectively (21). Mutational studies are sometimes inconsistent even among Japanese studies, suggesting that mutations in the NS5A region vary based on different geographical regions even in Japan.

The NS5A protein has a transcriptional activation function and represses IFN-induced gene expression (22). In addition, the NS5A protein interacts with antiviral protein PKR resulting in suppressed PKR activity (23). It is possible that mutations in the NS5A protein may affect the structural and/or biological functions of NS5A and inhibit IFN activity (23,24).

Mutations in E2-PePHD (aa 659-670), PKRBD (aa 2209-2274) and NS5A-V3 (aa 2356-2379) are also reported to be associated with IFN sensitivity (24,25).

Recent studies have shown that SNPs in the IL28B region are strongly associated with response to IFN therapy (26). In this study, genomic factors in the host were not analyzed due to the pre-treatment study design and informed consent. Therapeutic prediction can be more accurate upon examination of host factors as well as viral factors. In the near future, new drug therapies such as protease and polymerase inhibitors called new direct-acting antivirals (DAAs) will become available (27). Standard therapy for hepatitis C virus will include combination therapies using DAAs and pegylated-IFN plus ribavirin. However, the SVR rate by telaprevir-based pegylated-IFN plus ribavirin combination therapy (REALIZE study; phase III, randomized, double blind, placebo-controlled study) was found to be as high as 31% in patients who were non-responders to prior treatment (28). The viral response to pegylated-IFN and ribavirin combination therapy is important for the development of future combination therapies.

In conclusion, mutations in the NS5A region, particularly in patients with more than 6 aa mutations in the IRRDR region are strongly associated with the therapeutic response to pegylated-IFN and ribavirin combination therapy.

References

1. Seeff LB: Natural history of chronic hepatitis C. Hepatology 36 (Suppl 1): S35-S46, 2002.
2. Lavanchy D: The global burden of hepatitis C. Liver Int 29: 74-81, 2009.
3. Marcellin P: Hepatitis B and hepatitis C in 2009. Liver Int 29: 1-8, 2009.
4. Enomoto N, Sakuma I, Asahina Y, *et al*: Mutations in the nonstructural protein 5A gene and response to interferon in patients with chronic hepatitis C virus 1b infection. N Engl J Med 334: 77-81, 1996.
5. Enomoto N, Sakuma I, Asahina Y, *et al*: Comparison of full length sequences of interferon-sensitive and resistant hepatitis C virus 1b: sensitivity to interferon is conferred by amino acid substitutions in the NS5A region. J Clin Invest 96: 224-230, 1995.
6. El-Shamy A, Nagano-Fujii M, Sasase N, Imoto S, Kim SR and Hotta H: Sequence variation in hepatitis C virus nonstructural protein 5A predicts clinical outcome of pegylated interferon/ribavirin combination therapy. Hepatology 48: 38-47, 2008.
7. Kumthip K, Pantip C, Chusri P, *et al*: Correlation between mutations in the core and NS5A genes of hepatitis C virus genotypes 1a, 1b, 3a, 3b, 6f and the response to pegylated interferon and ribavirin combination therapy. J Viral Hepat 18: e117-e125, 2011.
8. Manns MP, McHutchison JG, Gordon SC, *et al*: Peginterferon alfa-2b plus ribavirin compared with interferon alfa-2b plus ribavirin for initial treatment of chronic hepatitis C: a randomised trial. Lancet 358: 958-965, 2001.
9. Fried MW, Shiffman ML, Reddy KR, *et al*: Peginterferon alfa-2a plus ribavirin for chronic hepatitis C virus infection. N Engl J Med 347: 975-982, 2002.
10. Hadziyannis SJ, Sette H Jr, Morgan TR, *et al*: Peginterferon-alpha2a and ribavirin combination therapy in chronic hepatitis C: a randomized study of treatment duration and ribavirin dose. Ann Intern Med 140: 346-355, 2004.
11. Yu ML, Dai CY, Huang JF, *et al*: Rapid virological response and treatment duration for chronic hepatitis C genotype 1 patients: a randomized trial. Hepatology 47: 1884-1893, 2008.
12. Yu JW, Wang GQ, Sun LJ, Li XG and Li SC: Predictive value of rapid virological response and early virological response on sustained virological response in HCV patients treated with pegylated interferon alpha-2a and ribavirin. J Gastroenterol Hepatol 22: 832-836, 2007.
13. Jafferbhoy H, Miller MH, El Wahed Z and Dillon JF: Pre-treatment prediction of response to pegylated-interferon plus ribavarin for chronic hepatitis C using RVR. J Hepatol 55: 1162-1164, 2011.
14. Tanioka D, Iwasaki Y, Araki Y, *et al*: Factors associated with adherence to combination therapy of interferon and ribavirin for patients with chronic hepatitis C: importance of patient's motivation and physician's treatment experience. Liver Int 29: 721-729, 2009.
15. Chung RT, Monto A, Dienstag JL and Kaplan LM: Mutations in the NS5A region do not predict interferon-responsiveness in American patients infected with genotype 1b hepatitis C virus. J Med Virol 58: 353-358, 1999.
16. Zeuzem S, Lee JH and Roth WK: Mutations in the nonstructural 5A gene of European hepatitis C virus isolates and response to interferon alfa. Hepatology 25: 740-744, 1997.
17. Paterson M, Laxton CD, Thomas HC, Ackrill AM and Foster GR: Hepatitis C virus NS5A protein inhibits interferon antiviral activity, but the effects do not correlate with clinical response. Gastroenterology 117: 1187-1197, 1999.
18. Torres-Puente M, Cuevas JM, Jimenez-Hernandez N, *et al*: Hepatitis C virus and the controversial role of the interferon sensitivity determining region in the response to interferon treatment. J Med Virol 80: 247-253, 2008.
19. Shen C, Hu T, Shen L, Gao L, Xie W and Zhang J: Mutations in ISDR of NS5A gene influence interferon efficacy in Chinese patients with chronic hepatitis C virus genotype 1b infection. J Gastroenterol Hepatol 22: 1898-1903, 2007.
20. Hung CH, Lee CM, Lu SN, *et al*: Mutations in the NS5A and E2-PePHD region of hepatitis C virus type 1b and correlation with the response to combination therapy with interferon and ribavirin. J Viral Hepat 10: 87-94, 2003.
21. Pascu M, Martus P, Höhne M, *et al*: Sustained virological response in hepatitis C virus type 1b infected patients is predicted by the number of mutations within the NS5A ISDR: a meta-analysis focused on geographical differences. Gut 53: 1345-1351, 2004.
22. Gale MJ, Korth MJ, Tang NM, *et al*: Evidence that hepatitis C virus resistance to interferon is mediated through repression of the PKR protein kinase by the nonstructural 5A protein. Virology 30: 217-227, 1997.
23. Gale MJ, Korth MJ and Katze MG: Repression of the PKR protein kinase by the hepatitis C virus NS5A protein: a potential mechanism of interferon resistance. Clin Diagn Virol 10: 157-162, 1998.
24. Hofmann WP, Zeuzem S and Sarrazin C: Hepatitis C virus-related resistance mechanisms to interferon alpha-based antiviral therapy. J Clin Virol 32: 86-91, 2005.
25. Gervain J, Czibula A, Simon J and Kalmar T: Structural analysis of the PKR-binding region of HCV 1b samples from patients with chronic hepatitis C and the correlation with IFN-sensitivity. Orv Hetil 144: 1179-1184, 2003 (In Hungarian).
26. Tanaka Y, Nishida N, Sugiyama M, *et al*: Genome-wide association of IL28B with response to pegylated interferon-alpha and ribavirin therapy for chronic hepatitis C. Nat Genet 41: 1105-1109, 2009.
27. Asselah T, Benhamou Y and Marcellin P: Protease and polymerase inhibitors for the treatment of hepatitis C. Liver Int 29: 57-67, 2009.
28. Forestier N and Zeuzem S: Triple therapy with telaprevir: results in hepatitis C virus-genotype 1 infected relapsers and non-responders. Liver Int 32: 44-50, 2012.

OPEN ACCESS Freely available online PLOS ONE

HCV NS5A Protein Containing Potential Ligands for Both Src Homology 2 and 3 Domains Enhances Autophosphorylation of Src Family Kinase Fyn in B Cells

Kenji Nakashima[1], Kenji Takeuchi[1,2], Kazuyasu Chihara[1,2], Tomoko Horiguchi[1], Xuedong Sun[1], Lin Deng[3], Ikuo Shoji[3], Hak Hotta[3], Kiyonao Sada[1,2]*

1 Division of Genome Science and Microbiology, Department of Pathological Sciences, School of Medicine, Faculty of Medical Sciences, University of Fukui, Eiheiji, Japan, **2** Organization for Life Science Advancement Programs, University of Fukui, Eiheiji, Japan, **3** Division of Microbiology, Center for Infectious Diseases, Kobe University Graduate School of Medicine, Kobe, Japan

Abstract

Hepatitis C virus (HCV) infects B lymphocytes and induces mixed cryoglobulinemia and B cell non-Hodgkin's lymphoma. The molecular mechanism for the pathogenesis of HCV infection-mediated B cell disorders remains obscure. To identify the possible role for HCV nonstructural 5A (NS5A) protein in B cells, we generated the stable B cell lines expressing Myc-His tagged NS5A. Immunoprecipitation study in the presence or absence of pervanadate (PV) implied that NS5A was tyrosine phosphorylated by pervanadate (PV) treatment of the cells. Therefore we examined pull-down assay by using glutathione S-transferase (GST)-fusion proteins of various Src homology 2 (SH2) domains, which associates with phosphotyrosine within a specific amino acid sequence. The results showed that NS5A specifically bound to SH2 domain of Fyn from PV-treated B cells in addition to Src homology 3 (SH3) domain. Substitution of Arg^{176} to Lys in the SH2 domain of Fyn abrogated this interaction. Deletion mutational analysis demonstrated that N-terminal region of NS5A was not required for the interaction with the SH2 domain of Fyn. Tyr^{334} was identified as a tyrosine phosphorylation site in NS5A. Far-western analysis revealed that SH2 domain of Fyn directly bound to NS5A. Fyn and NS5A were colocalized in the lipid raft. These results suggest that NS5A directly binds to the SH2 domain of Fyn in a tyrosine phosphorylation-dependent manner. Lastly, we showed that the expression of NS5A in B cells increased phosphorylation of activation loop tyrosine in the kinase domain of Fyn. NS5A containing ligand for both SH2 and SH3 domains enhances an aberrant autophosphorylation and kinase activity of Fyn in B cells.

Citation: Nakashima K, Takeuchi K, Chihara K, Horiguchi T, Sun X, et al. (2012) HCV NS5A Protein Containing Potential Ligands for Both Src Homology 2 and 3 Domains Enhances Autophosphorylation of Src Family Kinase Fyn in B Cells. PLoS ONE 7(10): e46634. doi:10.1371/journal.pone.0046634

Editor: Philippe Gallay, Scripps Research Institute, United States of America

Received April 12, 2012; **Accepted** September 2, 2012; **Published** October 16, 2012

Funding: This study was supported in part by research funding from the University of Fukui, Takeda Science Foundation, Yakult Foundation, and the Grant-in-Aids from the Japan Society for the Promotion of Science and the Ministry of Education, Culture, Sports and Technology, Japan. The funders had no role in study design, data collection and analysis, decision to publish, or preparation of the manuscript.

Competing Interests: The authors have declared that no competing interests exist.

* E-mail: ksada@u-fukui.ac.jp

Introduction

HCV is a small enveloped positive-sense RNA virus classified within the family *Flaviviridae* [1,2]. In addition to liver cells, HCV infects B cells, leading to mixed cryoglobulinemia and B cell non-Hodgkin's lymphoma [3–5]. HCV infection in B cells enhances the expression of lymphomagenesis-related genes, such as activation-induced cytidine deaminase (AID) [6,7]. However, the molecular mechanisms of HCV infection-mediated B cell disorders remain elusive.

Non-receptor type of protein-tyrosine kinase Fyn is a member of the Src family kinases, and has regulatory roles in immune receptor signaling. Recently, Fyn has been recognized as an important mediator of mitogenic signaling and regulator of cell cycle entry, growth and proliferation. As for pathological aspects, Fyn is overexpressed in various cancers, and overexpression of Fyn in cultured cells resulted in cancer-like phenotypes [8].

The Src family kinases all share a common structure and pattern of activation. The domains of these proteins include SH2, SH3, and kinase domains followed by a short C-terminal regulatory tail. The SH2 and SH3 domains are highly conserved regions and mediate protein-protein interactions: the SH2 domain binds to phosphotyrosine residue within the specific amino acid sequence, while the SH3 domain recognizes proline rich regions. HCV NS5A was shown to interact with various SH3 domains of intracellular signaling molecules, and the kinase activity of Fyn was upregulated in liver cell lines harboring HCV replicon [9]. Binding of ligands to both the SH2 and SH3 domains disrupts autoinhibitory intramolecular interactions and leads to the opened conformation. Then autophosphorylation of the activation loop tyrosine (Tyr^{420} in Fyn) and dephosphorylation of the C-terminal tail (Tyr^{531} in Fyn) by protein-tyrosine phosphatases lead to the activation of kinase activity [10].

Previously, we reported that Syk, another non-receptor type of protein-tyrosine kinase interacts with transiently expressed NS5A in PV treated BJAB B cells [11]. This suggested that protein-tyrosine phosphorylation is required for the association of NS5A with Syk, because PV is a nonspecific inhibitor of protein-tyrosine phosphatases and treatment of cells with PV causes increase in

protein-tyrosine phosphorylation in whole cells. Recently Pfannkuche *et al.* reported that NS5A binds to the SH2 domain of Src [12]. However, molecular mechanism of their interaction and effect of NS5A on the kinase activity of Src remain unclear.

In this study, we investigated the interaction between NS5A and the SH2 domain of Fyn in B cells.

Materials and Methods

Antibodies and cDNAs

Anti-NS5A and anti-glyceraldehyde-3-phosphate dehydrogenase (GAPDH) mAbs were purchased from Millipore (Bedford, MA, USA). Anti-Myc mAb and anti-Fyn antibody were obtained from Santa Cruz Biotechnology (Santa Cruz, CA, USA). Anti-phosphotyrosine (pTyr) (PY20) and human anti-IgM mAbs were from Zymed (South San Francisco, CA, USA). Anti-GST mAb was from Nacalai (Kyoto, Japan). Anti-phospho-Src family (Tyr416) antibody, which detects phosphorylated amount of Tyr^{420} in Fyn, was from Cell Signaling Technology (Danvers, MA, USA). The pEF1A-NS5A(Con1)-Myc-His plasmid and its deletion or substitution mutants were described previously [11]. Deletion of NS5A 127–146 (NS5A Δ127–146) was generated by the PCR-based method using four primers, 5′-TTGGTACCATGTCCGGCTCGTGGCTAAGAG-3′, 5′-GCTCTAGACAGCAGACGACGTCCTCA-3′, 5′-GGTTACGCGGGTGGGGGATCCCGAATTCTTCACAGAAGTG-3′, and 5′-CACTTCTGTGAAGAATTCGGGATCCCCCACCCGCGTAACC-3′, using NS5A cDNA as a template. Substitution of Tyr^{129} to Phe (Y129F) of NS5A 1–146 was generated by the site-directed mutagenesis using two primers, 5′-GGGGATTTCCACTTCGTGACGGGCA-3′ and 5′-TGCCCGTCACGAAGTGGAAATCCCC-3′, using NS5A 1–146 cDNA as a template. Substitutions of Tyr^{182} to Phe (Y182F), Tyr^{321} to Phe (Y321F), and Tyr^{334} to Phe (Y334F) of NS5A 147–447 were generated by the site-directed mutagenesis using two specific primers designed by QuikChange Primer Design Program (www.genomics.agilent.com), using NS5A 147–447 as a template. The resulted mutations were confirmed by the DNA sequencing.

Cell culture and transfection

B-lymphoid leukemia BJAB cells were kindly provided from Dr. Satoshi Ishido (RIKEN, Yokohama, Japan) [13] and maintained as described previously [14]. For the stable transfection of BJAB cells, 6 μg of linearized pEF1A-NS5A(Con1)-Myc-His was transfected into 5×10^6 cells/500 μl of cells by electroporation (240 V, 950 μF). Stably transfected cell lines were selected with 0.4 mg/ml of active G418 (Wako, Osaka, Japan) [15]. Cell lines were screened by level of protein expression by immunoblotting of detergent soluble lysates with anti-NS5A and anti-GAPDH mAbs as an internal control. Two positive cloned lines were selected for further analysis. For control cells, linearized empty vector was transfected by electroporation, and pooled clones resistant to 0.4 mg/ml of active G418 were utilized as control cells. COS cells were obtained from American Type Culture Collection (Manassas, VA, USA) and Ramos-T cells were kindly provided from Dr. Hamid Band (Nebraska Medical Center, NE, USA) [16]. Transient transfection of COS cells and Ramos-T cells were described previously [17]. Huh-7.5 cells were kindly provided from Dr. Charles M. Rice (The Rockefeller University, NY, USA) [18] and stably harboring an HCV replicon (pFK5B/2884 Gly) were described previously [11].

Cell activation, immunoprecipitation and immunoblotting

BJAB cells (10^8) were washed twice with serum free medium and treated with 100 μM PV or 10 μg/ml of anti-IgM mAb for 3 min at 37°C in the same medium. Either unstimulated or stimulated cells were washed twice with ice-cold PBS and then solubilized in the lysis buffer (1% Triton X-100, 50 mM Tris, pH7.4, 150 mM NaCl, 10 mM EDTA, 100 mM NaF, 1 mM Na_3VO_4, 1 mM phenylmethylsulfonyl fluoride and 2 μg/ml aprotinin) on ice. In some experiments, 0.5% Nonidet P-40 was used instead of 1% Triton. Precleared cell lysates were incubated with the indicated antibodies prebound to protein A-agarose beads (Sigma, St. Louis, MO, USA). After rotation for 90 min at 4°C, the beads were washed 4 times with the lysis buffer, and the immunoprecipitated proteins were eluted by the heat treatment for 5 min at 100°C with 2×sampling buffer. Precipitated proteins or cell lysates were separated by SDS-PAGE and transferred to polyvinylidene difluoride (PVDF) membrane (Millipore). After blocking in 5% milk in TBST (25 mM Tris, pH 8.0, 150 mM NaCl, and 0.1% Tween 20), the blots were incubated with the primary antibodies and then horseradish peroxidase-conjugated goat anti-rabbit IgG, goat anti-mouse IgG antibodies (Jackson ImmunoResearch Laboratories, West Grove, PA, USA), or horseradish peroxidase-conjugated protein G (Sigma) in TBST. To enhance the signals, Immuno-enhancer Reagent A (Wako) was utilized in the reaction with anti-pTyr (pY20) mAb. Finally, proteins were visualized by the enhanced chemiluminescence (ECL) reagent (Western Lightning, PerkinElmer Life Sciences, Boston, MA) [19]. Immunoblot quantification was performed using the program Scion Image (Scion, Frederick, MD, USA).

Pull-down assay

The cDNA for Fyn-SH2 (Trp^{149}-Ala^{257}) and –SH3 (Thr^{82}-Glu^{148}) were amplified by PCR using paired primers 5′-GGAATTCATGGTACTTTGGAAAACTTGGC-3′ and 5′-CCGCTCGAGATCTTTAGCCAATCCAGAAGT-3′ for –SH2, 5′-GGAATTCAACAGGAGTGACACTGTTTGTG-3′ and 5′-CCGCTCGAGCTCTTCTGCCTGGATGGAGTC-3′ for –SH3, using mouse Fyn(T) cDNA (a gift from Dr. Yasuhiro Minami, Kobe University, Kobe, Japan) as a template. The cDNA for c-Abl-SH2 (Typ^{146}-His^{221}) and -SH3 (Leu^{84}-Val^{138}) were amplified by PCR using paired primers 5′-CGGAATTCCTGGTATCATGGCCCTGTATCT-3′ and 5′-ATAGTTTAGCGGCCGCTAGCTGGGTAGTGGAGTGTGGT-3′ for -SH2, 5′-CGGAATTCCCTTTTTGTGGCACTCTATGAT-3′ and 5′-TAGTTTAGCGGCCGCTGACGGGGGTGATGTAGTTGCT-3′ for -SH3, using mouse c-Abl cDNA (a gift from Dr. David Baltimore, California Institute of Technology, CA, USA) as a template. The cDNA for Cbl-b N-terminal region containing SH2 domain (Ala^2-Pro^{349}) was amplified by PCR using 5′-CGGAATTCCGCAAACTCAATGAATGGCAGA-3′ and 5′-CCGCTCGAGCTAAGGTGTAGGTTCACATAATCC-3′, using human Cbl-b cDNA (a gift form Dr. Stanley Lipkowitz, National Naval Cancer Center, MD, USA) as a template. Resulted PCR fragments were subcloned into pGEX-4T.3 (GE Healthcare, Piscataway, NJ, USA) to make domain in-frame with the downstream of GST and verified by DNA sequencing. The GST-rat Lyn-SH2 and Syk-SH2 (N+C) expression constructs were provided by Dr. Reuben P. Siraganian (National Institutes of Health, MD, USA). Preparation of GST-rat Vav1-SH2, mouse c-Abl SH3 domain-binding protein-2 (3BP2)-SH2, human phospholipase C (PLC)-γ2-SH2 (N+C), and rat Lyn-SH3 domain expression constructs were described elsewhere [17,20,21]. Substitution of Arg^{176} to Lys (R176K) by a point mutation of pGEX-4T.3-Fyn-SH2 was generated by the site-directed mutagenesis using two primers 5′-TCAAAGAGAGCCAAACCACCAAAGG-3′ and 5′-TAAGAAAGGTACCTCTTGGGTTTCC-3′, using Fyn-SH2 cDNA wild type as a template. The resulted point mutation was confirmed by the DNA sequencing. All these SH2 and SH3 domains were fused downstream of GST. The GST fusion proteins were affinity-purified with glutathione Sepharose 4B beads (GE Healthcare). Extraction of GST-fusion proteins from bacteria was confirmed by the SDS-PAGE and Coomassie brilliant blue staining [22].

BJAB cells (10^8), Huh-7.5 cells stably harboring an HCV replicon (3×10^6), COS cells (10^6) or Ramos B cells expressing SV40 T antigen (Ramos-T cells) (10^7) were washed twice with serum free medium and stimulated with 100 μM PV for 3 min at 37°C. Either unstimulated or stimulated cells were solubilized in the binding buffer (1% NP-40, 50 mM Tris, pH7.4, 150 mM NaCl, 10 mM EDTA, 100 mM NaF, 1 mM Na_3VO_4, 1 mM phenylmethylsulfonyl fluoride and 2 μg/ml aprotinin). After centrifugation, the resulted supernatants were reacted with 20 μg of GST-fusion proteins prebound to glutathione Sepharose 4B beads for 90 min at 4°C. The beads were washed 4 times with the binding buffer. Proteins interacting with GST-fusion proteins were eluted by heat treatment for 5 min at 100°C with 2×sampling buffer, separated by SDS-PAGE, and analyzed by immunoblotting.

Far-western

Anti-NS5A immunoprecipitates from BJAB cells (3×10^7) were separated by SDS-PAGE and transferred to PVDF membrane. After blocking, the membranes were incubated with 2.5 μg/ml of GST or GST-Fyn-SH2 for 1 h at 4°C. After extensive washing, membranes were reacted with anti-GST mAb, subsequently reacted with horseradish peroxidase conjugated goat anti-mouse IgG antibody, and then subjected to ECL detection [17].

Subcellular fractionation

The low density detergent-insoluble fractions were prepared by sucrose density gradient centrifugation as described [23]. BJAB cells (10^8) were solubilized in 2.5 ml of 0.05% Triton in MNEV buffer (150 mM NaCl, 25 mM Mes, pH 6.5, 5 mM EDTA, 1 mM Na_3VO_4, and protease inhibitors) and dounced 10 times. Homogenates were cleared of intact cells by centrifugation for 10 minutes at 200 *g*. The resultant supernatants (2.4 ml) were mixed with equal volumes of 80% sucrose in MNEV buffer (final, 40% sucrose and 0.025% Triton), overlayered by 4.8 ml 30% and 2.4 ml 5% sucrose in MNEV buffer, and then centrifuged for 20 hours at 200 000 *g* (P40ST rotor, Himac CP80WX, Hitachi, Tokyo, Japan). After sucrose density gradient centrifugation, 9 fractions were collected from the top of the gradient and analyzed by the immunoblotting.

Statistical analysis

Quantification of Fyn was analyzed by ImageJ software. The two-tailed Student t-test was applied to evaluate the statistical significance of differences found. A P value of <0.05 was considered statistically significant.

In vitro kinase assay

Unstimulated BJAB cells were washed twice with ice-cold PBS and then solubilized in the lysis buffer. Precleared cell lysates were incubated with anti-Fyn antibody prebound to protein A-agarose beads. After rotation for 90 min at 4°C, the beads were washed 4 times with the lysis buffer, 2 times with the kinase buffer without ATP, then incubated with 20 μl of the kinase buffer (40 mM Hepes, pH 7.5, 10 mM $MgCl_2$, 2 mM $MnCl_2$, 4 μM ATP, 4 μCi [γ-^{32}P] ATP) and 2.5 μg of acid-treated enolase (Sigma) for 30 min at room temperature. Reaction was terminated and proteins were eluted by the heat treatment for 5 min at 100°C with 2×sampling buffer. Proteins were separated by SDS-PAGE and gel was incubated with 1N KOH for 1 h at 56°C to remove phosphoserine and most of phosphothreonine. After fixation, the gel was dried and radiolabeled proteins were visualized by autoradiography. Immunoprecipitation of Fyn was confirmed by the immunoblotting.

Results

HCV NS5A associates with the SH2 domain of Fyn

To identify HCV NS5A-interacting protein in B cells, we generated the stable B cell lines in which Myc-His tagged NS5A protein is constitutively expressed. Since we confirmed that the parental cells did not express NS5A, we choose the clones in which the level of NS5A expression was highest (Fig. 1A). In the following experiments, two cloned lines (clone 3 and 7) were examined, although some figures present the results from only one representative cell line. For control, vector plasmid was transfected into the same parental cells and G418-resistant clones were pooled and utilized as control cells.

Next, we performed immunoprecipitation study using anti-Myc mAb and found tyrosine phosphorylated proteins (Fig. 1B). This suggests that NS5A was tyrosine phosphorylated by PV treatment or another protein with similar size that associates with NS5A (Fig. 1B). Another experiment by affinity tag purification using Nickel column which could react with His-tag (His-Accept kit, Nacalai) also showed some tyrosine phosphorylated proteins in NS5A protein complex (data not shown). These findings suggest the possible involvement of protein-tyrosine phosphorylation associating with NS5A. Therefore, we tried to identify the protein which associates with NS5A through SH2 domain, which recognizes specific phosphotyrosine-containing amino acid sequence.

Then we carried out pull-down assay using GST-fusion proteins of various SH2 domains (Fig. 1C). Among these, the SH2 domain of Fyn dramatically bound to NS5A from PV-treated B cells. The SH2 domains of PLC-γ2 weakly bound to NS5A. The SH2 domains of Lyn, Abl, Vav, 3BP2, Syk or Cbl-b interacted with NS5A at very low level (long exposure, data not shown). GST-Lyn-SH3 was utilized as positive control because it was reported to interact with NS5A [9]. Therefore, this data demonstrated that HCV NS5A selectively binds to the SH2 domains of Fyn and PLC-γ2 in B cells. GST-human Fyn-SH2 also interacted with NS5A (Fig. S1). Moreover, the NS5A interaction with GST-Fyn-SH2 was observed even in the context of HCV RNA replication (Fig. 1D). Thus, HCV NS5A selectively associates with the SH2 domain of Fyn.

NS5A binds to the SH2 domain of Fyn in a tyrosine phosphorylation-dependent manner

PV treatment of cells dramatically enhances the binding of NS5A to the SH2 domain of Fyn, but not with that of Lyn or Abl (Fig. 2A). Substitution of Arg^{176} to Lys in the SH2 domain of Fyn, which caused the loss of association with phosphotyrosine residue, abrogated the binding of the SH2 domain of Fyn to NS5A (Fig. 2B). Arg^{176} is located in the consensus sequence within the SH2 domains to interact with phosphotyrosine residue. On the other hand, the SH3 domain of these kinases associated with NS5A to a comparable level (Fig. 2C). These results suggest that

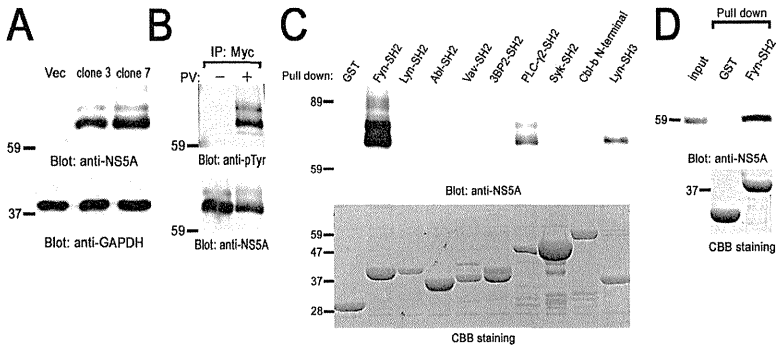

Figure 1. Identification of HCV NS5A-interacting proteins in B cells. (A) Generation of stable B cell lines expressing HCV NS5A. Detergent soluble cell lysates from vector cells (Vec) and Myc-His-NS5A expressing clones (clones 3 and 7) were separated by SDS-PAGE and analyzed with immunoblotting with anti-NS5A and anti-GAPDH mAbs. (B) BJAB cells expressing Myc-His-NS5A (clone 7) were treated without (−) or with (+) PV and solubilized in the lysis buffer. Cell lysates were immunoprecipitated with anti-Myc mAb and immunoprecipitated proteins were separated by SDS-PAGE and analyzed with immunoblotting with anti-pTyr (PY20) and anti-NS5A mAbs. PV-treated cells expressing Myc-His-NS5A (clone 7) (C) or Huh-7.5 cells stably harboring an HCV subgenomic replicon (D) were solubilized in the binding buffer. Precleared lysates were reacted with the indicated GST-fusion proteins and binding proteins were separated by SDS-PAGE and analyzed with immunoblotting with anti-NS5A mAb. The amount of GST-fusion proteins was confirmed by Coomassie brilliant blue (CBB) staining (C and D). Molecular sizing markers are indicated at left in kilodalton. The results were representative of three independent experiments. Similar results were obtained when another line was examined (B and C).
doi:10.1371/journal.pone.0046634.g001

increase in tyrosine phosphorylation of NS5A itself, or other associating proteins, allow the interaction with the SH2 domain of Fyn.

Central and/or C-terminal regions of NS5A binds to the SH2 domain of Fyn

To map the Fyn-SH2-binding region in NS5A, a series of deletion mutants were examined (Fig. 3). The results obtained reveals that N-terminal region (amino acids number 1–126) is not required for the interaction with the SH2 domain of Fyn in COS cells, although this region contains the region to interact with another kinase Syk (Fig. 3A) [11]. NS5A 127–146 and 147–447 could interact with the SH2 domain of Fyn. This demonstrates that deletion of the Fyn-binding region in the context of the full-length protein leads to loss of function. Similar results were obtained when HCV NS5A proteins were transiently expressed in Ramos B cells expressing SV40 T antigen (Ramos-T cells), and examined by pull-down assay (Fig. 3B). Deletion of 127–146 (NS5A Δ127–146) still allowed binding of NS5A to the SH2

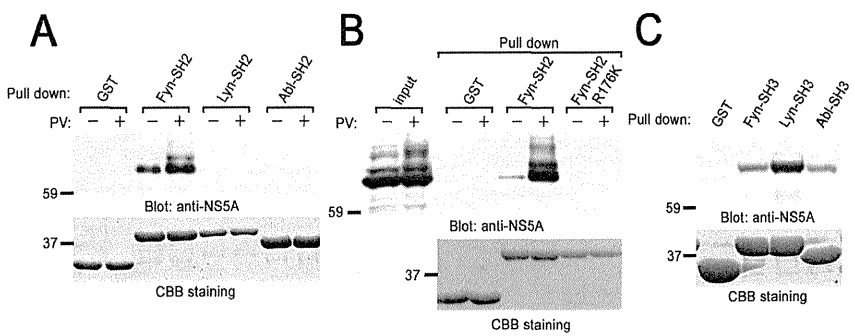

Figure 2. Pervanadate treatment of cells stimulates the binding of NS5A to the SH2 domain of Fyn in B cells. Either nontreated or PV-pretreated cells expressing Myc-His-NS5A (clone 7) were reacted with GST-fusion proteins of SH2 domains of various protein-tyrosine kinases (PTKs) (A), GST-Fyn-SH2 or GST-Fyn-SH2 R176K (B), or SH3 domains of various PTKs (C). Binding proteins were separated by SDS-PAGE and analyzed with immunoblotting with anti-NS5A mAb. The amount of GST-fusion proteins was confirmed by CBB staining. Molecular sizing markers are indicated at left in kilodalton. The results were representative of three independent experiments. Similar results were obtained when another line was examined.
doi:10.1371/journal.pone.0046634.g002

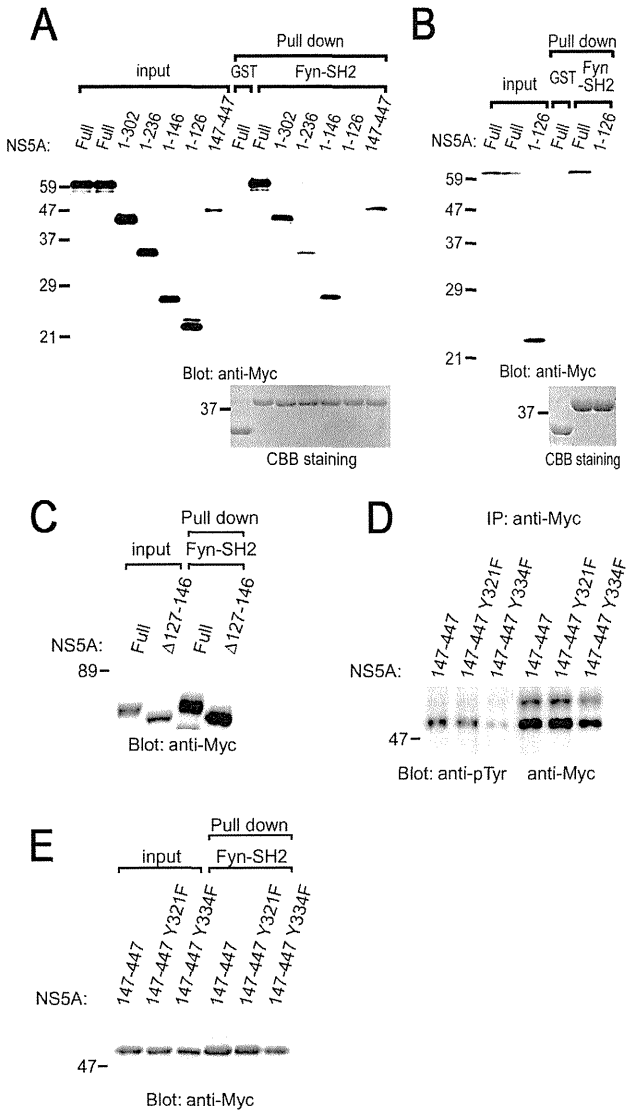

Figure 3. Structural analysis of the association of NS5A with the SH2 domain of Fyn in B cells. COS cells (A, C, E) or B cells (Ramos-T) (B) expressing different kinds of NS5A were stimulated with PV and subjected to pull-down assay using GST-Fyn-SH2. Binding proteins were separated by SDS-PAGE and analyzed with immunoblotting with anti-Myc mAb. The amount of GST-fusion proteins was confirmed by CBB staining. (D) COS cells expressing different kinds of NS5A mutants were stimulated with PV and subjected to immunoprecipitation. Precipitated proteins were separated by SDS-PAGE and analyzed with immunoblotting with anti-pTyr (PY20) and anti-Myc mAbs. Molecular sizing markers are indicated at left in kilodalton. The results were representative of three independent experiments.
doi:10.1371/journal.pone.0046634.g003

domain of Fyn (Fig. 3C). This suggests that NS5A Δ127–146 could interact with the SH2 domain of Fyn through NS5A 147–447.

Identification of Tyr^{334} as a tyrosine phosphorylation site in NS5A

In COS cells, full length and a series of deletion mutants of NS5A were tyrosine phosphorylated by PV treatment (Fig. S2). Because NS5A 1–126 could not bind to the SH2 domain of Fyn, we examined the possible involvement of tyrosine residue between amino acids number 127 and 146 for the binding. In this region, there is only one tyrosine residue that appears to be conserved. However, substitution of Tyr^{129} to Phe of truncated NS5A (NS5A 1–146 Y129F) still allowed tyrosine phosphorylation by PV and binding to the SH2 domain of Fyn in COS cells (Fig. S2 and S3). Thus, Tyr^{129} is not critical for the binding of NS5A to the SH2 domain of Fyn. In addition to this region (127 to 146), we examined the conserved tyrosine residues between 147 and 447 of NS5A (Tyr^{182}, Tyr^{321}, and Tyr^{334}). Among those, substitution of Tyr^{334} to Phe (Y334F) reduced tyrosine phosphorylation of NS5A 147–447, however this mutant could interact with the SH2 domain of Fyn (Fig. 3D and E). NS5A Y182F and Y321F were tyrosine phosphorylated as NS5A 147–447 (Fig. 3D and data now shown). Therefore, these results suggest that Tyr^{334} is required for tyrosine phosphorylation of NS5A, and existence of the multiple mechanisms for the binding of NS5A with Fyn including pTyr-SH2 domain interaction. Furthermore, we could not detect the increase in tyrosine phosphorylation of NS5A by *in vitro* kinase reaction with Fyn (data not shown), suggesting that some other protein-tyrosine kinases are required for phosphorylating NS5A.

The SH2 domain of Fyn directly binds to NS5A

Next we examined the mechanism of the interaction of the SH2 domain of Fyn and NS5A. Association of Fyn and NS5A in B cells were tested by the immunoprecipitation study (Fig. 4A). The result showed that NS5A was coprecipitated with anti-Fyn antibody, and vice versa. Therefore, NS5A complexes with Fyn in B cells. Far-western analysis further demonstrated that the SH2 domain of Fyn could directly bind to NS5A, suggesting that NS5A is tyrosine phosphorylated in B cells (Fig. 4B). We have shown that PV treatment of cells stimulates tyrosine phosphorylation of NS5A (Fig. 1B). These results demonstrate that NS5A could be tyrosine phosphorylated in B cells and directly associated with the SH2 domain of Fyn. In addition, we demonstrated the subcellular fractionation by sucrose density gradient centrifugation (Fig. 4C). Fractions 2–4 were regarded as low density detergent-insoluble fractions, whereas 5–9 were detergent-soluble fractions. As shown, NS5A broadly located in almost all of the fractions. In contrast, most of Fyn was located in detergent-insoluble fractions because of the lipid modification of Fyn (fractions 2–4), and some were in the detergent-soluble fractions (fractions 5–9). These results demonstrate that some of NS5A and Fyn are located in low density detergent-insoluble fractions in B cells.

Association with NS5A increases autophosphorylation and kinase activity of Fyn

Finally, we examined the effect of the expression of NS5A on the function of Fyn tyrosine kinase (Fig. 4D). Cross-linking of B cell receptor by anti-IgM mAb resulted in the increase in phosphorylation of a tyrosine residue in the activation loop of the kinase domain of Fyn, which parallels to its kinase activity [10]. Immunoprecipitation and immunoblotting experiments demonstrated that coexpression of NS5A increases phosphorylation of activation loop tyrosine and anti-IgM stimulation enhances this phenomenon. Immunoblot quantification also indicated the significant higher phosphorylation of the activation loop of Fyn in the unstimulated state in the NS5A expressing cells. In addition, we examined the biochemical kinase activity of Fyn by *in vitro* kinase assay (Fig. 4E). Coexpression of NS5A enhanced the kinase activity of Fyn as measured by both autophosphorylation and phosphorylation of exogenous substrate (enolase). This result biochemically demonstrated that association with NS5A increases tyrosine kinase activity of Fyn to phosphorylate tyrosine residues on Fyn itself and exogenous substrate. These results suggest that association of NS5A enhances an autophosphorylation and kinase activity of Fyn in B cells.

Discussion

We have demonstrated the possible tyrosine phosphorylation of NS5A in B cells and the interaction of NS5A with the SH2 domain of Fyn, in addition to SH3 domain. Previous reports demonstrated that cells harboring HCV replicon possesses the increased kinase activity of Fyn, which supports our conclusion of this study [9]. NS5A contains a highly conserved proline rich regions with Pro-X-X-Pro-X-Arg motif which is capable of the interaction with the SH3 domains of variety of cellular proteins, including Fyn [24]. Our finding reveals the second interaction site of Fyn to associate with NS5A. Therefore, NS5A could associate with both SH3 and SH2 domains. Through the two interactions, via SH3 and SH2 domains, it is predicted that NS5A could alter the conformation of Fyn to open active state. Physiological mechanism has generally been recognized that adaptor proteins with ligands of SH2 and SH3 domains bind to Src family kinases and positively regulates the kinase activity. Consistent with previous reports, our study demonstrated that NS5A protein containing potential ligands for both SH3 and SH2 domains increases autophosphorylation of Fyn in B cells.

Fyn has two tyrosine phosphorylation sites; one tyrosine in the activation loop is phosphorylated by autophosphorylation and the other in the C-terminal tail is phosphorylated by Csk to negatively regulate the kinase activity. In this manuscript, we examine the phosphorylation of tyrosine in the activation loop by using anti-phospho-Src family (Tyr416) antibody, which detects phosphorylated amount of a conserved tyrosine in the activation loop of Src family kinase (Fig. 4D). Therefore, we could conclude that tyrosine phosphorylation of Fyn was occurred in Tyr^{420} in the kinase domain.

The small interference RNA library screening study demonstrated that Csk is one of the protein-tyrosine kinases involved in the replication of HCV [25]. Csk is known to phosphorylate tyrosine residue in the C-terminal tail and negatively regulate Src family kinase, such as Fyn. Knock down of Fyn resulted in up-regulation of HCV replication [25]. This suggests that activation of Fyn suppresses HCV replication. In light of the aberrant increase in autophosphorylation of Fyn by NS5A coexpression, it is possible that NS5A negatively regulates HCV replication with activating Fyn kinase assumedly for persistent infection.

v-Src is the first discovered oncogene, and Fyn is a member of cellular Src family kinases and is also associated with cancer. Overexpression of Fyn in NIH3T3 fibroblast cells exhibited a cancer-like phonotype with increased anchorage-independent growth and prominent morphologic changes. Other studies have revealed that overexpression of Fyn results in promotion of the anti-apoptotic activity of Akt and dysregulation of anchorage-dependent cell growth. In this study, expression of NS5A enhanced autophosphorylation of Fyn in B cells, suggesting that

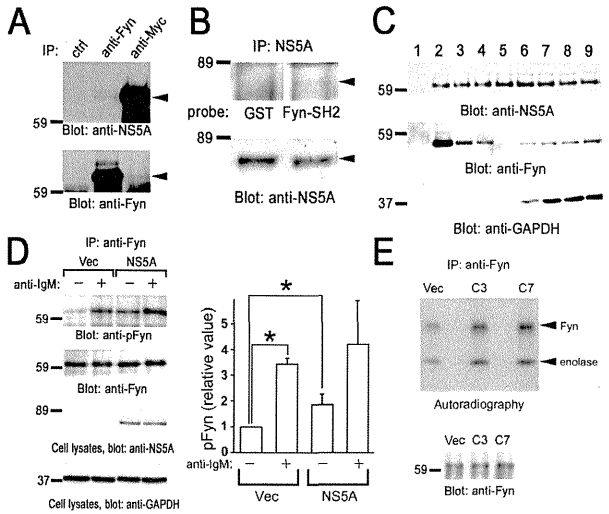

Figure 4. Association with NS5A increases the kinase activity of Fyn in B cells. (A) Endogenous interaction of Fyn with NS5A in BJAB cells. Cells were solubilized in the lysis buffer containing 0.5% Nonidet P-40. Detergent-soluble lysates from BJAB cells expressing Myc-His-NS5A (clone 7) were subjected to immunoprecipitation with anti-Fyn or anti-Myc antibodies. Protein interactions between NS5A and Fyn were analyzed by the immunoblotting with anti-NS5A mAb and anti-Fyn antibody, respectively. (B) Anti-Myc immunoprecipitates were separated by SDS-PAGE and subjected to far western analysis with GST or GST-Fyn-SH2 (GST-Fyn-SH2) (upper panel), and immunoblotting analysis with anti-NS5A mAb (lower panel). (C) Cell homogenates were fractionated by sucrose density gradient centrifugation. Proteins from these fractions were separated by SDS-PAGE and analyzed with immunoblotting with anti-NS5A mAb, anti-Fyn, and anti-GAPDH antibodies. (D) Control cells (Vec) and cells expressing Myc-His-NS5A (clone 7) were unstimulated (−) or stimulated (+) with anti-IgM mAb. Anti-Fyn immunoprecipitates (IP) were separated by SDS-PAGE and analyzed by immunoblotting with anti-phospho-Src family (Tyr416) antibody recognizing autophosphorylated Fyn (pFyn) and anti-Fyn antibody. Detergent-soluble lysates were separated by SDS-PAGE and analyzed by immunoblotting with anti-NS5A and anti-GAPDH mAbs. Densitometry analysis was performed on three experiments representative of Fig. 4D. Levels of pFyn were normalized to their respective total Fyn protein. The fold changes of pFyn are shown relative to unstimulated control cells. Data represent the mean ± SD of three independent experiments. *, $P<0.05$. (E) Anti-Fyn immunoprecipitates (IP) from control cells (Vec), cells expressing Myc-His-NS5A clone 3 (C3) and clone 7 (C7) were subjected to *in vitro* kinase assay using enolase as an exogenous substrate. Radioactive proteins were separated by SDS-PAGE and visualized by autoradiography. Immunoprecipitated Fyn was analyzed by immunoblotting. Molecular sizing markers are indicated at left in kilodalton. The results were representative of three independent experiments. Similar results were obtained when another line was examined.
doi:10.1371/journal.pone.0046634.g004

HCV-mediated activation of Fyn can promote aberrant growth and anti-apoptotic status leading to B lymphomagenesis [8].

Adaptor proteins have also been recognized candidates to promote oncogenes. For example, v-Crk (CT10 regulator of tyrosine kinase)/Crk-I are adaptor proteins composed of SH2 and SH3 domains but lack negative regulatory region (phosphotyrosine and C-terminal SH3 domain). Those adaptors function as constitutively activated ones, leading to tumorgenesis. Like that, NS5A presumably works constitutive activated adaptor for Fyn kinase [26].

In conclusion, present study demonstrated that NS5A binds to the SH2 domain of Fyn in tyrosine phosphorylation-dependent manner and that NS5A containing ligand for both SH2 and SH3 domains produces an aberrant increase in autophosphorylation and kinase activity of Fyn. Further studies are needed to clarify which tyrosine residues in NS5A are phosphorylated and bind to SH2 domain of Fyn. These data, however, may contribute to our understanding of the mechanisms that HCV infection causes B lymphomagenesis.

Supporting Information

Figure S1 GST-human Fyn-SH2 could react with NS5A. The cDNA for human Fyn-SH2 (Trp^{149}-Arg^{268}) were amplified by PCR using paired primers 5′-GGAATTCATGGTACTTTG-GAAAACTTGGC-3′ and 5′-GATCAACTGCAGGGATTCT-CG -3′, using cDNA from total RNA of BJAB cells as a template. Resulted PCR fragment was subcloned into the pGEX-4T.3 (GE Healthcare) to make domain in-frame with the downstream of GST and verified by DNA sequencing. PV-treated cells expressing Myc-His-NS5A (clone 7) were solubilized in the lysis buffer. Precleared lysates were reacted with GST or GST-human Fyn-SH2 and binding proteins were separated by SDS-PAGE and analyzed with immunoblotting with anti-NS5A mAb. The amount of GST-fusion proteins was confirmed by CBB staining. Molecular sizing markers are indicated at left in kilodalton. The results are representative of two independent experiments.
(TIF)

Figure S2 Tyrosine phosphorylation of NS5A and its mutants in COS cells. Full length and a series of deletion

mutants of NS5A were transiently expressed in COS cells. Cells were unstimulated (−) or stimulated (+) with PV and solubilized in the lysis buffer. Cell lysates were immunoprecipitated with anti-Myc mAb and immunoprecipitated proteins were separated by SDS-PAGE and analyzed with immunoblotting with anti-pTyr (PY20) and anti-Myc mAbs. Molecular sizing markers are indicated at left in kilodalton. The results were representative of three independent experiments.
(TIF)

Figure S3 Tyr^{129} is not critical for the binding of NS5A to the SH2 domain of Fyn. Indicated mutant forms of NS5A were transiently expressed in COS cells. Cells were unstimulated (−) or stimulated (+) with PV. Cells were solubilized in the binding buffer and precleared lysates were reacted with GST-Fyn-SH2. Detergent-soluble lysates and binding proteins were separated by SDS-PAGE and analyzed with immunoblotting with anti-Myc mAb. Molecular sizing markers are indicated at left in kilodalton. The results were representative of three independent experiments.
(TIF)

Acknowledgments

We are grateful to Dr. R. Bartenschlager (University of Heidelberg, Germany) for providing an HCV subgenomic replicon (pFK5B/2884 Gly), to Ms. Satomi Nishibata and Ms. Kuniyo Miyagoshi for the assistance, and to Dr. Shinkou Kyo (Kobe University Graduate School of Medicine, Toyooka Public Hospital, Hyogo, Japan) and Dr. Keiko Kawauchi (Mechanobiology Institute, Singapore) for experimental assistance.

Author Contributions

Conceived and designed the experiments: KN KT HH KS. Performed the experiments: KN KT TH XS KS. Analyzed the data: KN KT KC HH KS. Contributed reagents/materials/analysis tools: KN KT KC TH XS LD IS HH KS. Wrote the paper: KN HH KS.

References

1. Moradpour D, Penin F, Rice CM (2007) Replication of hepatitis C virus. Nat Rev Microbiol 5: 453–463.
2. Suzuki T, Aizaki H, Murakami K, Shoji I, Wakita T (2007) Molecular biology of hepatitis C virus. J Gastroenterol 42: 411–423.
3. Agnello V, Chung RT, Kaplan LM (1992) A role for hepatitis C virus infection in type II cryoglobulinemia. New Engl J Med 327: 1490–1495.
4. Morsica G, Tambussi G, Sitia G, Novati R, Lazzarin A, et al. (1999) Replication of hepatitis C virus in B lymphocytes (CD19(+)). Blood 94: 1138–1139.
5. Gisbert JP, Garcia-Buey L, Pajares JM, Moreno-Otero R (2003) Prevalence of hepatitis C virus infection in B-cell non-Hodgkin's lymphoma: Systematic review and meta-analysis. Gastroenterology 125: 1723–1732.
6. Machida K, Cheng KTH, Pavio N, Sung VMH, Lai MMC (2005) Hepatitis C virus E2-CD81 interaction induces hypermutation of the immunoglobulin gene in B cells. J Virol 79: 8079–8089.
7. Ito M, Murakami K, Suzuki T, Mochida K, Suzuki M, et al. (2010) Enhanced expression of lymphomagenesis-related genes in peripheral blood B cells of chronic hepatitis C patients. Clin Immunol 135: 459–465.
8. Saito YD, Jensen AR, Salgia R, Posadas EM (2010) Fyn A Novel Molecular Target in Cancer. Cancer 116: 1629–1637.
9. Macdonald A, Crowder K, Street A, McCormick C, Harris M (2004) The hepatitis C virus NS5A protein binds to members of the Src family of tyrosine kinases and regulates kinase activity. J Gen Virol 85: 721–729.
10. Bradshaw JM (2010) The Src, Syk, and Tec family kinases: Distinct types of molecular switches. Cell Signal 22: 1175–1184.
11. Inubushi S, Nagano-Fujii M, Kitayama K, Tanaka M, An C, et al. (2008) Hepatitis C virus NS5A protein interacts with and negatively regulates the non-receptor protein tyrosine kinase Syk. J Gen Virol 89: 1231–1242.
12. Pfannkuche A, Buther K, Karthe J, Poenisch M, Bartenschlager R, et al. (2011) c-Src is required for complex formation between the hepatitis C virus-encoded proteins NS5A and NS5B: A prerequisite for replication. Hepatology 53: 1127–1136.
13. Ishido S, Choi JK, Lee BS, Wang CY, DeMaria M, et al. (2000) Inhibition of natural killer cell-mediated cytotoxicity by kaposi's sarcoma-associated herpesvirus K5 protein. Immunity 13: 365–374.
14. Ogi K, Nakashima K, Chihara K, Takeuchi K, Horiguchi T, et al. (2011) Enhancement of B-cell receptor signaling by a point mutation of adaptor protein 3BP2 identified in human inherited disease cherubism. Genes Cells 16: 951–960.
15. Sada K, Miah SM, Maeno K, Kyo S, Qu X, et al. (2002) Regulation of FcεRI-mediated degranulation by an adaptor protein 3BP2 in rat basophilic leukemia RBL-2H3 cells. Blood 100: 2138–2144.
16. Rao N, Ghosh AK, Ota S, Zhou P, Reddi AL, et al. (2001) The non-receptor tyrosine kinase Syk is a target of Cbl-mediated ubiquitylation upon B-cell receptor stimulation. EMBO J 20: 7085–7095.
17. Shukla U, Hatani T, Nakashima K, Ogi K, Sada K (2009) Tyrosine Phosphorylation of 3BP2 Regulates B Cell Receptor-mediated Activation of NFAT. J Biol Chem 284: 33719–33728.
18. Blight KJ, McKeating JA, Rice CM (2002) Highly permissive cell lines for subgenomic and genomic hepatitis C virus RNA replication. J Virol 76: 13001–13014.
19. Nakashima K, Takeuchi K, Chihara K, Hotta H, Sada K (2011) Inhibition of hepatitis C virus replication through adenosine monophosphate-activated protein kinase-dependent and -independent pathways. Microbiol Immunol 55: 774–782.
20. Maeno K, Sada K, Kyo S, Miah SM, Kawauchi-Kamata K, et al. (2003) Adaptor protein 3BP2 is a potential ligand of Src homology 2 and 3 domains of Lyn protein-tyrosine kinase. J Biol Chem 278: 24912–24920.
21. Miah SM, Hatani T, Qu X, Yamamura H, Sada K (2004) Point mutations of 3BP2 identified in human inherited disease cherubism results in the loss of function. Genes Cells 9: 993–1004.
22. Chihara K, Nakashima K, Takeuchi K, Sada K (2011) Association of 3BP2 with SHP-1 regulates SHP-1-mediated production of TNF-α in RBL-2H3 cells. Genes Cells 16: 1133–1145.
23. Qu X, Sada K, Kyo S, Maeno K, Miah SM, et al. (2004) Negative regulation of FcεRI-mediated mast cell activation by a ubiquitin-protein ligase Cbl-b. Blood 103: 1779–1786.
24. Shelton H, Harris M (2008) Hepatitis C virus NS5A protein binds the SH3 domain of the Fyn tyrosine kinase with high affinity: mutagenic analysis of residues within the SH3 domain that contribute to the interaction. Virol J 5: 24. Available: http://www.virologyj.com/content/5/1/24.
25. Supekova L, Supek F, Lee J, Chen S, Gray N, et al. (2008) Identification of human kinases involved in hepatitis C virus replication by small interference RNA library screening. J Biol Chem 283: 29–36.
26. Birge RB, Kalodimos C, Inagaki F, Tanaka S (2009) Crk and CrkL adaptor proteins: networks for physiological and pathological signaling. Cell Commun Signal 7: 13. Available: http://www.biosignaling.com/content/7/1/13.

JVI Journals.ASM.org

Hepatitis C Virus Infection Suppresses GLUT2 Gene Expression via Downregulation of Hepatocyte Nuclear Factor 1α

Chieko Matsui,[a] Ikuo Shoji,[a] Shusaku Kaneda,[a] Imelda Rosalyn Sianipar,[a,b] Lin Deng,[a] and Hak Hotta[a]

Division of Microbiology, Center for Infectious Diseases, Kobe University Graduate School of Medicine, Chuo-ku, Kobe, Hyogo, Japan,[a] and Department of Physiology, Faculty of Medicine, Universitas Indonesia, Jakarta, Indonesia[b]

Hepatitis C virus (HCV) infection causes not only intrahepatic diseases but also extrahepatic manifestations, including type 2 diabetes. We previously reported that HCV replication suppresses cellular glucose uptake by downregulation of cell surface expression of glucose transporter 2 (GLUT2) (D. Kasai et al., J. Hepatol. 50:883–894, 2009). GLUT2 mRNA levels were decreased in both HCV RNA replicon cells and HCV J6/JFH1-infected cells. To elucidate molecular mechanisms of HCV-induced suppression of GLUT2 gene expression, we analyzed transcriptional regulation of the GLUT2 promoter using a series of GLUT2 promoter-luciferase reporter plasmids. HCV-induced suppression of GLUT2 promoter activity was abrogated when the hepatocyte nuclear factor 1α (HNF-1α)-binding motif was deleted from the GLUT2 promoter. HNF-1α mRNA levels were significantly reduced in HCV J6/JFH1-infected cells. Furthermore, HCV infection remarkably decreased HNF-1α protein levels. We assessed the effects of proteasome inhibitor or lysosomal protease inhibitors on the HCV-induced reduction of HNF-1α protein levels. Treatment of HCV-infected cells with a lysosomal protease inhibitor, but not with a proteasome inhibitor, restored HNF-1α protein levels, suggesting that HCV infection promotes lysosomal degradation of HNF-1α protein. Overexpression of NS5A protein enhanced lysosomal degradation of HNF-1α protein and suppressed GLUT2 promoter activity. Immunoprecipitation analyses revealed that the region from amino acids 1 to 126 of the NS5A domain I physically interacts with HNF-1α protein. Taken together, our results suggest that HCV infection suppresses GLUT2 gene expression via downregulation of HNF-1α expression at transcriptional and posttranslational levels. HCV-induced downregulation of HNF-1α expression may play a crucial role in glucose metabolic disorders caused by HCV.

Hepatitis C virus (HCV) is the main cause of chronic hepatitis, liver cirrhosis, and hepatocellular carcinoma. HCV is a single-stranded, positive-sense RNA virus that is classified into the *Flaviviridae* family, *Hepacivirus* genus (21). More than 170 million people worldwide are chronically infected with HCV. The 9.6-kb HCV genome encodes a polyprotein of approximately 3,010 amino acids (aa). The polyprotein is cleaved co- and posttranslationally into at least 10 proteins by viral proteases and cellular signalases: the structural proteins core, E1, E2, and p7 and the nonstructural proteins NS2, NS3, NS4A, NS4B, NS5A, and NS5B (21).

Persistent HCV infection causes not only intrahepatic diseases but also extrahepatic manifestations, such as type 2 diabetes. Clinical and experimental data suggest that HCV infection is an additional risk factor for the development of diabetes (26, 29, 30). HCV-related glucose metabolic changes and insulin resistance have significant clinical consequences, such as accelerated fibrogenesis, reduced virological response to alpha interferon (IFN-α)-based therapy, and increased incidence of hepatocellular carcinoma (29). Therefore, the molecular mechanism of HCV-related diabetes needs to be clarified.

We have sought to identify a novel mechanism of HCV-induced diabetes. We previously demonstrated that HCV suppresses hepatocytic glucose uptake through downregulation of cell surface expression of glucose transporter 2 (GLUT2) in a human hepatoma cell line (19). The uptake of glucose into cells is conducted by facilitative glucose carriers, i.e., glucose transporters (GLUTs). GLUTs are integral membrane proteins that contain 12 membrane-spanning helices. To date, a total of 14 isoforms have been identified in the GLUT family (24). GLUT2 is expressed in the liver, pancreatic β-cells, hypothalamic glial cells, retina, and enterocytes. Glucose is transported into hepatocytes by GLUT2 (34). We previously reported that GLUT2 expression was reduced in hepatocytes obtained from HCV-infected patients (19). We also demonstrated that GLUT2 mRNA levels were lower in HCV replicon cells and in HCV J6/JFH1-infected cells than in the control cells. GLUT2 promoter activity was suppressed in HCV-replicating cells. However, the molecular mechanism of HCV-induced suppression of GLUT2 gene expression remains to be elucidated.

In the present study, we aimed to clarify molecular mechanisms of HCV-induced suppression of GLUT2 gene expression. We analyzed transcriptional regulation of the GLUT2 promoter in HCV replicon cells. We demonstrate that HCV infection downregulates hepatocyte nuclear factor 1α (HNF-1α) expression at both transcriptional and posttranslational levels, resulting in suppression of GLUT2 promoter. We propose that HCV-induced downregulation of HNF-1α may play a crucial role in glucose metabolic disorders caused by HCV.

MATERIALS AND METHODS

Cell culture. The human hepatoma cell line Huh-7.5 (4) was kindly provided by Charles M. Rice (The Rockefeller University, New York, NY).

Received 8 June 2012 Accepted 11 September 2012
Published ahead of print 19 September 2012
Address correspondence to Hak Hotta, hotta@kobe-u.ac.jp, or Ikuo Shoji, ishoji@med.kobe-u.ac.jp.

doi:10.1128/JVI.01418-12

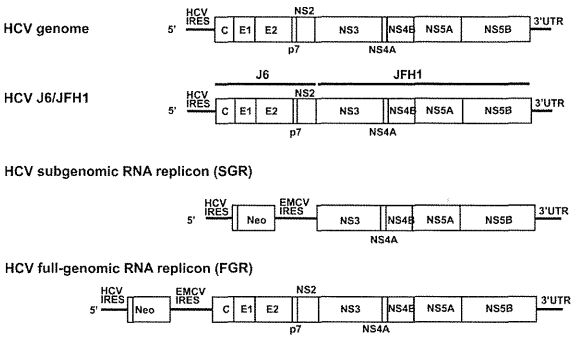

FIG 1 The HCV genome, chimeric HCV J6/JFH1, and the HCV RNA replicons. Schematic diagrams of the HCV genome, the chimeric HCV J6/JFH1 genome, SGR, and FGR are shown. IRES, internal ribosome entry site; EMCV, encephalomyocarditis virus; Neo, neomycin resistance gene.

Cells were cultured in Dulbecco's modified Eagle's medium (DMEM) (high glucose) with L-glutamine (Wako, Osaka, Japan) supplemented with 50 IU/ml penicillin, 50 μg/ml streptomycin (Gibco, NY), 10% heat-inactivated fetal bovine serum (Biowest, France), and 0.1 mM nonessential amino acids (Invitrogen, NY) at 37°C in a 5% CO_2 incubator. Cells were transfected with plasmid DNA using FuGENE 6 transfection reagents (Promega, Madison, WI).

Huh-7.5 cells stably harboring an HCV-1b subgenomic RNA replicon (SGR) were prepared as described previously (18), using pFK5B/2884Gly (a kind gift from R. Bartenschlager, University of Heidelberg, Heidelberg, Germany). The SGR cells express the genomic region from NS3 to NS5B of the HCV Con1 strain (19) (Fig. 1). Cells harboring a full-genome HCV-1b RNA replicon (FGR) derived from Con1 (27) or pON/C-5B (17, 19) (a kind gift from N. Kato, Okayama University, Okayama, Japan) were also used. The FGR cells express all of the HCV proteins (the region ranging from the core protein to NS5B).

The pFL-J6/JFH1 plasmid that encodes the entire viral genome of a chimeric strain of HCV-2a, J6/JFH1 (23), was kindly provided by Charles M. Rice. The HCV genome RNA was synthesized *in vitro* using pFL-J6/JFH1 as a template and was transfected into Huh-7.5 cells by electroporation (6, 9, 23, 37). The virus produced in the culture supernatant was used for infection experiments (6).

Cells were treated with 1,000 IU/ml of IFN-α (Sigma, St. Louis, MO) for 10 days to eliminate HCV replication (19).

Luciferase reporter assay. We constructed the human GLUT2 promoter-luciferase reporter plasmid by cloning a 1.6-kb genomic fragment that encompasses the human GLUT2 promoter region from −1291 to +308, yielding pGLUT2(−1291/+308)-Luc (2, 19), into the pGL4 vector plasmid (Promega). The pGLUT2(−1291/+308)-Luc construct contains a 1,291-bp fragment of the human GLUT2 promoter upstream of the minimal promoter and the coding sequence of the *Photinus pyralis* (firefly) luciferase. We also used seven different GLUT2 promoter-luciferase reporter plasmids, i.e., pGLUT2(−1193/+308)-Luc, pGLUT2 (−1155/+308)-Luc, pGLUT2(−1100/+308)-Luc, pGLUT2(−1030/+308)-Luc, pGLUT2(−206/+308)-Luc, pGLUT2(+29/+308)-Luc, and pGLUT2(+126/+308)-Luc, which lack the binding sequence of the CCAAT/enhancer binding site (C/EBP), cyclic AMP (cAMP) response element (CRE), AP-1 binding site, HNF-1α binding site, CAAT box, TATA-like motif, and transcriptional initiation, respectively (Fig. 2A). The reporter plasmid pRL-CMV-*Renilla* (where CMV is cytomegalovirus) (Promega) was used as an internal control. Cells were transfected with each pGLUT2-Luc construct together with pRL-CMV-*Renilla*. At 48 h after transfection, samples were harvested and assayed for luciferase activity. The luciferase assays were performed using a dual-luciferase reporter assay system (Promega). Luciferase activity was measured by a Lumat LB 9501 instrument (Berthold Technologies GmbH & Co., Bad Wildbad, Germany). Firefly luciferase activity was normalized to *Renilla* luciferase activity for each sample. The number of relative light units (RLU) of the SGR cells or FGR cells transfected with each reporter plasmid is expressed as a ratio of the number of Huh-7.5 cells transfected with each reporter plasmid.

Expression plasmids. Expression plasmids for core protein, p7, NS2, NS3, NS4A, NS4B, NS5A, and NS5B were described previously (9, 10, 18). To express E1 and E2 (E1/E2), the cDNA fragment of nucleotides (nt) 825 to 2676 derived from the HCV Con1 strain was amplified by PCR using the plasmid pFKI389neo/core-3′/Con1 (a kind gift from R. Bartenschlager) as a template. Specific primers used for PCR were as follows: sense primer, 5′-CCAGTGTGGTGAATTCAC CATGGTGAACTATGCAACAGGGAA-3′; antisense primer, 5′-CGAAG GGCCCTCTAGAGATGTACCAGGCAGCACAGA-3′. To express NS3 and NS4A (NS3/4A), the cDNA fragment of nt 3420 to 5474 derived from the HCV Con1 strain was amplified by PCR. Specific primers were as follows: sense primer, 5′-CCAGTGTGGTGAATTCACCATGGCGCCTA TTACGGCCTACTC-3′; antisense primer, 5′-CGAAGGGCCCTCTAGA GCACTCTTCCATCTCATCGAA-3′. These amplified PCR products were purified, and each of them was inserted into the EcoRI-XbaI site of pEF1/myc-His A (Invitrogen) using an In-Fusion HD-Cloning kit (Clontech, Mountain View, CA). To express a series of NS5A deletion mutants as hemagglutinin (HA)-tagged proteins, each fragment was amplified by PCR and cloned into the NotI site of pCAG-HA. pEF1A-NS5A (Con1)-myc-His was used as a template (18). The primer sequences used in this study are available from the authors upon request. The sequences of the inserts were extensively verified by sequencing (Operon biotechnology, Tokyo, Japan). The plasmids pEF1A-NS5A(1–126)-myc-His, consisting of residues 1 to 126 in NS5A, and pEF1A-NS5A(1–147)-myc-His were described previously (18).

Antibodies. The mouse monoclonal antibodies (MAbs) used in this study were anti-FLAG (M2) MAb (F-3165; Sigma), anti-NS5A MAb (MAB8694; Millipore), anti-core protein MAb (2H9) (37), and anti-glyceraldehyde-3-phosphate dehydrogenase (GAPDH) MAb (MAB374; Millipore). Polyclonal antibodies (PAbs) used in this study were anti-HNF-1α rabbit PAb (sc-8986; Santa Cruz Biotechnology), anti-HNF-1α goat PAb (sc-6548; Santa Cruz Biotechnology), anti-NS5B goat PAb (sc-17532; Santa Cruz Biotechnology), anti-NS3 rabbit PAb (described elsewhere), and anti-actin goat PAb (C-11; Santa Cruz Biotechnology). Horseradish peroxidase (HRP)-conjugated anti-mouse IgG antibody (Cell signaling), HRP-conjugated donkey anti-goat IgG (Santa Cruz Biotechnology), and HRP-conjugated anti-rabbit IgG (Cell signaling) were used as secondary antibodies.

Real-time quantitative reverse transcription-PCR (RT-PCR). Total cellular RNA was isolated using RNAiso reagent (TaKaRa Bio, Kyoto, Japan), and cDNA was generated using a QuantiTect Reverse Transcription system (Qiagen, Valencia, CA). Real-time quantitative PCR was performed using SYBR Premix *Ex Taq* (TaKaRa Bio) with SYBR green chemistry on an ABI Prism 7000 system (Applied Biosystems, Foster, CA), as described previously (11, 19). The β-glucuronidase (GUS) gene was used as an internal control. The primers used for real-time PCR are as follows: for HNF-1α (NM_000545), 5′-AGCTACCAACCAAGAAGGGGC-3′ (nt 601 to 621) and 5′-TGACGAGGTTGGAGCCCAGCC-3′ (nt 801 to 781); HNF-1β (NM_000458), 5′-GTTACATGCAGCAACACAACA-3′ (nt 600 to 620) and 5′-TCATATTTCCAGAACTCTGGA-3′ (nt 801 to 782); GUS (NM_000181), 5′-ATCAAAAACGCAGAAAATACG-3′ (nt 1797 to 1817) and 5′-ACGCAGGTGGTATCAGTCTTG-3′ (nt 2034 to 2014).

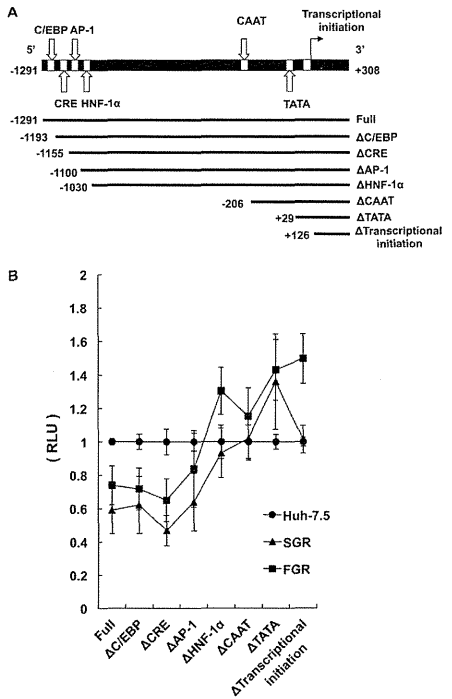

FIG 2 HNF-1α-binding site is important for HCV-induced suppression of GLUT2 promoter. (A) A series of constructs in which genomic GLUT2 promoter DNA fragments were fused to a promoterless firefly luciferase gene of the pGL4 vector were generated with the 3′ end always terminating at bases +308 from transcriptional start site. The 5′ ends began at bases −1291, −1193, −1155, −1100, −1030, −206, +29, and +126 The regions that represent potential binding sites for transcription factors are shown, including a CCAAT/enhancer binding site (C/EBP), cAMP response element (CRE), AP-1 binding site, HNF-1α binding site, CAAT box, and TATA-like motif. The nucleotide at the beginning of the construct is indicated. (B) Huh-7.5 cells, SGR cells, and FGR cells (2.5×10^5 cells/six-well plate) were transfected with each GLUT2 plasmid (0.5 μg) together with pRL-CMV-*Renilla* (25 ng). pRL-CMV-*Renilla* was used as an internal control. At 48 h posttransfection, cells were harvested and assayed for luciferase activities using a dual-luciferase reporter assay system. RLU is expressed as a ratio of the Huh-7.5 cells transfected with each reporter plasmid.

Immunoblot analysis. Immunoblot analysis was performed essentially as described previously (9, 33). The cell lysates were separated by 8% sodium dodecyl sulfate-polyacrylamide gel electrophoresis (SDS-PAGE) and transferred to polyvinylidene difluoride membrane (Millipore Corp., Billerica, MA). The membranes were incubated with primary antibody, followed by incubation with peroxidase-conjugated secondary antibody. The positive bands were visualized using ECL Western blotting detection reagents (GE Healthcare, Buckinghamshire, United Kingdom). To detect endogenous HNF-1α protein, ECL Plus Western blotting detection reagents were used (GE Healthcare).

Immunoprecipitation. Cultured cells were lysed with a buffer containing 150 mM NaCl, 20 mM Tris-HCl (pH 7.4), 0.1% SDS, 1% NP-40, and Complete protease inhibitor cocktail (Roche Diagnostics, Indianapolis, IN). The lysate was centrifuged at 12,000 × *g* for 20 min at 4°C, and the supernatant was immunoprecipitated with appropriate antibodies. Immunoprecipitation was performed as described previously (10). Briefly, the cell lysates were immunoprecipitated with control IgG and Dynabeads protein A (Invitrogen) and incubated with appropriate antibodies at 4°C overnight. After being washed with the washing buffer (0.1 M Na-phosphate buffer, pH 7.4) five times, the immunoprecipitates were analyzed by immunoblotting.

Statistical analysis. Results were expressed as means ± standard errors of the means (SEM). Statistical significance was evaluated by analysis of variance (ANOVA), and statistical significance was defined as a P value of <0.05.

RESULTS

HNF-1α-binding site is important for HCV-induced suppression of GLUT2 promoter. To gain an insight into potential regulatory sequences involved in HCV-induced suppression of GLUT2 gene transcription, a 1.6-kb genomic fragment that encompasses the human GLUT2 promoter (−1291 to +308) and a series of deletion mutants were analyzed (Fig. 2A). The ability of the upstream region of the GLUT2 gene to function as a promoter was assessed by its capacity to drive the expression of a luciferase reporter gene. GLUT2 promoter activity was assessed by measuring luciferase activity of the cell extracts derived from transiently transfected Huh-7.5 cells, SGR cells, and FGR cells. As shown in Fig. 2B, a deletion of the promoter sequence to −1100 [pGLUT2(−1100/+308)-Luc [ΔAP-1]] showed lower luciferase activities in HCV replicon cells than in the control cells. Successive removal of nucleotides from −1100 to −1030 completely or almost completely abolished the suppression of the luciferase activity in both FGR and SGR cells, suggesting that the HNF-1α-binding site is important for HCV-induced suppression of GLUT2 promoter.

HCV infection reduces HNF-1α mRNA levels. It is worth noting that HNF-1α is known to play a crucial role in diabetes. Mutations in the HNF-1α gene have been reported to cause a monogenic form of diabetes mellitus with autosomal dominant inheritance, termed maturity onset diabetes of the young 3 (MODY3) (25, 40). Cha et al. (7) reported that HNF-1α functions as a transcriptional transactivator in human GLUT2 gene expression in a human hepatoma cell line. These findings motivated us to further investigate a role of HNF-1α in HCV-induced glucose metabolic disorders in a human hepatoma cell line. To determine

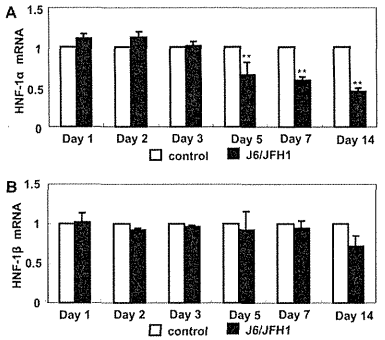

FIG 3 Quantitative RT-PCR analysis of mRNA for HNF-1α and HNF-1β in HCV J6/JFH1-infected cells. Huh-7.5 cells (2.5×10^5 cells/six-well plate) were infected with HCV J6/JFH1 at a multiplicity of infection of 2. Cells were cultured and harvested at the indicated times. Total RNA was extracted, and the levels of HNF-1α mRNA and HNF-1β mRNA were determined by quantitative RT-PCR. Mock-infected cells served as negative controls. **, $P < 0.01$, compared with mock-infected cells.

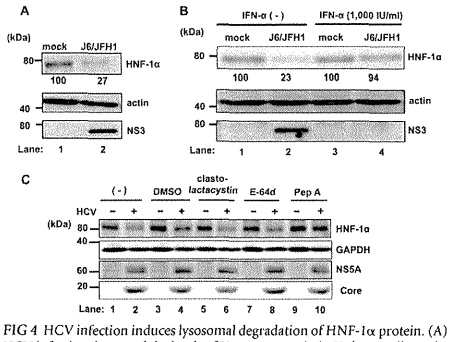

FIG 4 HCV infection induces lysosomal degradation of HNF-1α protein. (A) HCV infection decreased the levels of HNF-1α protein in Huh-7.5 cells. Huh-7.5 cells (2.5×10^5 cells/six-well plate) were infected with HCV J6/JFH1 at a multiplicity of infection of 2. Cells were cultured and harvested at 5 days postinfection. Cells were analyzed by immunoblotting with anti-HNF-1α, anti-NS3, and anti-actin antibodies. The level of actin served as a loading control. The relative levels of protein expression were quantitated by densitometry and are indicated below the respective lanes. (B) HCV-induced downregulation of HNF-1α protein was restored by treatment of the cells with IFN-α. Huh-7.5 cells were plated at 2.5×10^5 cells/six-well plate and cultured for 12 h. The cells were infected with HCV J6/JFH1 at a multiplicity of infection of 2 and cultured for 5 days. The cells were replated at 2.5×10^5 cells/six-well plate and cultured in complete DMEM with or without 1,000 IU/ml IFN-α for 10 days to eliminate HCV. The cells cultured in DMEM without IFN-α served as negative controls. (C) HCV-induced reduction of HNF-1α protein was restored by treatment of the cells with lysosomal protease inhibitor. Huh-7.5 cells were plated at 2.0×10^5 cells/six-well plate and cultured for 12 h. At 5 days postinfection, proteasome inhibitor (30 μM clasto-lactacystin β-lactone) or lysosomal protease inhibitors (40 μM E-64d and 20 μM pepstatin A) were administered to the cells. Cells were cultured for 12 h, harvested, and analyzed by immunoblotting as indicated. The level of GAPDH served as a loading control. DMSO, dimethyl sulfoxide; PepA, pepstatin A.

whether HCV infection suppresses HNF-1α mRNA expression, we quantified mRNA levels of HNF-1α and HNF-1β in HCV J6/JFH1-infected cells and in mock-infected cells by real-time RT-PCR. HNF-1α mRNA levels were significantly reduced in HCV J6/JFH1-infected cells from 5 days postinfection (dpi) to 14 dpi (Fig. 3A). On the other hand, HNF-1β mRNA levels remained unchanged until 14 dpi (Fig. 3B). These results suggest that HCV infection specifically downregulates HNF-1α mRNA expression.

HCV infection reduces HNF-1α protein levels. To determine whether HCV infection reduces HNF-1α protein levels, endogenous HNF-1α protein levels were examined by immunoblot analysis. The HNF-1α protein level was much lower in J6/JFH1-infected cells than in the mock-infected control (Fig. 4A, upper panel, lane 2). To determine whether HCV infection is specifically involved in reduction of HNF-1α protein, we eliminated HCV by treatment of the cells with IFN-α (Fig. 4B, lower panel, compare lane 2 with lane 4). Upon elimination of HCV, the HNF-1α protein expression level recovered to the level of the mock-infected control (Fig. 4B, upper panel, compare lane 2 with lane 4). These results suggest that HCV infection specifically reduces HNF-1α protein levels.

HCV-induced reduction of HNF-1α protein is restored by treatment of the cells with a lysosomal protease inhibitor. As shown in Fig. 3A, HNF-1α mRNA levels in HCV J6/JFH1-infected cells decreased slowly at day 5 postinfection. One possible explanation is that suppression of HNF-1α mRNA is an indirect effect caused by HCV infection. The degree of the reduction of the HNF-1α protein was larger than that of HNF-1α mRNA (Fig. 4A), suggesting the involvement of protein degradation in reduction of HNF-1α protein levels. To determine whether protein degradation is involved in HCV-induced reduction of HNF-1α protein, we assessed the role of proteasome or lysosome proteases in the reduction of HNF-1α protein. We treated the cells with a proteasome inhibitor, clasto-lactacystin β-lactone, or lysosome protease inhibitors E-64d and pepstatin A. Clasto-lactacystin β-lactone had no effect on the levels of HNF-1α protein (Fig. 4C, upper panel, lane 6). This result suggests that proteasome is not involved in the reduction of HNF-1α protein. E-64d is a cysteine protease inhibitor, and pepstatin A is an aspartic protease inhibitor. Pepstatin A, but not E-64d, restored the levels of HNF-1α protein (Fig. 4C, upper panel, lanes 10 and 8). These results suggest that a lysosomal protease, such as an aspartic protease, is involved in HCV-induced reduction of HNF-1α protein.

Overexpression of NS5A protein suppresses GLUT2 promoter activity. To determine which HCV protein is involved in the suppression of GLUT2 promoter, we examined the effects of transient expression of HCV proteins on GLUT2 promoter activity. Huh-7.5 cells were cotransfected with each HCV protein expression plasmid together with the GLUT2 promoter-luciferase plasmid. The pRL-CMV-*Renilla* plasmid was cotransfected as an internal control. At 48 h posttransfection, cells were harvested and assayed for luciferase activity. As shown in Fig. 5A, overexpression of the NS5A expression plasmid significantly reduced GLUT2 promoter activity. On the other hand, other HCV protein expression plasmids failed to suppress GLUT2 promoter activity (Fig. 5A, left and right panels). These results suggest that NS5A protein is involved in the suppression of GLUT2 promoter activity.

Overexpression of NS5A protein reduces the levels of endogenous HNF-1α protein. To investigate a role of NS5A in the suppression of the GLUT2 promoter, we examined the effect of NS5A protein on the levels of endogenous HNF-1α protein. Huh-7.5 cells were transfected with increasing amounts of either an NS5A expression plasmid or NS5B expression plasmid. At 48 h posttransfection, cells were harvested, and the levels of endogenous HNF-1α protein were analyzed by immunoblot analysis. To detect endogenous HNF-1α protein, highly sensitive Western blotting detection reagents (ECL Plus Western blotting detection reagents) were used. Overexpression of NS5A (Fig. 5B, left panel) but not NS5B (Fig. 5B, right panel) significantly reduced endogenous HNF-1α protein. These results suggest that NS5A protein specifically reduces endogenous HNF-1α protein levels.

To determine if NS5A-dependent reduction of HNF-1α protein is due to lysosomal degradation, we treated the cells with lysosome protease inhibitors. Pepstatin A, but not E-64d, recovered the levels of HNF-1α protein (Fig. 5C, middle panel, lanes 5 and 6), which is consistent with the results found in HCV-infected cells. These results suggest that NS5A is responsible for HCV-induced lysosomal degradation of HNF-1α protein. Taken together, our results suggest that HCV infection suppresses GLUT2 promoter activity via NS5A-dependent lysosomal degradation of HNF-1α protein.

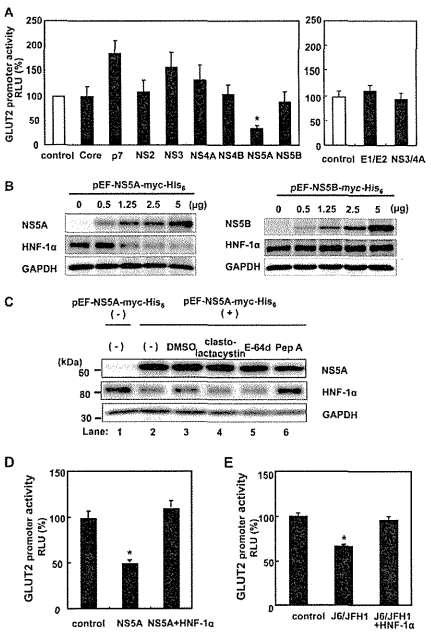

FIG 5 HCV NS5A protein is involved in suppression of GLUT2 promoter activity and lysosomal degradation of HNF-1α protein. (A) Huh-7.5 cells were plated at 1×10^5 cells/12-well plate. After cells were cultured for 12 h, cells were cotransfected with each HCV protein plasmid (0.5 μg), the human GLUT2 promoter reporter plasmid (0.5 μg), and pRL-CMV-*Renilla* (25 ng). pRL-CMV-*Renilla* was used as an internal control. At 48 h posttransfection, cells were harvested. Luciferase assays were performed by using a dual-luciferase reporter assay system. (B) Huh-7.5 cells were plated at 4×10^5 cells/six-well plate and cultured for 12 h. Cells were transfected with increasing amounts of either NS5A plasmid or NS5B plasmid as indicated. At 48 h posttransfection, cells were harvested. Whole-cell lysates were analyzed by immunoblotting with anti-HNF-1α, anti-NS5A, and anti-NS5B antibodies. The level of GAPDH served as a loading control. (C) Huh-7.5 cells (2.5×10^5 cells/six-well plate) were transfected with pEF1A-NS5A-myc-His_6. At 2 days posttransfection, proteasome inhibitor (30 μM clasto-lactacystin β-lactone) or lysosomal enzyme inhibitors (40 μM E-64d and 20 μM pepstatin A) were administered to the cells. Cells were cultured for 12 h and harvested, and the levels of endogenous HNF-1α protein were analyzed by immunoblotting with anti-HNF-1α goat PAb. The level of GAPDH served as a loading control. (D) Huh-7.5 cells (1.0×10^5 cells/12-well plate) were transfected with the human GLUT2 promoter reporter plasmid (0.5 μg) and pRL-CMV-*Renilla* (25 ng). The plasmid pEF1A/myc-His (0.5 μg) was cotransfected to the control cells. Cells were transfected with the plasmid pEF1A-NS5A-myc-His (0.5 μg) together with either empty plasmid pCMV4 (10 ng) or pCMV-HNF-1α (10 ng). At 48 h posttransfection, cells were harvested. Luciferase assays were performed by using a dual-luciferase reporter assay system. *, $P < 0.05$, compared with control. (E) Huh-7.5 cells (1.2×10^6 cells /10 cm-dish) were infected with HCV J6/JFH1 at a multiplicity of infection of 2 and cultured for 5 days. At day 5 postinfection, cells were plated at 1.0×10^5 cells/12-well plate and cultured for 12 h. Mock-infected cells were plated similarly. Cells were transfected with the human GLUT2 promoter reporter plasmid (0.5 μg) and pRL-CMV-*Renilla* (25 ng) together with either empty plasmid pCMV4 or pCMV-HNF-1α, cultured for 48 h, and harvested. Luciferase assays were performed by using a dual-luciferase reporter assay system. *, $P < 0.05$, compared with control.

pression of the GLUT2 promoter, we examined the effect of NS5A protein on the levels of endogenous HNF-1α protein. Huh-7.5 cells were transfected with increasing amounts of either an NS5A expression plasmid or NS5B expression plasmid. At 48 h posttransfection, cells were harvested, and the levels of endogenous HNF-1α protein were analyzed by immunoblot analysis. To detect endogenous HNF-1α protein, highly sensitive Western blotting detection reagents (ECL Plus Western blotting detection reagents) were used. Overexpression of NS5A (Fig. 5B, left panel) but not NS5B (Fig. 5B, right panel) significantly reduced endogenous HNF-1α protein. These results suggest that NS5A protein specifically reduces endogenous HNF-1α protein levels.

To determine if NS5A-dependent reduction of HNF-1α protein is due to lysosomal degradation, we treated the cells with lysosome protease inhibitors. Pepstatin A, but not E-64d, recovered the levels of HNF-1α protein (Fig. 5C, middle panel, lanes 5 and 6), which is consistent with the results found in HCV-infected cells. These results suggest that NS5A is responsible for HCV-induced lysosomal degradation of HNF-1α protein. Taken together, our results suggest that HCV infection suppresses GLUT2 promoter activity via NS5A-dependent lysosomal degradation of HNF-1α protein.

To verify a role of HNF-1α in the HCV-induced suppression of GLUT2 promoter activity, we examined the effects of ectopic expression of HNF-1α on GLUT2 promoter activity in NS5A-transfected cells as well as in HCV J6/JFH1-infected cells. As shown in Fig. 5D, overexpression of NS5A decreased GLUT2 promoter activity, and ectopic expression of HNF-1α restored GLUT2 promoter activity (Fig. 5D). Moreover, HCV J6/JFH1 infection significantly decreased GLUT2 promoter activity, and ectopic expression of HNF-1α restored GLUT2 promoter activity (Fig. 5E). These results are consistent with the notion that HNF-1α protein is a key regulator for HCV-induced suppression of GLUT2 promoter activity.

NS5A protein interacts with HNF-1α protein in Huh-7.5 cells and in FGR Con1 cells. It was previously reported that *in vitro* translated HNF-1 protein was pulled down with glutathione *S*-transferase (GST)-NS5A protein (32). To determine whether NS5A physically interacts with HNF-1α protein in cultured cells, Huh-7.5 cells were cotransfected with each FLAG-tagged NS5A expression plasmid together with the HNF-1α expression plasmid. Immunoprecipitation analysis revealed that HNF-1α protein was coimmunoprecipitated with FLAG-NS5A protein using anti-FLAG MAb (Fig. 6A, third blot, lane 8). No band was detected using control IgG for immunoprecipitation (Fig. 6A, third blot, lane 7). Conversely, immunoprecipitation analysis revealed that NS5A protein was coimmunoprecipitated with HNF-1α protein using anti-HNF-1α rabbit PAb (Fig. 6B, fourth blot, lane 8). Moreover, NS5A protein was coimmunoprecipitated with endogenous HNF-1α protein (Fig. 6B, fourth blot, lane 6), suggesting that NS5A protein indeed interacts with HNF-1α protein.

To confirm that HCV NS5A protein can interact with HNF-1α protein in HCV-replicating cells, we performed immunoprecipitation analysis using FGR Con1 (RCYM1) cells. NS5A protein was coimmunoprecipitated with endogenous HNF-1α protein (Fig. 6C, fourth blot, lane 2). Transfection of HNF-1α protein increased the level of coimmunoprecipitated NS5A protein (Fig. 6C, fourth blot, lane 4), suggesting that HCV NS5A protein indeed interacts with HNF-1α protein in HCV-replicating cells.

HNF-1α binds domain I of NS5A protein. To map the HNF-

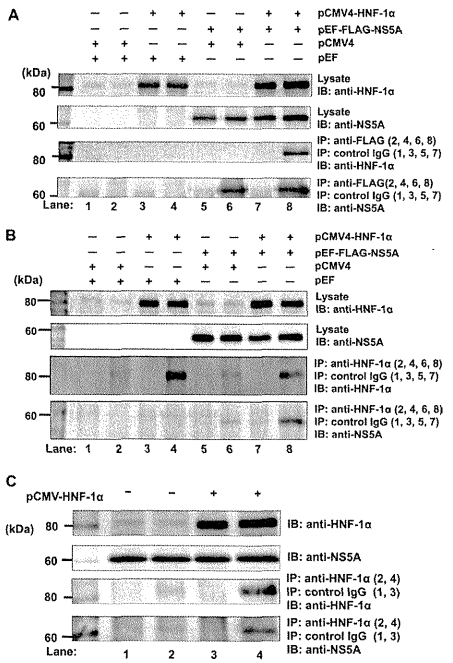

FIG 6 NS5A protein interacts with HNF-1α protein. (A) Huh-7.5 cells were plated at 1.2×10^6 cells/10-cm dish and cultured for 12 h. Cells were transfected with plasmids as indicated. At 48 h after transfection, cells were harvested. Cell lysates were immunoprecipitated with either anti-FLAG mouse MAb (lanes 2, 4, 6, and 8) or control IgG (lanes 1, 3, 5, and 7), and bound proteins were immunoblotted with anti-HNF-1α rabbit PAb (third blot) or anti-NS5A mouse MAb (fourth blot). Protein expression of HNF-1α or FLAG-NS5A was confirmed using the same cell lysates by immunoblotting with either anti-HNF-1α rabbit PAb (first blot) or anti-NS5A mouse MAb (second blot). (B) Cell lysates were immunoprecipitated with either anti-HNF-1α rabbit PAb (lanes 2, 4, 6, and 8) or control IgG (lanes 1, 3, 5, and 7), and bound proteins were immunoblotted with either anti-HNF-1α rabbit PAb (third blot) and anti-NS5A mouse MAb (fourth blot). (C) Full-genome replicon Con1 (RCYM1) cells were plated at 1.2×10^6 cells/10-cm plate and transfected with or without pCMV-HNF-1α plasmid and cultured for 48 h. Cells were harvested and assayed for immunoprecipitation with anti-HNF-1α rabbit PAb (lanes 2 and 4) or control IgG (lanes 1 and 3). Bound proteins were immunoblotted with anti-HNF-1α goat PAb (third blot) or anti-NS5A mouse MAb (fourth blot). Input samples were immunoblotted with either anti-HNF-1α PAb (first blot) or anti-NS5A MAb (second blot). IP, immunoprecipitation; IB, immunoblotting.

1α-binding site on NS5A protein, coimmunoprecipitation analyses were performed. By use of a panel of NS5A deletion mutants (Fig. 7A), FLAG-HNF-1α protein was found to coimmunoprecipitate with all of the HA-NS5A proteins except HA-NS5A consisting of aa 357 to 447 [HA-NS5A(357–447), HA-NS5A(250–447), or HA-NS5A(214–447) (Fig. 7B, lower left panel). These results suggest that domain I of NS5A consisting of aa 1 to 213 is important for HNF-1α binding. FLAG-HNF-1α protein was also found to coimmunoprecipitate with NS5A(1–126)-myc-His_6 and NS5A(1–147)-myc-His_6. These data led to the conclusion that the HNF-1α-binding domain of NS5A protein was aa 1 to 126.

DISCUSSION

In this study, we aimed to clarify molecular mechanisms of HCV-induced suppression of GLUT2 gene expression. The reporter assays of the human GLUT2 promoter suggest that the HNF-1α-binding site is crucial for HCV-induced suppression of GLUT2 promoter activity (Fig. 2). HCV infection significantly reduced the levels of HNF-1α mRNA (Fig. 3A). Moreover, HCV infection remarkably decreased HNF-1α protein levels (Fig. 4A). Our results suggest that HCV infection suppresses GLUT2 gene expression via NS5A-mediated lysosomal degradation of HNF-1α protein (Fig. 5). Immunoprecipitation analyses revealed that NS5A protein physically interacts with HNF-1α protein (Fig. 6) and that domain I of NS5A is important for HNF-1α binding (Fig. 7). Taken together, our results suggest that HCV infection suppresses GLUT2 transcription via downregulation of HNF-1α expression at both transcriptional and translational levels (Fig. 8).

We demonstrated that HNF-1α protein levels were greatly reduced compared to the reduced levels of HNF-1α mRNA. We demonstrated that pepstatin A, but not E64-d, restored the levels of HNF-1α protein, suggesting that an aspartic protease is involved in the degradation of HNF-1α protein. Pepstatin A is widely used for investigation of autophagy and lysosomal degradation. Further studies are needed to elucidate how HCV induces lysosomal degradation of HNF-1α protein and how HNF-1α protein is selectively downregulated by HCV infection. Our data suggest that the HCV NS5A protein is responsible for the HCV-induced degradation of HNF-1α protein. Using a panel of NS5A deletion mutants, we demonstrated that domain I of NS5A is important for association with HNF-1α protein. NS5A domain I is relatively conserved among HCV genotypes compared to domains II and III, suggesting that NS5A–HNF-1α interaction is common to all the HCV genotypes. Domain I coordinates a single zinc atom per protein molecule and is essential for HCV RNA replication (35). The crystal structure of NS5A domain I revealed the presence of a zinc coordination motif and a C-terminal disulfide bond (36). NS5A domain I was found to bind many host proteins, RNA, and membranes (16). It is possible that physical interaction between NS5A protein and HNF-1α protein is important for selective degradation of HNF-1α protein. One possible mechanism is that NS5A protein may recruit HNF-1α protein to the lysosome. Further study is necessary to test this possibility.

We observed that deletion of the GLUT2 transcriptional start site enhances expression of the GLUT2 reporter in FGR cells (Fig. 2B). Cha et al. (7) previously reported that deletion down to nucleotide +73 of the GLUT2 promoter resulted in a marked increase and that further deletion to nucleotide +188 caused a drastic decrease in luciferase activity, indicating the presence of negative- and positive-regulator elements in the 5′ untranslated region. The role of these elements in HCV-infected cells remains to be elucidated.

We demonstrated that HCV J6/JFH1 infection reduced the HNF-1α mRNA level and HNF-1α protein level. Our results contradict an earlier report (32) demonstrating that expression of HNF-1 mRNA was increased in subgenomic replicon Huh.8 cells (3). We observed downregulation of HNF-1α mRNA and

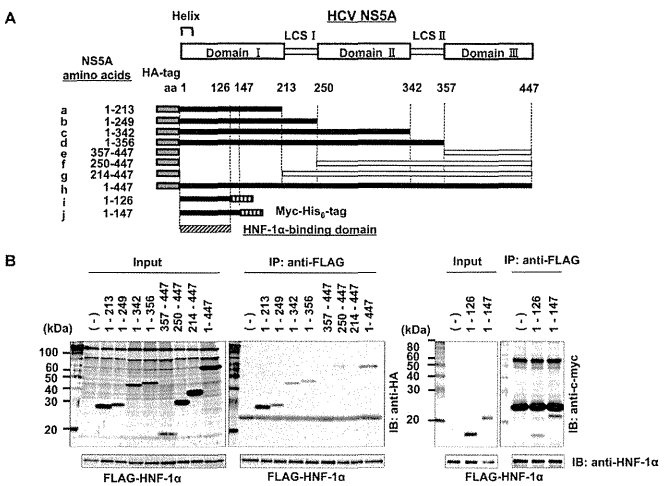

FIG 7 Mapping of the HNF-1α-binding domain for NS5A protein. (A) Schematic representation of the hepatitis C virus NS5A protein. NS5A consists of three domains (domains I, II, and III) with domains separated by low-complexity sequences (LCS I and II). The position of the amino-terminal amphipathic helix membrane anchor is shown (labeled helix). The NS5A deletion mutants (a to j) contain the NS5A amino acids indicated to the left. Each NS5A deletion mutant contains either HA tag in the N terminus (a to h) or myc-His_6 tag in the C terminus (i and j). The gray region of each represents the HA tag sequence. The lattice region of each represents the myc-His_6 tag (i and j). Closed boxes represent proteins that are bound specifically to HNF-1α protein, and open boxes represent those that are not bound. (B) Huh-7.5 cells were transfected with each NS5A mutant plasmid together with a FLAG-HNF-1α expression plasmid. At 48 h posttransfection, cells were harvested, and cell lysates were immunoprecipitated with anti-FLAG beads. Input samples and immunoprecipitated samples were immunoblotted with anti-HA MAb (two left panels, top), anti-c-myc MAb (two right panels, top), or anti-HNF-1α PAb (all panels, bottom).

HNF-1α protein in SGR cells as well as in FGR cells (data not shown). We also demonstrated that the ectopic expression of NS5A protein decreased the endogenous HNF-1α protein level. The reasons for these discrepancies remain to be elucidated.

We along with other groups previously reported that HCV NS5A protein is involved in mitochondrial reactive oxygen species (ROS) production (11, 13, 38). Mitochondrial ROS generation is known to induce the autophagy pathway (22) and lysosomal membrane permeabilization (8). Therefore, it is necessary to determine whether NS5A-induced ROS production enhances autophagic degradation or lysosomal membrane permeabilization. Several groups have reported that autophagy vesicles accumulate in HCV-infected cells and that autophagy proteins can function as proviral factors required for HCV replication (14). Autophagy degrades macromolecules and organelles. Based on the means by which cargo is delivered to the lysosomes, three different autophagy pathways are described: macroautophagy, microautophagy, and chaperone-mediated autophagy (CMA). At first, autophagy was considered a nonselective bulk degradation process. CMA, however, results in specific degradation of the cytosolic proteins in a molecule-by-molecule fashion. Most known substrates for CMA contain a peptide sequence biochemically related to KFERQ (12). Although the typical KFERQ peptide motif is not found in HNF-1α protein, it is possible that KFERQ-like sequences can be generated by post-translational modifications. It is also possible that HNF-1α protein possesses other degradation motifs. The molecular mechanism underlying NS5A-dependent lysosomal degradation of HNF-1α protein needs to be elucidated.

HNF-1α is a homeodomain-containing transcription factor, which is expressed in the liver, pancreatic β cells, and other tissues (1). Intriguingly, HNF-1α is known to play a crucial role in diabetes. Heterozygous germ line mutations in the gene encoding HNF-1α are responsible for an autosomal dominant form of non-insulin-dependent diabetes, MODY3 (40). Mutations in the HNF-1α gene disrupt GLUT2 function as a glucose sensor in pancreatic β cells, resulting in severe insulin secretory defects (39). It is unclear whether HNF-1α mutations in the liver affect glucose homeostasis in MODY3 patients. Two strains of HNF-1α-deficient mice have been reported. The mice of the first strain, created using standard methods for making knockout mice, are born normally, but most die postnatally around the weaning period after a progressive wasting syndrome (31). Mice of the second strain, created using the Cre-loxP recombination method, had a normal life span (20). The knockout mice of the second strain were dwarfed, diabetic, and infertile. Moreover, the knockout mice had enlarged livers and exhibited progressive liver damage.

HNF-1α was also identified as a tumor suppressor gene involved in human liver tumorigenesis since biallelic inactivating mutations of the HNF-1α gene were found in 50% of hepatocellular adenomas and, in rare cases, of well-differentiated hepatocellular carcinomas developed in the absence of cirrhosis (5).